LIBRARY
DEPOSITED
THESIS
16 XI 67
OXFORD

Some studies

on

THE IONIC BASIS OF THE CURRENT-VOLTAGE RELATIONS IN CARDIAC MUSCLE

by

RONALD ERIC McALLISTER

A Thesis, submitted to
The Board of the Faculty of Biological Sciences,
University of Oxford,
for the Degree of Doctor of Philosophy

August, 1967

ABSTRACT

Measurements of the electrical properties of the cardiac Purkinje fibre membrane (sheep) have been made with intracellular electrodes; and in a separate study, computations based on a mathematical model of the membrane have been performed.

Evidence has been found that the instantaneous potassium permeability of the membrane varies as a function of the difference between the K equilibrium potential and the membrane potential, rather than of the latter alone. Superimposed upon this, there is a time-dependent slow increase in K conductance on depolarization, corresponding to the delayed rectification described by the Hodgkin-Huxley relation when n^2 is used in place of n^4. The time constant is voltage dependent and may be up to hundreds of msec. This increase and its subsequent decline can account for repolarization from the plateau of the action potential, and for pacemaker activity. During long-lasting outward currents applied across the membrane there is a gradual depolarization of the K equilibrium potential; evidence suggests that K ions accumulate transiently in an extracellular space adjacent to the membrane.

Solutions to Noble's (1962) modified Hodgkin-Huxley equations have been computed for a membrane with part of its capacitance in series with a constant resistance. Rates of depolarization and repolarization have thereby been increased to experimentally-observed values; also, a possible explanation for the pre-plateau notch in some action potentials has resulted. An evaluation of the ramp-shaped voltage clamp as an analytical tool has been attempted, by computing solutions of the same equations under such conditions. The equations have also been solved when g_{K2} is a function of n^2.

ACKNOWLEDGEMENTS

I am very grateful to Professor Sir Lindor Brown for permission to study in the University Laboratory of Physiology, and for his ready and effective assistance in smoothing the path at any time that this was within his power.

My debt to my supervisor, Dr. Denis Noble, is much greater than I can acknowledge. My decision to change from the physical to the biological sciences earned me dismissal from my college; notwithstanding, he provided opportunity and encouragement in very full measure and saw me well established in a new career. I can think of no way in which he was not a most ideal supervisor during all the three years of our association.

I am very grateful to the Rhodes Trustees for a Scholarship for three years' study in Oxford, and to the Warden of Rhodes House, Mr. E.T. Williams, for his helpful interest and advice. The National Research Council of Canada kindly provided me with a Scholarship to cover my final year of research in Oxford.

The academic, technical, and supporting staff of the Laboratory have unfailingly provided welcome assistance whenever asked. The staff of the University Computing Laboratory have been similarly helpful. To all these, I should like to express my sincere gratitude, and in particular to Mr. A.J. Spindler.

Mrs. Audrey Richards has worked wonders in typing my handwritten thesis draft.

And finally, I must acknowledge my great debt to my wife Carol, who spent many hours creating respectable photographs and figures to amplify the text that follows.

CONTENTS

ABSTRACT

ACKNOWLEDGEMENTS

CHAPTER 1 : INTRODUCTION 1

1.1 Histology of cardiac muscle 2

1.2 The Purkinje fibre 9

1.3 Electrophysiological properties 12

1.4 Mathematical background 21

1.4a Thermodynamic considerations 22
1.4b Approximations and assumptions 28
1.4c The Hodgkin-Huxley equations 33
1.4d Modifications for cardiac muscle 36

1.5 Aims of this study 38

CHAPTER 2 : EXPERIMENTS WITH CONSTANT CURRENTS 39

2.1 Methods 39

2.1a The preparation 39
2.1b The bath and superfusion apparatus 41
2.1c Electrodes 42
2.1d Electronic apparatus 44

2.2 Results 46

2.2a Current-voltage relations in Na-free solutions 46
2.2b Experiments with increased external K concentrations 49
2.2c Effects of prolonged current pulses 59
2.2d Temperature effects 61

2.3 Discussion 65

CHAPTER 3 : EXPERIMENTS WITH VOLTAGE CLAMPS 70

3.1 Methods 70

3.2 Results of voltage clamps 72

3.3 Discussion 80

CHAPTER 4 : COMPUTATIONS 87

4.1 Methods 89

4.1a The computed membrane action potential 89
4.1b The ramp-shaped voltage clamp 93

4.2 Results of computations 95

4.2a Results with g_{K2} as a function of n^2 95
4.2b Results with the series-RC component included 97
4.2c Ramp voltage clamp results 103

4.3 Discussion of computed results 106

CHAPTER 5 : SUMMARY OF THE RESULTS OF THIS STUDY 116

6 : APPENDIX 120

6.1 KDF-9 Algol program for computing the cardiac action potential, with a series-RC segment in the membrane 122

6.2 KDF-9 Algol program for computing cardiac muscle membrane currents during a ramp voltage clamp 132

REFERENCES 139

'It is difficult to avoid the conclusion that there can be little progress in unifying and consolidating the cardiac phenomena until an analysis of the cardiac cell membrane such as has been done for the squid axon becomes possible. Until then it may not be possible to know whether or not the squid data apply even qualitatively to cardiac cell membranes and, to the extent they do apply, what quantitative differences exist.'

- Kenneth S. Cole, 1957

(Ann. N.Y. Acad. Sci. 65, 658-662)

CHAPTER 1 INTRODUCTION

The heart is a highly specialized organ composed in the main of (excitable) muscle tissue of three functionally different types, and including interwoven myelinated and unmyelinated nerve fibres and endings (both afferent and efferent) together with nerve cells and small ganglia beneath the epicardium near the sinus venosus. The interstitial spaces contain the capillaries, connective tissue, and collagenous fibrils which complete the structure. The musculature consists of: the relatively small nodal cells, which form the pacemaker area and include few myofibrils; the conduction system of narrow cylindrical cells joined in strands, becoming continuous with the normal myocardium after running for varying distances through it, and containing sparse numbers of disoriented myofibrils; and the myocardium, a mass of variously-shaped but roughly cylindrical cells containing closely-packed myofibrillar bundles which occasionally branch and interconnect, and large numbers of mitochondria filling most of the spaces between the myofibrils. Although the tissue is innervated, the basic operation is initiated and temporally controlled by the pacemaker region: so that while the nervous supply can modify the rate, the organ can also function independently.

The muscle in general is striated, although in the more specialized conducting and pacemaker cells this is apparent only in the individual myofibrils. Functionally it behaves as a syncytium,

and in this respect it differs electrophysiologically from skeletal muscle.

In other respects, the electrophysiological picture is enhanced by a comparison with other muscles and with nerve; in fact as discussed below, it does not require extensive modification in order to adapt the Hodgkin-Huxley (1952) equations to cardiac muscle and so obtain a mathematical model of the excitable membrane. The general results of electrophysiological experimentation and analysis, from many workers in various preparations, all indicate that the fundamental principles underlying the operation of excitable tissues are quite general; and hence, that much useful qualitative information, later to be quantitatively adapted to other tissues, can be obtained from the quantitative study of one particular membrane. Thus some of the results presented herein should find wide applicability in the study of the electrophysiology of all types of muscle, and possibly of nerve as well.

1.1 HISTOLOGY OF CARDIAC MUSCLE

Until about fifteen years ago, it was generally believed that the mass of cardiac muscle was, both functionally and morphologically, a multi-nucleated syncytium. Intercalated discs were known to take plate, step, and irregular forms, but were regarded as limited intracellular structures rather than cell boundaries. Then the combined weight of several independent observations began to require changes in this scheme. Occasional sections showed contraction of the myofibrils on one side of a disc, with none on the other. Under mechanical stress

or trypsin digestion, separation usually occurred at the disc. Myofibrils were observed not to pass through the disc without interruption. Cultured heart cells could exhibit spontaneous beating at different rates in adjacent cells. (However in other cardiac muscle preparations the spread of excitation from cell to cell occurred at a rate which suggested direct coupling. Cedergren & Harary (1964) found that cultured single heart cells beat synchronously when in contact; and Weidmann (1966) found a very low resistance to the diffusion of radio-potassium in Purkinje fibres). By 1957, the idea of the distinct cellular composition of cardiac muscle was firmly established, after the work of van Breeman (1953), Sjöstrand & Anderssen (1954), and Moore & Ruska (1957) in amplifying the above observations; and it has been amply confirmed by the many demonstrations since then using new staining and fixing techniques and the better resolving power of the newer electron microscopes. Muir (1957) illustrated the development of the disc from embryonic to adult form in the rabbit heart: he found small, mononucleated, spindle-shaped cells in the embryo to have 'simple' (or roughly linear) intercalated discs; in the newborn heart these had begun to assume the step-like character noted in the adult, where the cell boundary runs parallel to the longitudinal axis of the cell between the myofibrils, but crosses the myofibrils at right angles to this axis and exhibits the thick dark 'myofibrillar anchor plaques' at these crossings; and in the adult heart the transverse parts of the disc membranes interdigitate very extensively, and the anchor plaques thicken and fill in all the finger-like projections between the cells. Since, with the exception of the

adult heart, the disc region (with anchor plaques) was seen to be relatively thin - 0.16μ as opposed to the fully-developed thickness of 0.7μ - some of the failures of the early light microscopists to see intercalated discs in their entirety are understandable. The increased interdigitation at the disc with development was postulated to be an effect of increasing tension (due to growth), this being transmitted to the disc membrane only at the myofibrillar anchor plaques and so leaving the longitudinal parts of the 'steps' relatively undistorted.

Electron-microscopic observations over the next few years confirmed the cellular nature of the myocardium by delimiting the continuous sarcolemma (Moore & Ruska, 1957), and several different forms of intercellular contact (Sjöstrand et al, 1958; Muir, 1965). The latter were found to consist of four main types:

(1) Normal intercellular contacts, with no specialized areas of membrane, and a constant spacing between the adjacent cell boundaries of about 200A.

(2) Longitudinal connecting surfaces, or desmosomes, which consist of a densely osmiophilic thickening in each of the apposed membranes and a decreased intercellular space.

(3) Interfibrillar connecting surfaces, or myofibrillar insertion (anchor) plaques. These resemble the desmosomes, but occur in the intercalated disc where a myofibril approaches: they often occur in pairs, one in each cell, so that the myofibril may appear continuous except for a definite intercellular break of 95A. Grimley & Edwards (1960) found that the desmosomal thickenings were often

associated with the Z-band region of the adjacent myofibrils; and as they were observed in various orientations and positions, these authors suggested that a natural consequence of development was the rotation of desmosomes to become myofibrillar insertion plaques in the disc.

(4) The tight junction, or nexus, which can occur in the longitudinal or disc parts of the cell and often appears to be a fusion of the two sarcolemmal membranes (Dewey & Barr, 1961 and 1964).

A study of these interconnections now became of great importance in order to explain the transmission of excitation through the muscle. The most obvious possibility was that the excitatory current flowed through the membranes at the nexus areas. If these were really areas of fusion, then there would be effectively a single membrane with a negligible difference in concentrations of ions on either side; and if the membrane characteristics were like those of the sarcolemma, the resultant depolarization would mean that the nexuses were areas of high conductivity (Dewey & Barr, 1964). This view was supported by the observation on frog atrial muscle fibre bundles that hypertonic bathing solution caused conduction block at a sucrose gap shunted by an external circuit, whereas normal solution did not; and that this same hypertonic solution caused the nexus regions to separate (Barr, Berger & Dewey, 1964). Because of the complexity of the disc region, the full extent of the nexal regions has not yet been determined, and therefore a useful prediction of the axial resistance between cells cannot be made. It is unlikely that they are very widespread, however, as they present no barrier to the diffusion of ferritin

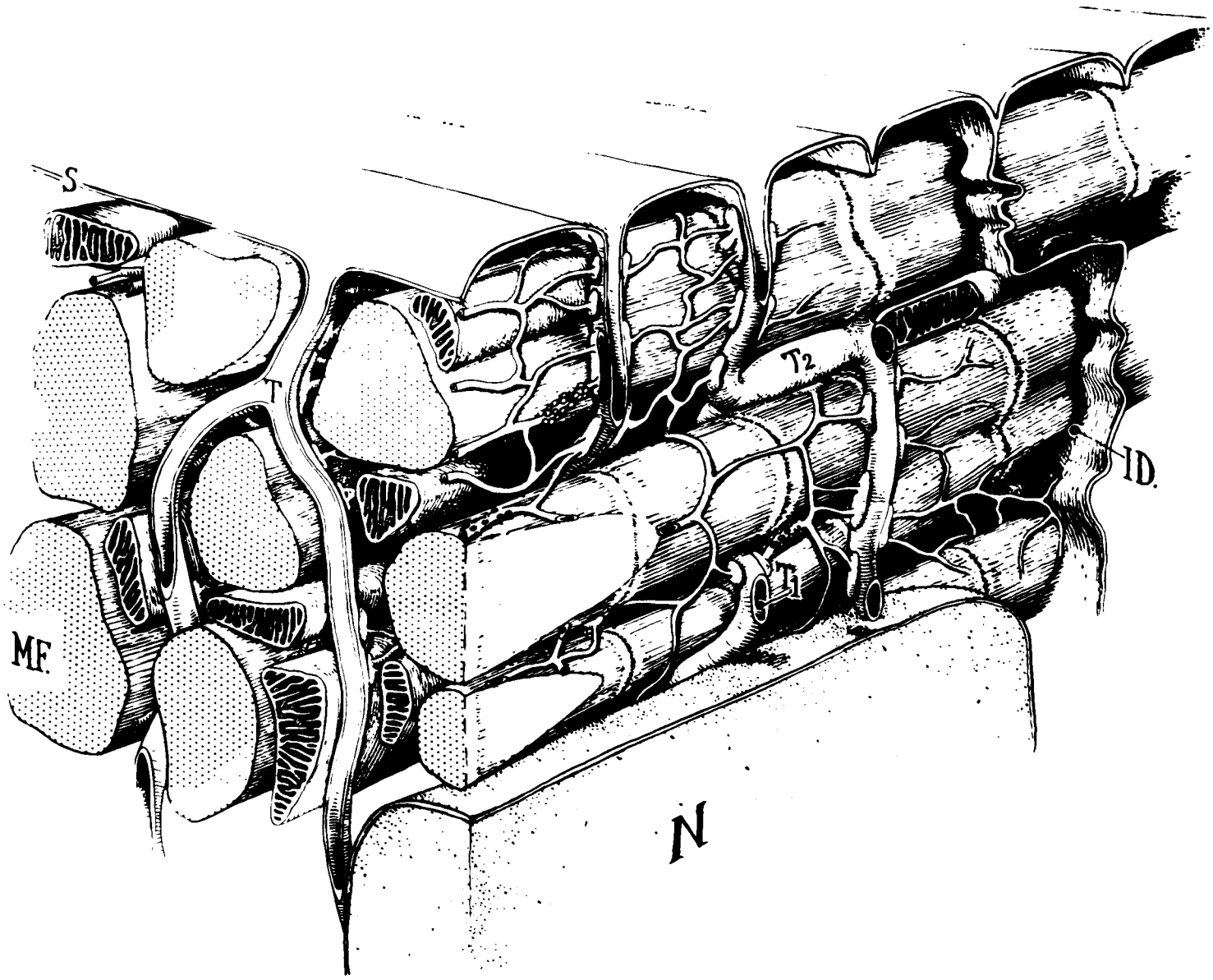


Figure 1 : Model of a portion of a myocardial fibre, showing transverse system (T), longitudinal connections between transverse tubules (T2), intercalcated disc (ID), myofilaments (M), sarcolemma (S), and nucleus (N). From Nelson & Benson, 1963.

granules throughout the intercellular spaces at the disc (Muir, 1965; Forssmann & Girardier, 1966); although they have been observed to extend for upwards of one sarcomere length (1.5μ), generally in areas of the 'stepped' intercalated disc parallel to the fibre axis (Dewey, Barr & Berger, 1965).

Even given the cellular structure of the myocardium and a low-resistance intercellular contact, the problem of the spread of excitation to the interior of the cells still exists; for the contraction in response to external stimulation occurs with too little delay to allow for the diffusion time of an excitatory agent (Hill, 1948). A reticular structure, the muscle analogue of the endoplasmic reticulum of other cells, provided a possible avenue of approach. As electron-microscopy techniques improved, it became apparent that two systems of tubules - the transverse tubular system and the longitudinal system or sarcoplasmic reticulum - permeated the entire cell volume between and adjacent to the myofibrils and the very numerous mitochondria (Porter, 1956; Edwards, Ruska et al, 1958; see Figure 1). The transverse system originates near the sarcolemma and approaches the myofibrils with a regular spatial relationship to each sarcomere - e.g. at the Z-line region in cardiac muscle; while the longitudinal system runs along the myofibrils between the Z-lines and becomes distended wherever it meets the transverse system (forming the 'triad' or 'dyad' arrangement commonly seen in electronmicrographs). It had been a general observation that the longitudinal and transverse tubules were not continuous, excitation being supposed to occur electrotonically across the adjacent membranes (e.g. Walker & Schrodt, 1965); however, Forsmann & Girardier

(1966) have reported openings between the two systems in heart muscle and penetration of ferritin granules into the longitudinal system following external application. They suggest that cardiac muscle is different from skeletal muscle in this respect, because in the latter the calcium relaxing factor has an internal source whereas it is believed to come from the extracellular fluid in cardiac muscle. Most research workers in considering the functional importance of these structures, have dealt with three possibilities; the first is generally believed to be of prime importance in excitation.

(1) Conduction of the action potential down the walls of the tubules (supposing these membranes to be similar to the sarcolemma). The velocity of propagation down a 300A tubule has been estimated as a few cm/sec, permitting excitation of an entire muscle fibre in 1-2 msec (Huxley, 1964). The microstimulation experiments of Huxley & Taylor (1958), whereby local contractions of a sarcomere could only be elicited when the current was applied to the areas of sarcolemma nearest the transverse tubules, indicated the importance of this system in the initiation of contraction; but they produced no evidence of an 'all-or-none' effect indicative of action potentials, and so left open the next two possibilities.

(2) Diffusion of a transmitter (and perhaps metabolites) passively down the lumen of the tubules. Hill's calculations place some limits on the effectiveness of this, however.

(3) Passive conduction of local currents from the cell interior to the extracellular fluid across the (possibly inexcitable) tubule membranes (Girardier, 1963). This is consistent with the graded

responses seen on microstimulation by Huxley & Taylor, and would appear to offer a reasonable alternative to (1).

Evidence is still being sought to distinguish the actual functional importance of these tubular systems, and some combination of the above possibilities is not excluded.

1.2 THE PURKINJE FIBRE

The mass of cardiac muscle presents a difficult problem to the electrophysiologist, because of its functionally syncytial nature. Locally-applied stimulating currents spread in all directions, with the result that point electrodes must record very low current densities. Spatial control of membrane potential with applied currents, and therefore the voltage clamp, is impossible with normal techniques. Muscle contraction tends to break the glass micropipette electrodes which are required for intracellular measurements.

Electrical properties of a cell membrane are ideally measured by means of electrodes on both sides of it. The ideal cell on which to experiment will be non-contractile; spatially well-defined; easily accessible; symmetrical; and large enough to penetrate with normal microelectrodes - i.e., ones with a bore capable of passing useful currents. Fortunately, such a cardiac muscle preparation is available.

The conducting system in the hearts of some mammals, notably sheep, cattle, and dogs, frequently includes 0.5-2 mm diameter cord-like extensions (the 'false tendons') away from the inner walls of the ventricles. They have come to be known as cardiac Purkinje fibres, after the Bohemian histologist who first described them in sheep heart

in 1838. Although it is not a general feature, in the ungulates the myofibrillar arrangement within these cells is so sparse and disorganized that contraction is usually extremely slight. Muir (1957) studied sheep Purkinje fibres with the electron microscope and found one to six parallel strands of cells joined end-to-end, bound into a fibre by a dense outer layer of collagenous connective tissue. The cells were roughly cylindrical, with a diameter of 30-40μ (normal myocardial cells are about 10μ in diameter), and 5-15% of the cross-sectional area was occupied by myofibrils. Normal myocardial cells have 65-75% of the cross-sectional area so occupied, and Muir pointed out that it would be consistent to suppose the two types of cell to contain the same number of myofibrils - implying, perhaps, that the cell volume increased with specialization. Caesar, Edwards & Ruska in 1958 carried out similar observations and commented on the close similarity of general appearance with that of normal myocardial cells, and even moreso with that of embryonic cardiac cells. The cell membranes were also similar except that in Purkinje fibres the outer 'basement' membrane, a semi-opaque 400-500A layer outside the (supposed) protein-lipid-protein basic membrane, was found to extend around the bundle of cells but not into it; i.e., the interior parts of the cells were separated only by their respective plasmalemmas and the interspace. Both Muir and Caesar et al. found small capillaries and myelinated nerve fibres in the surrounding connective tissue sheath, but not among the muscle fibres. A determination of the length of the conducting cells, and the certain definition of the intercalated disc as the cell boundary, was achieved by Muir in 1965 by centrifuging sheep Purkinje fibres loaded

with ferritin granules; the granules collected at the cell end-walls, and showed the cells to average a length of 130-170μ, about the same as normal sheep myocardium. Other electron micrographs showed that the intercellular spaces were clear and much smaller than in normal myocardium, which has capillaries and collagen between the cells. The intercellular contacts were greatly increased by interdigitation, and specialized contacts (membrane fusions, desmosomes) occurred much more frequently. Even the non-specialized intercellular areas were characterized by a smaller gap, 130A versus the usual 200A. This would suggest that transverse conduction is as easy as longitudinal, and that the fibre therefore behaves electrically like a uniform cable of the same dimensions.

Domestic sheep from local abattoirs provide a ready supply of Purkinje fibres, for the left ventricles generally contain upwards of a dozen easily-excised and non-branching preparations. These easily-available, non contractile, well-oriented and discrete groups of cells, with dimensions one to two orders of magnitude larger than the 1μ tip of a useful microelectrode, satisfy all the conditions necessary to a useful study of the cell properties; but there is also one other property at least equally advantageous. Even with such a cable-like preparation (and, e.g., nerve axon), the geometrical properties permit a very considerable spread of current in both directions along the cable from a point electrode. This spread must be allowed for in analysing the experimental results, and also prevents the adequate voltage clamping of any large area of membrane. Cardiac muscle, however, has been found capable of 'healing over' a cut surface so

that the healed surface presents an effective ion barrier, and Purkinje fibres have this characteristic ability (Weidmann, 1952); the process, according to Deleze (1963), is dependent on the presence of Ca in solution in usual (millimolar) concentration. As demonstrated in 1964 by Deck, Kern & Trautwein, this healing occurs even when a section of Purkinje fibre only 1-2 mm long is isolated from the rest, either by ligation or cutting; such a section of fibre is viable when maintained in heated, oxygenated Tyrode solution (Table 1,A). Thus a preparation short enough to permit uniform polarization of the cell membrane by internally-applied current was obtained (Weidmann, 1952, found the characteristic cable length or space constant to be about 1.8 mm; if a fibre is more than a space constant long, cable complications begin to increase), and accurate voltage-clamping experiments without serious cable problems could be carried out for the first time on cardiac muscle.

1.3 ELECTROPHYSIOLOGICAL PROPERTIES OF THE CARDIAC PURKINJE FIBRE

Although some electrophysiological information on Purkinje fibres has been obtained earlier with extracellular recording methods (e.g. Goldenberg & Rothberger, 1936), little progress was made until the advent of the microelectrode, invented by Ling & Gerard for intracellular use with frog skeletal muscle fibres in 1949. This made possible a whole new era of experimental measurement, ushered in for Purkinje fibres by Weidmann and his associates in 1949-51. The action potential (AP) was known to consist of a rapidly-rising initial spike followed quickly by a partial repolarization which slowed and became a

long-lasting 'plateau' at or above the midway point. While the initial spike (lasting up to 10 msec) was similar to, but somewhat longer lasting than, a nerve action potential, the plateau continued for hundreds of msec before ending in a sudden and complete final phase of repolarization to the resting or diastolic level (see Figure 27 for the general shape). The cycle often repeated spontaneously, or it could be initiated by a brief depolarizing stimulus to a 'threshold' level. In spontaneous 'beating', a gradual depolarization toward the threshold often occurred between action potentials; although it was unknown whether this diastolic depolarization was an after-potential (a consequence of the AP) or a pre-potential (a generator of the AP), it was strongest in certain areas known as 'pacemaker' areas, and an AP was initiated first in these areas and then propagated throughout the myocardium. Both frequency of beating and temperature affected the shape of the AP; and the refractory period after an AP, during which no amount of depolarizing stimulus would evoke a new AP, decreased with increasing frequency (Goldenberg & Rothberger, 1936).

Coraboeuf & Weidmann (1949a, b) found resting potentials or maximum diastolic potentials (for beating fibres) normally approaching -80mV, with an inversion of membrane potential to as much as +40mV during the spike of the AP. Draper & Weidmann (1951) made more extensive and careful measurements of the AP's properties, checking that the cut ends of the fibre, the general anaesthetic applied to the animal, electrode junction potentials, etc. did not invalidate their results. They then found resting potentials averaging -90mV, and total action potential amplitudes up to 135mV. The rate of rise of membrane

potential during the spike was of the order of 600 V/sec at its maximum, and the AP duration was 300-500 msec at normal beating rates. They also varied the ionic content of the bathing solution: a cessation of spontaneous activity but unchanged AP's occurred in Ca-free solutions, and a gradual diminution of the potential reversal or 'overshoot' occurred as the Na content of the solution was reduced, until at 20% of normal Na electrical activity ceased. Increasing the frequency of excitation decreased the AP duration, the resting potential, and the overshoot.

The next phases in the study of Purkinje fibre electrophysiology were to measure the passive electrical properties, the effects of ions, drugs, and external influences, and the active electrical properties. Weidmann began the first of these in 1951 (b) with measurements of membrane resistance (R_m) to short, small hyperpolarizing intracellular current pulses applied during the action potential; he noted an increase during diastolic depolarization, a rapid transient fall during the spike, and a slow increase again during the plateau to a higher level than at the resting potential. Passing longer (100 msec) pulses during the pacemaker, he also noted a larger R_m in the depolarizing direction than in the hyperpolarizing direction (later to be known as 'anomalous' or inward rectification), and effects on the membrane potential termed post-nodal enhancement (depolarization after the end of a hyperpolarizing pulse) and its opposite, post-cathodal depression. For hyperpolarizing currents passed late in the plateau, a premature repolarization could be invoked in an all-or-nothing manner, which appeared to propagate as an off-response. Weidmann was able to conclude that the spike of the AP

represented a rapid rise in membrane permeability to Na followed by a less-rapid decrease, and that either slow Na or K permeability changes, or both, caused the final repolarization from the plateau. In his next paper (1952) he went further by investigating the cable properties of the fibres, proving that current leakage at the healed end was negligible (as would be expected from its area, if the resistance per unit area were of the same order of magnitude as that of the normal exterior membrane) by plotting the potential profile along the fibre while injecting current at one point via a second microelectrode. At the same time he showed that the connective tissue sheath of the fibre was not a barrier to current flow by slowly lowering his recording electrode through this layer; and he obtained the following mean values for the electrical parameters by analysing the voltage profile in terms of the cable equations: space constant (λ), 1.9 mm; intracellular resistivity (R_i), 105 ohm cm (that of Tyrode solution is 51 ohm cm, implying that little of the intracellular ion content is in bound form); membrane resistance (R_m), 1940 ohm cm^2; and membrane capacitance (C_m), 12.4 $\mu F/cm^2$.

Shortly afterwards another group began a series of electrophysiological experiments on Purkinje fibres which has continued to the present day: that led by W. Trautwein in Heidelberg. In 1953, Trautwein, Gottstein & Federschmidt made a careful study of temperature effects on the action potential, finding that membrane potential rates of change exhibited a relatively high Q_{10} of about 1.7 at a constant frequency of stimulation; i.e., the AP slowed markedly in all its phases for a lowering of temperature to 30°C, and activity ceased at about 25°.

With Dudel (T & Dudel, 1954), Trautwein showed a linear relation between AP duration and 1/frequency; and with Gottstein & Dudel (T,G & D) in the same year demonstrated a remarkable insensitivity of Purkinje fibres to oxygen deficiency, injury beginning only after high-frequency beating for more than one hour and first manifesting itself as an increase of pacemaker activity.

Weidmann continued his researches up to their culmination in a book devoted solely to the topic in 1956(a). With Coraboeuf (C & W, 1954), he found the same slowing of the AP at low temperatures as Trautwein, and observed progressive permanent damage at temperatures above 45^{o}. His Q_{10} value for the spike was similar, but because he did not maintain a constant beating frequency, his Q_{10}'s for the later phases were much higher(a factor of 3 - 4); it seems likely that effects purely due to the beating frequency were being included in these values. The Q_{10} of the membrane resistance, as measured with small current pulses, was 1.5. Continuing, he showed (1955a) that R_m increased on depolarization to a maximum of about 4 times resting level at -40mV, and thereafter decreased to about half this maximum on further depolarization: the resulting curve of current versus membrane potential has since become very familiar. A further milestone was the introduction (1955b) of a localized voltage clamp to studies on what are now known as 'long' (several space constants) Purkinje fibres; this permitted the study of time-dependent resistance (or its inverse, conductance) changes at fixed voltage levels, the only way of separating time- and voltage-dependent effects. As a result, he could demonstrate that the rate of upstroke during the depolarization phase of the AP depended on the

previous level of membrane potential in the same way as that of squid nerve, and was therefore subject to the form of quantitative analysis described in mathematical form by Hodgkin & Huxley three years earlier (1952 a-d). He was thus plotting the time and voltage dependence of the Na conductance parameter h; and since the time constants of increase and decrease were short, he inferred that Na currents had little effect on the slow changes in membrane potential during the plateau or pacemaker. An increased extracellular Ca concentration was shown (1955c) to shift the h-versus-voltage relation in a depolarizing direction, so that threshold was increased; hence the known 'stabilizing' effect of Ca. In 1956(b) as a result of experiments in which high K concentrations were injected into the circulation of turtle hearts, he suggested the possibility of a transient accumulation of K ions in a restricted space adjacent to the outer surface of the excitable membrane, the resultant high K concentration toward the end of the plateau promoting repolarization by either affecting Na kinetics or increasing g_K; the existence of such a space is postulated in a somewhat different context in Section 2.2c of this thesis. He further demonstrated (1957) the depolarization of the resting potential in external K concentrations of less than 2mM (in the presence of Na), which was unexpected on the basis of the simple Nernst equation.

The Heidelberg group (Trautwein & Dudel, 1958 a and b; Dudel & Trautwein) in 1958 began to study the pacemaker potential in more detail by applying acetylcholine and showing that its effect was solely to increase g_K, as indicated earlier by Harris & Hutter's (1956) flux measurements; they then concluded from its effects on the AP that

the pacemaker was probably due to a decrease in g_K, and that the same mechanism worked in reverse to promote repolarization from the plateau. By adding ACh to solutions containing increased K concentrations, the close proximity of the resting potential to E_K at K concentrations above 10mM could be demonstrated, as well as a slight chloride effect which increased with depolarization and caused the resting potential to fall below the predicted E_K above -40mV. Later (Trautwein & Kassebaum, 1961), by measuring the resistance during the pacemaker to small hyperpolarizing pulses while a constant degree of polarization was being applied, a definite dependence of the g_K decrease on both time and voltage was confirmed.

An Australian group under Johnson entered the field in 1960. Unfortunately their technique of measuring current-voltage relations was inadequate to the task of providing any new information in this respect (Noble, 1962b), but they were able to infer that a component of K conductance probably increased during the plateau (Johnson, Tille & Wilson, 1960).

Meanwhile Hutter & Noble (1960) demonstrated that the relative permeability of the membrane to anions was in the order $I > NO_3 > Br > Cl >> CH_3SO_4$, by observing changes in resting potential and AP shape and frequency when these ions were substituted in the bathing solution, and also by noting the changes in membrane potential in response to small current pulses. Chloride was found to contribute to the depolarizing current during the pacemaker and to the repolarizing current during the plateau, implying an effective equilibrium potential somewhere between these levels. Since the contribution to membrane

conductance was shown to be less than 30% and Cl appeared to be passively distributed across the membrane, it was possible to roughly compute E_{Cl} as -50mV. At the same time, Hall, Hutter & Noble (1963) were using long intracellular current pulses to plot the current-voltage relation over the complete physiological range of potential for Purkinje fibres in Na-free solutions, and found both the 'anomalous' decrease in conductance on depolarization noted by Weidmann, and a time-dependent and voltage-dependent rise in conductance on maintained depolarization beyond -30mV. Although for depolarization the conductance behaved anomalously, the resting value was found to be approximately predicted by the constant-field equation for K conductance even when external K concentration was increased to 141mM; and, further, this was probably also true when $[K]_o$ was reduced below normal, providing the electrochemical gradient for K ions was restored to near zero by polarizing current. This dependence of g_K on the electrochemical gradient rather than on membrane potential alone will be discussed in Section 2.2b below; it added much to the successful predictions of electrophysiological phenomena which Noble was computing from his modification of the Hodgkin-Huxley equations at this time, as discussed in Section 1.4d, and provided an explanation of the membrane depolarization seen by Weidmann in low-K solutions containing Na.

Carmeliet (1961), who was investigating anion conductance at the same time as Hutter & Noble, confirmed their findings for chloride, and in addition obtained some evidence that it is probably passively distributed by polarizing the membrane for several minutes andobserving effects on the membrane potential which would be

expected from an alteration of E_{Cl}. Hecht & Hutter in 1963 investigated the effects of pH, and found an increase in outward current and rates of time-dependent potential changes in alkaline solutions (and the opposite in acidic ones). They also noted that in different preparations they had seen either time-dependent rises or falls in conductance during prolonged depolarizations, the difference arising from causes unknown then or since.

Deck, Kern & Trautwein in 1963 successfully applied the most useful tool for electrophysiological analysis, the complete voltage clamp, to Purkinje fibres. This was achieved by using only a short (2mm) segment of the fibre, which remained functional because of the healing-over effect at the cut ends; as a result, the polarization of the membrane by applied intracellular currents was effectively uniform throughout the length of the fibre, and cable complications were completely avoided. They could not manage to suppress the initial spike on depolarization in Na-containing solutions, nor has anyone else to date; the currents required are beyond the capabilities of useful microelectrodes, and the response time of the clamp circuitry is a further limiting factor. However, they were able to show (Deck & Trautwein, 1964) that there was a slow increase in outward current during depolarization and a slowly-decaying outward current when the membrane potential was returned to the resting level after a depolarization lasting about one AP-duration; these could be related to the conductance changes causing repolarization from the plateau. When Na was removed by substitution of choline, these slow changes were altered; outward current slowly declined during depolarization, and the positive

current on repolarization was practically eliminated. By subtracting the two current-voltage relations, they tried to obtain one for Na alone, and concluded that the repolarization phase of the AP was due entirely to a slow decline in g_{Na} with a time constant of 100 msec which could not be accounted for by Noble's modification of the Hodgkin-Huxley equations. At the same time they showed that the outward current on repolarization reversed if the level of repolarization exceeded the K equilibrium potential; it was therefore assumed that a g_K change was triggered by the repolarization phase.

It was at this stage in the study that the experiments described in succeeding chapters of this thesis were begun, in order to verify and extend the voltage clamp results and fit them to a mathematical framework. The results have provided experimental information on the time-dependent g_K changes, the dependence of the inward rectification on the K electrochemical gradient, and the accumulation of K outside the excitable membrane; these will be discussed in later chapters, with reference to papers which have appeared since 1963.

1.4 MATHEMATICAL BACKGROUND

The membrane conductance changes which determine the size and time course of the action potential are measurable and subject to mathematical analysis; such analysis affords a very clear means of comparison with data from other excitable membranes, by separating and rendering measurable the individual influences contributing to the gross electrical behaviour.

Hodgkin & Huxley, in 1952, formulated a set of mathematical

equations which could describe the electrical behaviour of the squid axon with accuracy. They made use of the known geometry of the axon and the electrical parameters which they measured, together with the known behaviour of ions in solution under the influence of an electric field and in the presence of a semi-permeable membrane, and their result is still the most useful generalization of (empirical) membrane electrical behaviour. Noble, in 1962, modified the equations to apply to heart muscle, in the light of experimental data obtained with O.F. Hutter from the sheep Purkinje fibre. A summary of the background and results of these papers is given below, as the main object of the work presented in this thesis is the confirmation and extension of the theory.

1.4a Thermodynamic Considerations

The basic theory of the electrochemical thermodynamics (as outlinedfor example, in Bayliss, 1959, or Höber, 1945) provides for the description of a thermodynamic system in terms of certain fundamental, or 'state', variables -- temperature, volume, pressure, entropy -- together with several useful derivatives of these. The internal energy of a closed system (one which maintains a constant mass, but may exchange energy with other external systems) is described by

$$U = G + TS - PV \qquad (1)$$

and hence

$$dU = dG + TdS + SdT - PdV - VdP \qquad (2)$$

Here U = internal energy, T = temperature, S = entropy, P = pressure,

V = volume, and G = Gibbs free energy. Like all physical systems, this one will undergo no change unless either work is done on it, or its own potential energy decreases; this is the essence of the first law of thermodynamics. The internal energy of the system is considered as being of two types, bound energy and free energy. In any change of state, the former is unavailable for doing any work, whereas the latter can be recovered and used to do useful work providing that the system is manipulated in the appropriate way. The Gibbs free energy is the useful energy extracted by other means than the pressure acting through a change in volume of the system. In considering electrolytic solutions of differing concentrations, either contiguous at an interface or separated by a membrane, pressure and temperature can be taken as constant; this is the situation for excitable cells. In this case, equation (2) becomes

$$dU = dG + TdS - PdV \ , \qquad (3)$$

and the only bound energy term is TdS. Such a system will be in equilibrium when its free energy is at a minimum; otherwise changes will spontaneously occur until the excess of free energy is dissipated by doing work and/or being converted to bound energy.

In order to obtain quantitative results in applying thermodynamic theory to any real system, it is necessary to know the relations between the state variables which exist under any conditions for that system: i.e., the equation of state. This is never known exactly, because of the multitude of factors involved (from atomic sizes to molecular electric fields, etc.); it is always necessary to use an approximation, to be checked against experimental measurements. The

concept of an 'ideal' gas or solution is the initial and most useful one; in this, it is assumed that the individual molecules are of uniform size and remain so separated as not to interact, and therefore that the 'gas law' of the early experimentalists is exact :

$$PV = nRT \tag{4}$$

This approximation allows the individual state variables of each species of molecule to be calculated without regard to the others; although all occupy the same volume and are at the same temperature, the 'partial' pressure of each is proportional to the relative number of molecules present. The solvent and solutes in a solution are all considered to be 'perfect gases', and may all be treated alike: the distinction between solvent and solute theoretically disappears. In practice, it is found that this approximation is valid for dilute solutions.

In solutions at a given temperature and volume, the ideal gas law relation between partial pressure and nodal content leads to a simple calculation of free energy differences. If there are two solutions with solutes in different concentrations, the partial pressure of the solute will be higher in one. If the concentrations are made equal by adding to the more concentrated solution some more solvent at the same temperature and pressure (therefore with the same specific internal energy), the solute molecules spread into this additional volume and do work equal to

$$\int_{V_1}^{V_2} P\,dV = \int_{V_1}^{V_2} RT\,\frac{dV}{V} = RT \ln \frac{V_2}{V_1}$$

per mole, where V_1 is the initial volume and V_2 the final one. Since the amount of solute is unchanged in this 'thought-experiment', the ratio of the volumes is equal to the inverse ratio of the concentrations, so that the work done is also expressed by

$$RT \ln \frac{[A]_1}{[A]_2} \quad , \qquad (5)$$

where [A] is the concentration of the solute concerned. In such a dilution, of course, both the specific free energy and the specific internal energy are unchanged, and entropy increases; but if the energy difference between the solutions can be exploited in some other, more reversible way, then useful energy would be derived directly from a change in specific free energy. The theoretical maximum of useful energy - the difference in potential free energy between two solutions of differing concentrations - is given by equation (5). In practice, it is found that the physicochemical behaviour of solutions is different from that predicted by the ideal gas law; but this first approximation can be made more valid by defining the 'activity' of a solute in solution by the equation

$$\Delta G = RT \ln \frac{a_1}{a_2} \quad , \qquad (6)$$

where the activity, a, is related to the concentration by an experimentally determined 'activity coefficient', λ. For very dilute solutions, λ approaches 1, so that equation (5) can be used effectively; it is found empirically that this is sufficient for the biological electrolyte solutions of interest in mammalian muscle studies.

Electrolyte solutions, however, include changed particles;

therefore some or all of the free energy can be manifested as electrical energy. The particular case of interest here is one in which two solutions of differing concentrations and compositions are separated by a semi-permeable barrier, or membrane. In this case there are two forces at work to lower the free energy of the system: in addition to the concentration gradient at the boundary tending to cause transfer of material, there is an electric force which may assist or oppose this. There is also a resistance to movement of the particles, caused by interactions of solvent and solute, which may differ for each species of molecule involved. The force on a charged particle is related to its velocity of movement along the potential gradient by the equations

$$v = -\mu \frac{\partial V}{\partial x}, \quad \text{and (force per unit charge)} = -\frac{\partial V}{\partial x}, \qquad (7)$$

where μ is the 'mobility' and V the electrical potential difference. Since there is a charge $zN_0e = zF$ coulombs per mole of fully- dissociated ions of sign and valence z (N_0 is Avogadro's number), the resistance to movement may be expressed as

$$\frac{\text{(force per mole)}}{\text{velocity}} = \frac{zF}{\mu} \quad .$$

It is a general rule that force is the negative of the gradient of potential energy (any sort), and since the potential energy of the solute arising solely from its concentration is its free energy G, then the related force causing diffusion across the boundary is $-\frac{\partial G}{\partial x}$. The amount of free energy must always be referred to some arbitrary state, which is by convention taken as a concentration of

unity; it therefore follows from equation (6) that $G = RT \ln a = RT \ln \lambda [A]$, and

$$\frac{\partial G}{\partial x} = RT \frac{\partial}{\partial x} \ln [A] \qquad (8)$$

for a dilute solution. Since the frictional force opposing the motion of the particles will be the same regardless of the type of force applied, equations (7) and (8) may be combined to give the net velocity of diffusion for any ion species A as

$$v = -\mu \frac{\partial V}{\partial x} - \frac{\mu}{zF} RT \frac{\partial}{\partial x} \ln [A] \quad . \qquad (9)$$

The total flux of positive ions (velocity x concentration) must be equal to that of the negative ions by the condition of electrical neutrality in a conductor:

$$\Sigma M_+ v_+ = \Sigma M_- v_- \quad , \qquad (10)$$

where M represents concentration. A very slight increase in the relative number of ions of one sign on either side of the boundary increases the attractive force on those of the other sign, ensuring that equation (10) holds after the first instant. This slight imbalance manifests itself as a potential difference across the boundary. For the particular case of two similar electrolyte solutions of differing concentrations separated byaa boundary layer impermeant to one of the ions, the net velocity of the permeant ion at equilibrium must be zero; therefore integration of equation (9) across the boundary gives

$$V_c - V_d = \Delta V = -\frac{RT}{zF} \ln \frac{[A]_c}{[A]_d} \quad , \qquad (11)$$

where the subscripts c and d indicate the concentrated and dilute solutions. This is known as the Nernst equation.

1.46 Approximations and assumptions

The only requirement placed on the boundary in deriving the Nernst equation is that the free energy and electric potential are continuous across it, and hence differentiable; this will always be so in a real situation, although it is possible for the transition regions to be very sharp. If there is more than one permeant ion, the calculation of the equilibrium potential becomes more difficult, for the mobilities of the ions become factors; and where ions of positive and negative charge are both permeant, equation (10) must be satisfied. Moreover, if the boundary between the two electrolyte solutions is a layer of some <u>different</u> material (a membrane), then equation (9) will yield a different particle velocity for each phase according to the value of each μ therein; and equations (10) and (11) must be applied to each interface using some known relation to express the electrolyte concentration just inside the membrane surfaces (usually these are related to the external concentrations by a constant, the partition coefficient). In this case, the electrical potential difference between electrolyte solutions is the sum of the diffusion potentials at each interface plus the resistive potential drop in the membrane itself if currents flow. Still another complicating factor arises from the presence of impermeant ions: such a situation implies that there can be no equilibrium state for a passive system, since equation (11) indicates that the required boundary potential would be infinite if

one of the concentrations were zero. Therefore the fact that biological cells are observed to maintain a steady trans-membrane potential, although containing impermeant ions (e.g. proteins) and several permeant ions with different equilibrium potentials when considered separately, indicates that these systems are not passive. Instead, some active process is 'pumping' at least one of the ions so as to maintain a steady state wherein the net current across the membrane is zero despite a flux of each of the permeant ions. Excitable cell membranes are also observed to exhibit time and voltage-dependent changes in resistance to ion flow or excitation, and the resultant changes in ion fluxes will be superimposed on the 'steady-state' ones. Obviously the real system can be approximated only, if a workable method of theoretical analysis is to be obtained; the approximations initially tried, and the resultant predictions, will be outlined below (Goldman, 1943; Hodgkin & Katz, 1949).

Where several ion species are present, there exists the possibility that each will affect the physical and electrical properties of the others; such interrelations, even if understood, would cause the components of equation (10) to assume a form which cannot be solved satisfactorily, if at all. Therefore, the first approximation desirable is

(1) All the properties of each individual ion species remain independent of the concentrations of the other ions in solution. This means that each type of ion will have an equilibrium configuration: its net flux will be zero when the boundary potential reaches a characteristic, concentration-dependent value. Furthermore, as outlined

in Section 1.1, biological cells behave as if bounded by a membrane, and observations with the electron microscope have revealed one. Therefore, all considerations from here will follow widely-accepted practice in assuming the existence of a membrane phase separating the two electrolyte solutions (an alternative view is reviewed by Troshin, 1964). Two more useful approximations are, then,

(2) The concentration of an ion immediately inside the membrane surface is a constant function (β) of its external concentration.

(3) The membrane is homogeneous throughout.

The important point in (2), the 'independence principle', is that β is a constant: that is, it is unaffected by any applied influences such as voltage, and is the same on both sides of the membrane. The result of this condition is that the diffusion potential at each boundary is equal and opposite, so that the trans-membrane equilibrium potential (that required to balance the concentration free energy and make $v = o$ in equation (9)) is given by equation (11) and is continuous from one electrolyte solution to the other. The justification for this is found only in comparison with experimental results. That (3) is morphologically incorrect is readily seen from good electron micrographs; the homogeneity condition as a first approximation is also only empirically justified.

The method of movement of the ions through the membrane must be specified in any model. The first and most obvious approximation here is to assume,

(4) The behaviour of the ions inside the membrane is analogous to that in aqueous solution. This requires that they move

according to the ordinary laws of diffusion under any applied force.

Since the trans-membrane potential of a cell is unlikely to by the equilibrium potential for many of the ions in solution within and outside it, it is necessary to describe the membrane electrical behaviour in terms of currents flowing through it at any given potential difference; the dynamic equilibrium potentials will then be ones at which the net current flowing is zero. The current is given by multiplying the flux by the amount of charge per mole, so that

$$I = \Sigma I_A = \Sigma z_A F [A] \upsilon_A \quad , \qquad (12)$$

where I is the net current, A the ion species involved, and υ is given by equation (9). By the use of the independence principle and equation (9), then, the current I_A may be expressed as

$$I_A = - \mu_A z_A F [A] \left(\frac{\partial V}{\partial x} + \frac{RT}{z_A F} \frac{\partial}{\partial x} \ln [A] \right) ; \qquad (13)$$

and I_A is itself a constant, as there can be no significant current sources or sinks in the membrane.

In order to solve this equation for the current in terms of the internal and external concentrations, the spatial dependence of the electric potential V within the membrane must be given. Such a profile cannot be measured directly by any known technique, and further assumptions about the molecular structure of the membrane must be made in order to predict it. In keeping with the assumption of membrane homogeneity, then, the fifth and final fundamental approximation in this analysis is

(5) The electric field, $-\frac{\partial V}{\partial x}$, within the membrane is constant. Then equation (13) gives

$$I_A = P_A \frac{z_A e_m F^2}{RT} \frac{[A]_o - [A]_i \exp \frac{z_A F e_m}{RT}}{1 - \exp \frac{z_A F e_m}{RT}} \quad , \qquad (14)$$

where the 'constant-field permeability', P_A, of a membrane of thickness x is given by

$$P_A = \frac{\mu_A \beta_A RT}{xF} \quad .$$

The independence principle implies that the electromotive force for any ionic current is the difference between the membrane potential and the equilibrium potential for that ion; and current is proportional to e.m.f. The fundamental variable, therefore, is the relation between e.m.f. and current, not membrane potential and current; and this 'conductance', g, is defined by

$$I_A = g_A (e_M - E_A) \quad . \qquad (15)$$

This value of the conductance, which can be obtained as a function of membrane and equilibrium potentials from equation (14), is valid only when a steady state has been reached :

$$g_A = \frac{\partial I_A}{\partial e} = \frac{P_A z_A F^2}{RT} \frac{[A]_o - [A]_i \exp \frac{z_A F e}{RT}}{1 - \exp \frac{z_A F e}{RT}} - \frac{P_A z_A^2 F^3 e}{R^2 T^2} \frac{[A]_i \exp \frac{z_A F e}{RT}}{1 - \exp \frac{z_A F e}{RT}} +$$

$$\frac{P_A z_A^2 F^3 e}{R^2 T^2} \frac{[A]_o - [A]_i \exp \frac{z_A F e}{RT}}{\left[1 - \exp \frac{z_A F e}{RT}\right]^2} \exp \frac{z_A F e}{RT} \quad . \qquad (16)$$

On the other hand, it is by no means usual for an excitable cell to be in a steady state. Time-dependent changes in g cannot be predicted from this constant-field analysis. The electrophysiological study of excitable cells includes experimental measurements of the time-dependent conductance changes as well as voltage-dependent ones; an empirical mathematical model of the results can then be used to check the assumptions made above, and to suggest some for a theoretical treatment of time dependence.

1.4c The Hodgkin-Huxley Equations

Hodgkin & Huxley (& Katz, 1952; 1952a-d) conducted experiments on the giant axon of the squid, using an electronic feedback technique to control the potential of the entire axon membrane ('voltage-clamping'). By varying the concentrations of ions in the external medium, they were able to analyse the currents flowing through the mebrane into components attributable to various ions, and obtain measurements of their time and voltage dependences. With a.c. frequency and phase angle measurements, Cole & Curtis (1939) had shown that the squid axon membrane behaved electrically like a parallel resistance and capacitance. Hodgkin & Huxley treated their results on the basis of this analysis, assuming a lumped pure capacitance in parallel with an e.m.f.-resistance branch for each ion contributing to the total membrane current: the circuit is shown in Figure 2. Because the membrane potential was held constant between changes, the capacitive current disappeared rapidly, and could be measured and subtracted from the records.

The ionic currents were assumed to obey equation (15). Currents of ions other than K and N_a were found to be of little import-

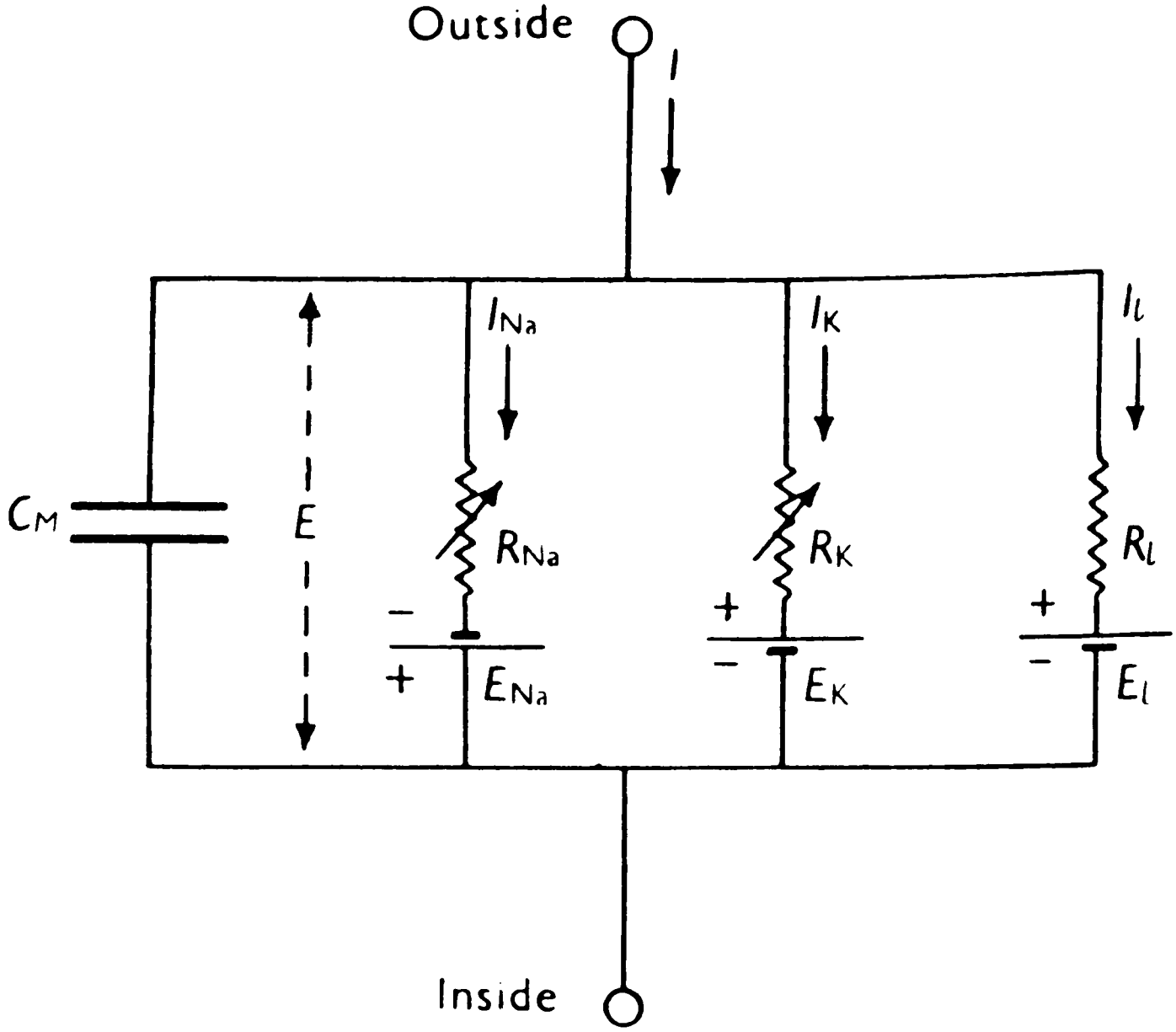


Figure 2 : Hodgkin & Huxley's equivalent membrane circuit. Modern convention is to regard the outside as the reference level, and positive currents as flowing outward. From Hodgkin & Huxley (1952d).

ance in determining the electrical behaviour, and so they were ignored. Although the values of g_K and g_{Na} were found to be constant immediately following instantaneous changes in membrane potential, both thereafter showed a very marked time and voltage dependence. The maximum value of each conductance depended on the membrane potential; and whereas g_{Na} rose rapidly to its maximum value and then declined, g_K rose much more slowly to its maximum and remained there for the duration of the depolarization. Moreover, the rates of rise and fall were dependent on the magnitude of the conductance just before the change; and also on the value of the membrane potential during the clamp, even beyond the level of depolarization where the conductances had attained an absolute maximum. Thus the conductances were not constant, as predicted by equation (16); rather, they exhibited not only a voltage dependence, but also a time dependence with voltage-dependent rates.

That the conductances (permeabilities) varied with membrane potential and not current became obvious when the membrane was clamped beyond the equilibrium potential for Na or K; the resultant current reversal left the conductance changes unaffected. This suggested to Hodgkin & Huxley that charged elements in the membrane moved under the influence of the electric field and affected the ionic permeabilities. They assumed that these elements could take an 'open' or a 'closed' position at the simplest form of self-limiting rate (e.g., as found for ordinary chemical reactions); if n is the proportion in the open position (and therefore 1 - n the proportion closed), then the time dependence is given by

$$\frac{dn}{dt} = a_n n - b_n (1 - n) \quad , \qquad (17)$$

where a_n and b_n are rate-governing 'constants' - which can themselves be dependent on voltage. The experiments indicated that g_{Na} could be described by two variables of this type changing in opposite directions with voltage and at different rates, but that one would suffice for g_K. The solution of equation (17) is an exponential with the rate of change and the final value dependent on a_n, b_n, and the initial value :

$$n = n_\infty - (n_\infty - n_o) \exp((-a_n - b_n)t) \text{ and } n_\infty = \frac{a_n}{a_n + b_n} \quad . \quad (18)$$

The potassium conductance g_K was assumed proportional to n; then a suitable power of this was chosen to fit the time-dependence of n from equations (18) to that measured experimentally on changing the membrane potential in a step-wise fashion. The best fit, which accounted for the observed delay in the increase of g_K after depolarization, was given by a fourth power. The sodium conductance parameters, m and h, were chosen to control respectively the onset and decline of g_{Na}; and the actual time course was best fit when m was raised to the third power. Thus, the conductances were expressed as

$$g_K = \overline{g_K}\, n^4 \quad \text{and} \quad g_{Na} = \overline{g_{Na}}\, m^3 h \quad . \quad (19)$$

The rate constants determining m, n and h were described by purely empirical exponential functions, and the scaling factors $\overline{g_K}$ and $\overline{g_{Na}}$ were also empirically determined.

The currents in Figure 2 obey the following equation :

$$I_m = C_m \frac{de}{dt} + \overline{g_K} n^4 (e - E_K) + \overline{g_{Na}}\, m^3 h\, (e - E_{Na}) + \overline{g_L}\, (e - E_L) \quad , \quad (20)$$

where g_L is the leakage conductance to other ions with a collective equilibrium potential of E_L, and is assumed constant; I_m is the total current flowing through the membrane. With uniform polarization, any current leaving the cell from one part of the membrane must complete its circuit by returning through another part of the membrane with the same conductance and e.m.f. as the first; clearly, then, this current I_m must be zero. (For non-uniform polarization of the membrane, different parts will have different e.m.f's, and currents will flow between them: in this case the net current leaving any one part of the membrane need not be zero, but is related to that at the other parts by equations describing currents in a leaky conducting cable). Numerical solution of this equation gave good quantitative approximations to the action potential, and varying the parameters describing the membrane produced facsimiles of many other phenomena seen in various experimental situations; by applying the cable equation, conduction velocities and excitability phenomena could also be adequately described.

1.4d Modifications for Cardiac Muscle

The excitable membrane of cardiac muscle, while exhibiting an analogous electrical behaviour to that of squid nerve, has nevertheless several significant distinguishing differences. The most obvious of these is the time dependence; whereas the nerve action potential is complete in a few msec, that of cardiac muscle has a duration of several hundred msec. After an initial fast sodium conductance change, a 'plateau' occurs where the repolarization is greatly slowed; the

length of the action potential is governed mainly by this plateau, which is followed by a fairly rapid repolarization. In some cardiac cells, notably the pacemaker and Purkinje cells, the fast repolarization is followed by a slow depolarization until the threshold for the next initiation of an action potential is reached, and automaticity is thereby established. Moreover, whereas the nerve membrane impedance falls during the action potential, that of cardiac muscle increases during the plateau. Clearly then, the Hodgkin-Huxley equations required modification if they were to apply to cardiac muscle membranes; Noble, in 1962, published the first such modified equations, adapted to describe qualitatively the active electrical behaviour of the cardiac Purkinje fibre. He introduced a breakdown of the potassium conductance into two components, one (g_{K1}) generating an instantaneous depolarization-induced decrease in conductance, or 'anomalous rectification' (anomalous because opposite in direction to the constant-field predictions), and the other (g_{K2}) analogous to the Hodgkin-Huxley potassium-conductance function - but with rate constants reduced by a factor of 100. Sodium conductance was assumed to obey the same functions as in the Hodgkin-Huxley analysis, except for the addition of a very small constant term unlikely to affect the results (it was added for computational convenience). The scaling constants for all these functions were chosen to agree with the limited amount of data then available, most of it from constant-current analysis; since information on fast g_{Na}-changes was completely lacking, the rate constants governing m were chosen on a purely mathematical basis so that equation (20) could generate action potentials. Solution of this

equation by electronic computer then reproduced quite faithfully most of the electrical phenomena of cardiac muscle then known to occur.

1.5 AIMS OF THE PRESENT STUDY

The work on the cardiac Purkinje fibre which forms the basis of this thesis may be conveniently divided into three parts: studies with constant trans-membrane currents, with voltage-clamping of the membrane, and with a computer-analysis of the membrane behaviour predicted by the modified Hodgkin-Huxley equations. The first two parts will describe membrane properties of this preparation, some of which have hitherto remained largely unrecognized, and certain basic experiments will suggest improved values of some of the necessary empirical constants for Noble's equations. The third part will test some of these values in the mathematical model, as well as the effects of a resistance in series with some of the membrane capacitance - as has been measured by other workers in experiments. Implications of the results will be discussed.

CHAPTER 2 EXPERIMENTS WITH CONSTANT CURRENTS

The first series of experiments (begun in the latter part of 1964) included investigations with intracellular microelectrodes of the effects of passing constant-current pulses of varying amplitude, duration, and configuration. The concentrations of ions in the external medium were maintained at desired values, and temperature was controlled throughout the experiments.

2.1 METHODS

2.1a The Preparation

Sheep hearts were obtained from either of two local abattoirs at the time of their normal slaughtering operations, usually near 8.00 a.m. At one abattoir, the sheep were initially stunned with a bolt fired through the skull, then allowed to bleed freely from the opened throat (in a prone position). As soon as bleeding ceased, the animal's chest was opened and the heart immediately excised, very often still beating regularly. At the other abattoir, the animals were first suspended by the hind legs, and allowed to bleed from the opened throat without previous stunning; they were then skinned and eviscerated in the normal fashion, and the heart subsequently excised. In either case, immediately after being received, the heart was placed in a large vacuum flask containing one to two litres of oxygenated, ice-cold Tyrode solution (Table 1,A); often the left auricle and ventricle were carefully opened at this stage to allow free entry of

the Tyrode solution and prevent the formation of large blood clots. This part of the operation was completed within 2-3 min or 10-15 min of the animal's death, depending on the abattoir visited. Despite significant differences in the apparent condition and handling of the hearts from the two sources, the condition of the Purkinje fibres showed very little variation between sources: if more viable preparations were obtained from one, it was from the second-mentioned above. A much more definite correlation was obtained between preparation viability and time of year; in three successive years, the period from mid-January to the end of March (perhaps related to the lambing period) saw a long series of hearts with Purkinje fibres showing little electrical activity and having connective tissue sheaths so thick and tough as to be often impregnable with microelectrodes.

The hearts were removed to the laboratory as soon as possible, usually within a quarter-hour. They were dissected under Tyrode solution at normal room temperature (about 20°C), and on warming it was not uncommon to find a resumption of normal beating of the whole heart. The left ventricle was usually found to contain well over a dozen Purkinje fibre bundles, extending between areas of the ventricular wall and often branching extensively; diameters varied from about 0.25 to 1.0 mm or larger. Straight sections of these were selected, usually about 0.5 mm in diameter, and a length of about 1.5-2 mm was excised with fine scissors; these were then picked up with some solution in a pipette and transferred to fresh, oxygenated Tyrode solution at a controlled temperature of 35°C, where they were kept until required for the experiment. Subsequent observations led to the belief that,

in order to obtain preparations with good electrical activity, an hour or more should be allowed to elapse before proceeding with the experiment; this may have been because the complete healing-over of the cut ends was being achieved slowly.

2.1b The Bath+Superfusion Apparatus

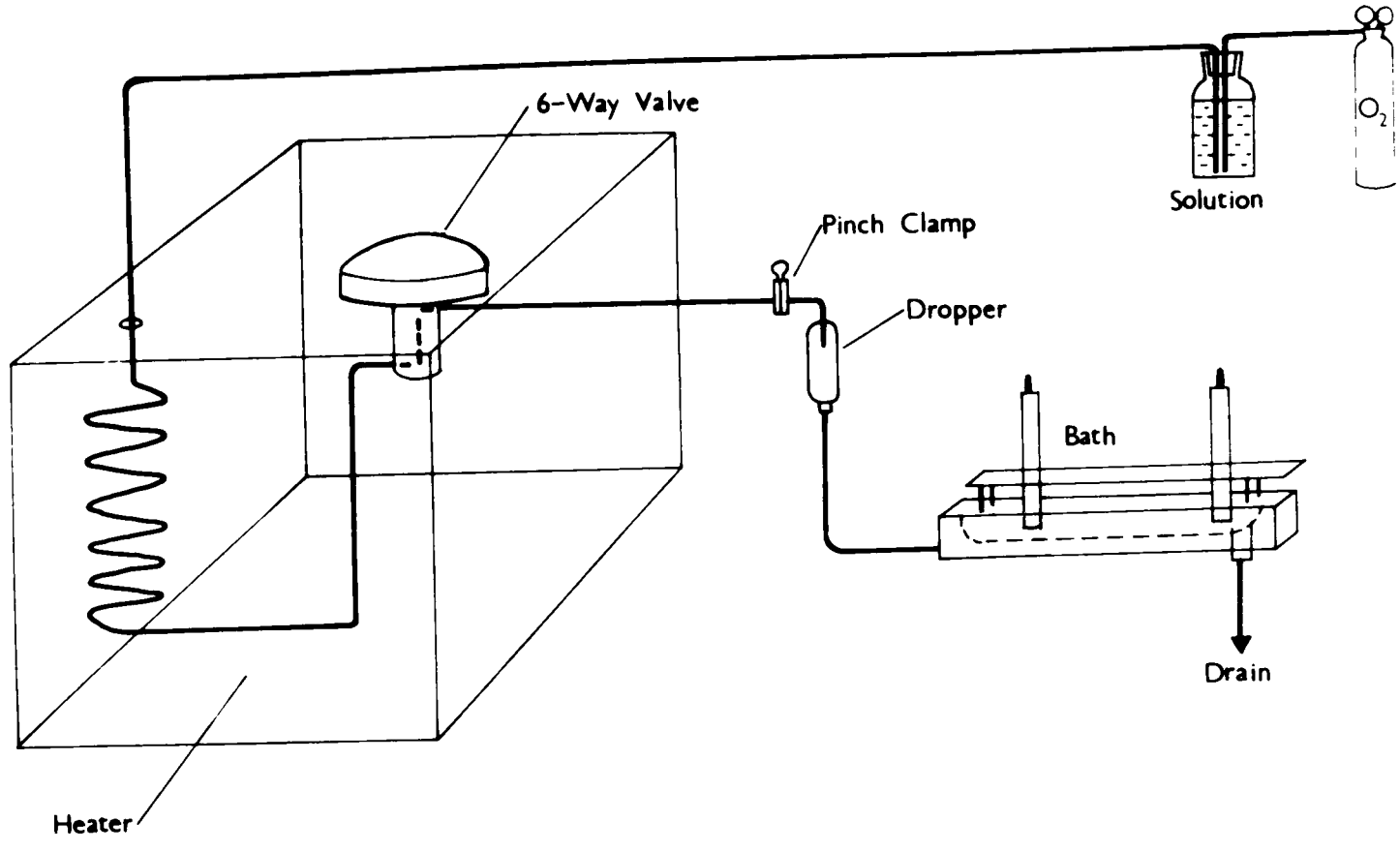
The compositions of the various solutions which bathed the fibre are detailed in Table 1. These were prepared within twelve hours previous to the experiment and stored in a refrigerator at 0-5°C in 2-litre glass jars. During an experiment, up to six of these jars were situated near the fibre bath and fitted with rubber stoppers connected by rubber tubing to the regulator of an oxygen cylinder. Oxygen pressure slightly above atmospheric was applied, both to ensure good oxygenation of the solutions and to force them along a second set of tubes towards the bath. Figure 3 illustrates the arrangement. These led to a set of six glass coils immersed in a water-filled constant-temperature bath, where the solutions were heated to the desired temperature as indicated by a thermocouple in the bath beside the preparation; in practice the temperature of the solutions dropped by only a few degrees between heater and fibre, and the temperature of the heater was therefore normally at about 44°C. The fluid path from each jar of solution was separate until reaching the outlet from the heater; here a rotary valve allowed switching any one of the six circuits to the outlet tube leading to the fibre bath. The rate of flow was controlled by a screw-adjustable pinch clamp above a dropper unit in the outlet tube; 1-2 drops per second was normal, except during solution changes when much higher flows could be admitted.

TABLE 1

Composition of Solutions

(Concentrations are in millimolar. All solutions contain 1 gm/ litre glucose. Distilled water was used throughout)

Solution	Na	K	Cl	Mg	Ca	HPO_4^{--}	$H_2PO_4^-$	$CH_3SO_4^-$	Choline
A	140	4	144.6	0.5	1,8	1.65	0.7	0	0
B	0	4	144.6	0.5	1.8	1.65	0.7	0	140
C	0	24	144.6	0.5	1.8	1.65	0.7	0	100
D	0	9	139.6	0.5	1.8	1.65	0.7	5	135
E	0	14	134.6	0.5	1.8	1.65	0.7	10	130
F	0	19	129.6	0.5	1.8	1.65	0.7	15	125
G	0	24	124.6	0.5	1.8	1.65	0.7	20	120
H	0	29	119.6	0.5	1.8	1.65	0.7	25	115
I	0	34	114.6	0.5	1.8	1.65	0.7	30	110
J	0	100	48.6	0.5	1.8	1.65	0.7	96	44
K	0	100	144.6	0.5	1.8	1.65	0.7	0	44
L	0	16	144.6	0.5	1.8	1.65	0.7	0	128
M	0	10	144.6	0.5	1.8	1.65	0.7	0	134



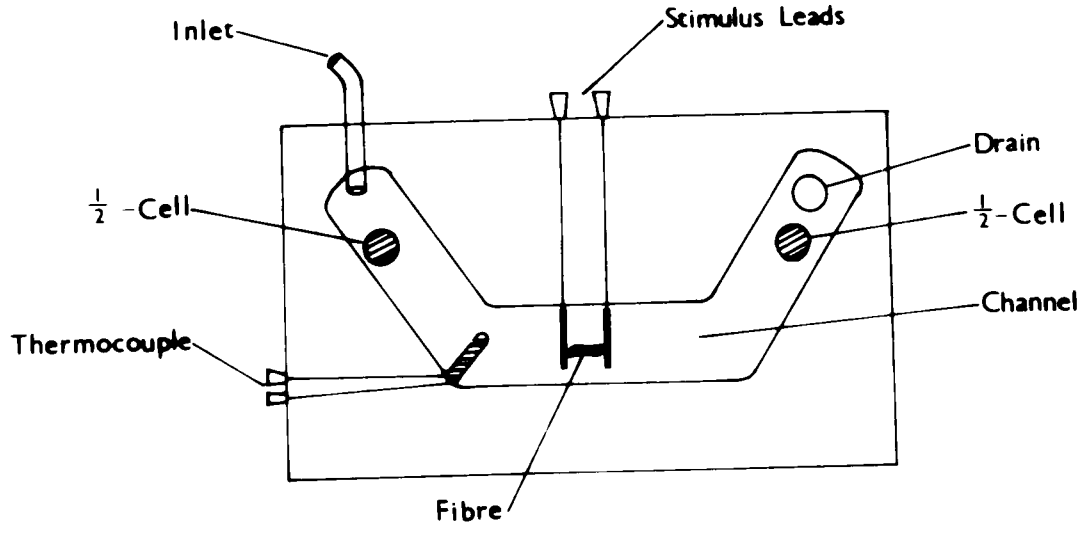


Figure 3 : Top : general arrangement of the superfusion apparatus.
Below : a top view of the fibre bath.

The fibre bath consisted of a ¼" deep channel machined into a 3" x 5" block of Perspex, as shown in the lower part of Figure 3. The fresh solution entered at the left, travelled along the channel past the thermocouple, around and over the fibre in the middle of the bath, and drained by gravity at the right end of the channel. The copper-constantan thermocouple wires were isolated from the solution by a thin-walled glass sheath. In the centre of the bath, beneath the fibre, were two silver wires ½ cm apart; these were used to stimulate the fibre for the initiation of action potentials when required. Above the bath was mounted a variable-magnification (1-100X) Zeiss stereoscopic dissecting microscope, and illumination was from beneath the fibre. Micromanipulators from the Cambridge Engineering Laboratory, on the A.F. Huxley (1961) design, were rigidly mounted on the left and right of the bath; these provided micrometer movements in three dimensions, with coarse and fine motion controls allowing positioning of the microelectrode tips to within a few μ.

2.1c Electrodes

The glass microelectrodes were drawn from 6" Pyrex glass tubes of about 1 mm internal diameter and 2 mm external diameter (the tubes in any one shipment varied widely in size, and often careful selection was required in order to obtain reasonable uniformity in the end product). The puller used was constructed in the laboratory; the heating element was a Nichrome strip ¼" wide, partially encircling the glass tube which was held in place by rubber-padded screw-clamps at each end. On the pressing of a single switch, force was applied to

the movable lower stage by a solenoid arrangement, and the pre-set (variable-transformer-controlled) heater current was turned on automatically. As the tube lengthened, the lower stage tripped a microswitch at a pre-set position, which increased the pulling force, and a similar switch turned off all the circuits when the process was completed. By varying the heater current, the strength of the first pull, and the time of initiation of the second pull, considerable control could be gained over the shape of the microelectrode tips; but such control was necessarily empirical, and varied from week to week. Each pulling process produced two microelectrodes.

A sample of each batch was checked by viewing under a water-immersion microscope, at an overall magnification of about 900X; the water would enter the electrode tip and fill it to a variable extent, and trials showed that filling to the extent of about one field of view was indicative of a tip size leading to 10-20 megohm final resistance. Suitable electrodes were then mounted on a Perspex holder and immersed in 3M KCl; they were filled by first heating to boiling point, then applying vacuum so that controlled boiling occurred for 10-15 min without heating. Filled electrodes were stored in 3M KCl in darkness until use, which was preferably within not more than 24 hours to prevent excessive tip erosion or blockage. Immediately before use they were either checked for resistance electronically - 10-20 megohms was the suitable range, combining small tip size and adequate current-carrying capacity - or viewed under the water-immersion microscope to observe tip shape and presence of any obstructing air bubbles. The best microelectrodes had a uniform taper for the last 100μ to within

10-20μ of the tip, then a slight rounding followed by another uniform taper to the end (which could not be resolved optically).

The microelectrodes and the bath were connected to the external electronic circuiting via conventional Ag-AgCl non-polarizing electrodes, two in the bath and two acting as microelectrode holders. These were stored in darkness when not in use, to preserve the AgCl.

2.1d Electronic Apparatus

The stimulation, time-delay unit, and two long current pulse stimulators were as described in Kay, Phillips & Teal (1958). In addition, the following units were in use:

(a) one Tektronix 502A dual-trace oscilloscope

(b) one Shackman 35 mm oscilloscope recording camera

(c) one precision voltage calibrator, constructed from a standard cell and four chains of high-precision decade resistors, providing accurate voltage offsets of 0.1-200mV

(d) one double-sided, high impedance cathode follower, drawing a current of less than 10^{-12}A, and with an output impedance of 10K-ohms to feed the 1 megohm differential-amplifier inputs of the oscilloscope

(e) one galvanometer fed by the leads from the thermocouple in the fibre bath (in comparison with one in the constant-temperature heating bath), the system producing a deflection of 0.6cm per C degree difference

(f) one Devices 4-channel heated-stylus recorder with variable chart speeds to 10 mm/sec.

(g) four Solartron operational amplifiers.

The time delay unit, synchronized with the oscilloscope sweep, controlled the relative time of initiation of the whole-fibre stimulus (to elicit action potentials) and the constant-current pulses being passed through one of the intracellular microelectrodes. The amount of current passed was monitored on one trace of the oscilloscope, by either recording the difference in potential across a known resistance from earth in series with the circuit, or feeding this current through an operational amplifier (at virtual earth) and recording at its output. The amplitude of the current was made largely independent of membrane resistance fluctuations by inserting a very large resistance in series with the membrane. The trans-membrane potential was measured with another intracellular microelectrode; it was compared with an 'indifferent' electrode in the bathing solution via the cathode follower, and the output was passed through the voltage calibrator and on to the differential input of the other oscilloscope trace. (Because the properties of the microelectrode can change on insertion, retraction, and even because of vibration during an experiment, there is always some degree of uncertainty in the absolute measurement of membrane potential. This point should be borne in mind whenever absolute membrane potential is used in graphs). Parallel connections were run from the oscilloscope and the temperature-measuring galvanometer to the heated-stylus recorder, so that a continuous, low chart-speed record of the whole experiment was available immediately, and slow phenomena could be easily observed while objectionable high-frequency noise was filtered out with the built-in filters.

Instrumental pick-up of local 50-Hz noise was a continual problem and limited the resolution of current measurements; extensive anti-noise measures were attempted. The fibre bath was on a metal table with three shielding walls, with a working space of about 3' by 4'. All wire leads were of specially-shielded low-noise microphone cable, and earths from all shields were led to a common earthing copper strip by separate leads carefully chosen to avoid any accidental earth loops. Normally currents to 10^{-8}A could be accurately measured.

2.2 RESULTS

2.2a Current-Voltage Relations in Na-Free Solutions

When a Purkinje fibre had been impaled by both microelectrodes and showed characteristic action potentials on stimulation (they are not normally self-exciting in 4 mM K solutions), the existence of a uniform degree of polarization of all parts of the membrane was tested by passing short negative intracellular current pulses during the early part of the action potential plateau. If the fibre is long enough for the cable properties to affect the polarization, then regenerative repolarization (cut-off of the action potential) will only occur late in the plateau and with relatively high threshold (Noble & Hall, 1963). However, in every case it was found that the short preparations being used exhibited complete cut-off at a low threshold, and very early in the plateau (~~to greater than~~ after about 100 msec); it was therefore concluded that effectively uniform membrane polarization was obtained in every preparation.

Using bathing solutions with choline chloride replacing

sodium chloride to eliminate excitatory responses (B in Table 1), current-voltage relations were obtained by passing constant currents of 1-2 sec duration via one of the intracellular microelectrodes. The voltage response showed transients in onset and decay due to the membrane time constant; where required, it was possible to roughly compensate for the onset capacitive current by using measurements from the decay transient, if the initial and final levels of depolarization during the pulse were nearly equal (there is no 'break response', so the transient at the end of the current pulse is primarily due to the passive properties of the circuit only). Figure 4 shows a typical record of this part of an experiment, although the pulse duration is greater than was usual. For depolarizations to below some threshold for a particular fibre, response was constant; above that threshold, the membrane potential of several fibres was observed to decline slowly. Occasionally there were, as illustrated in Figure 5, other transient responses before the steady state was reached; these will be discussed in Section 2.2d. There were often 'forbidden zones' of membrane potential, which could be crossed in either direction by very slight changes of membrane current. Such regions of negative conductance are seen in Figures 4 and 5, and in the voltage-clamp record of Figure 6. In plotting the current-voltage relations, the measurements were taken near the end of the pulse, when a steady state was most likely. The resulting curves showed marked inward rectification for depolarizations to about -50mV; beyond this, outward rectification appeared at some more positive level. The curve labelled '4mM' in Figure 7 is an example, and the relatively small number of points in the near-vertical region is an

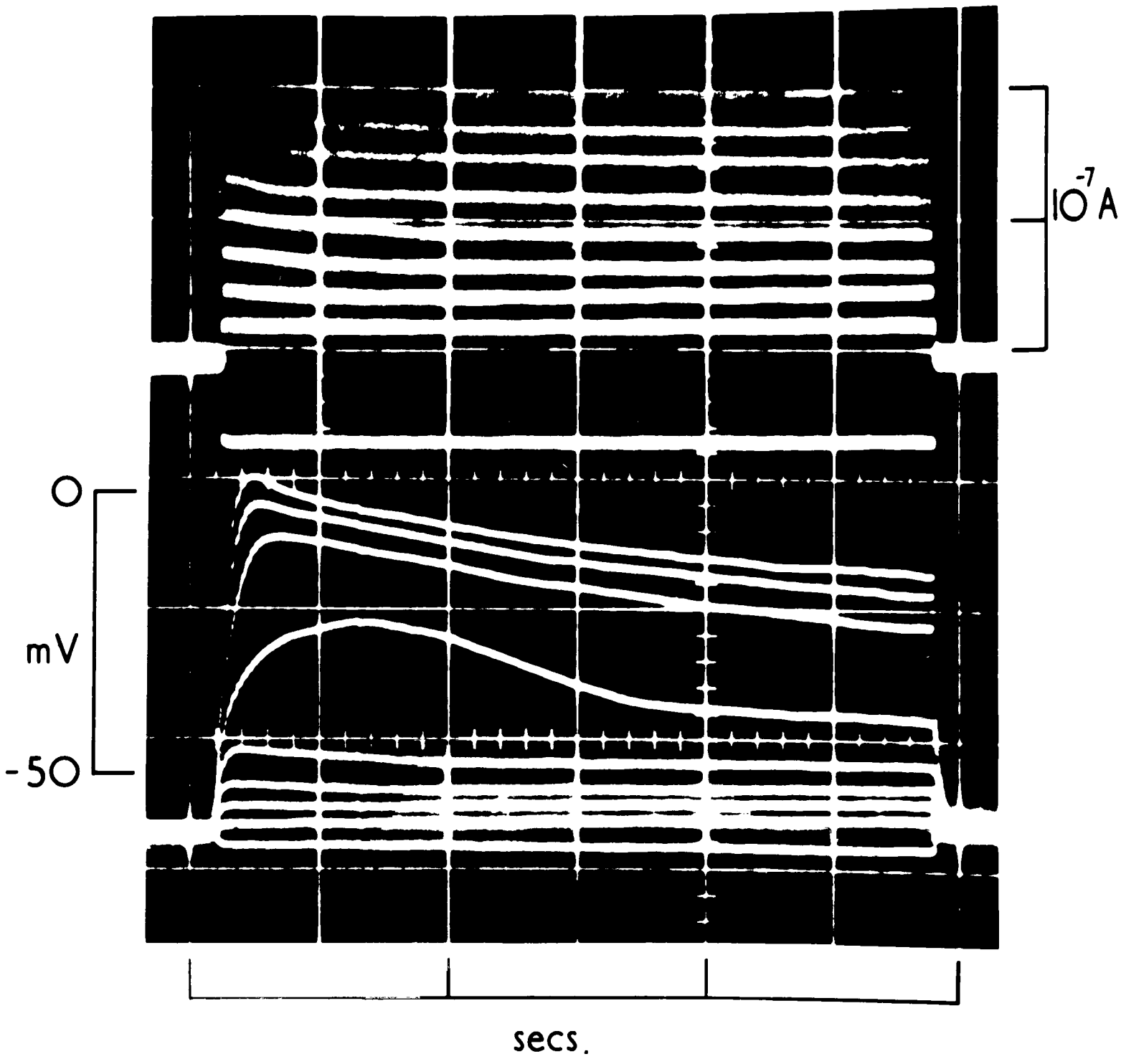


Figure 4 : Effect of depolarizing currents on a short Purkinje fibre in Na-free solution containing 24mM K. Top : superimposed records of current passed through the membrane. Bottom : superimposed records of membrane potential changes. Records as in Figure 5 were obtained before and after this exposure to high K solution.

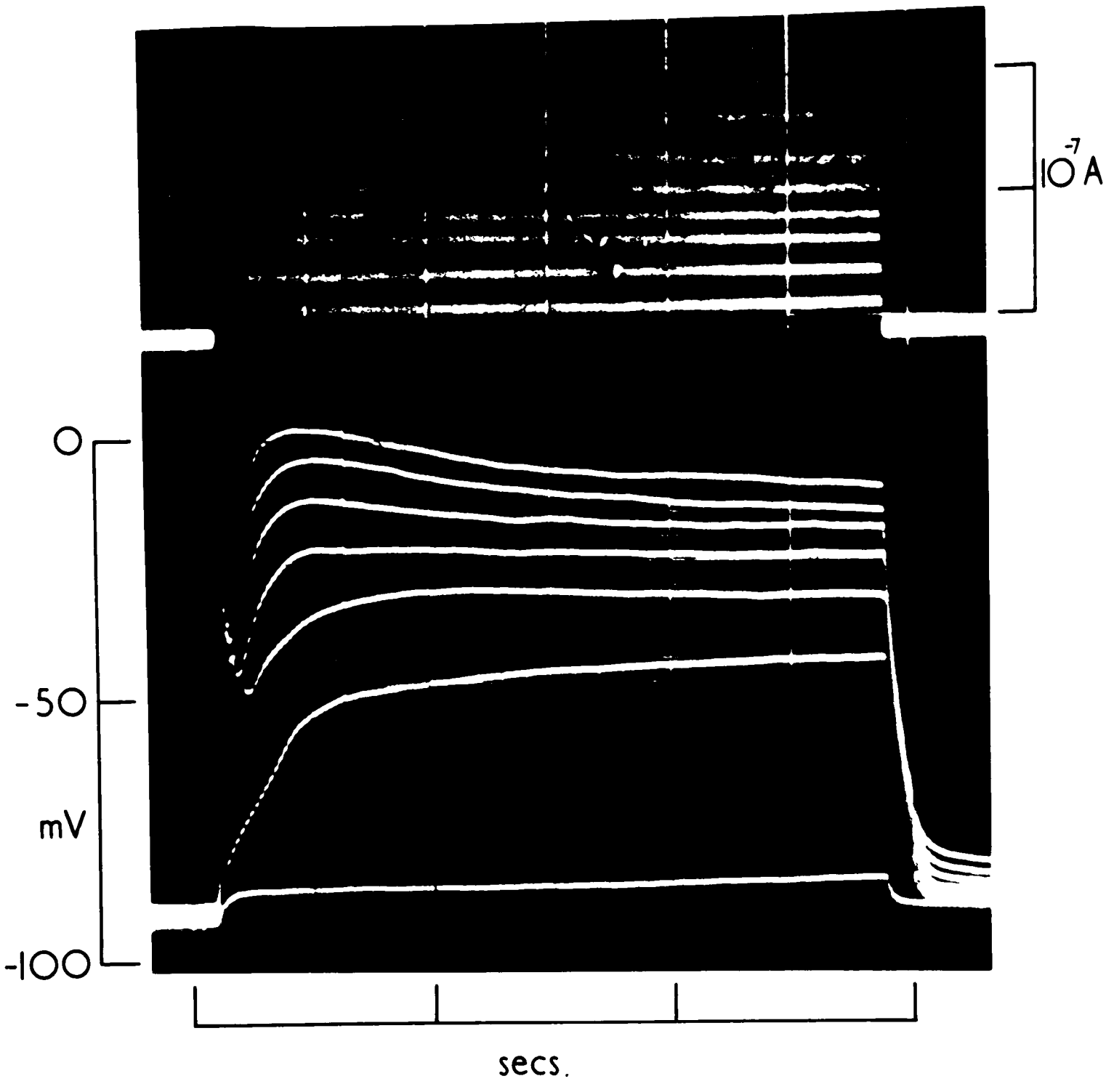


Figure 5 : Response of a short Purkinje fibre in Na-free solution to depolarizing currents. Top : superimposed records of currents passed through the membrane. Bottom : superimposed records of membrane potential changes. The fibre (the same as in Figure 4) was superfused continuously with Na-free solution containing 4mM K^{+} for over two hours before records were taken.

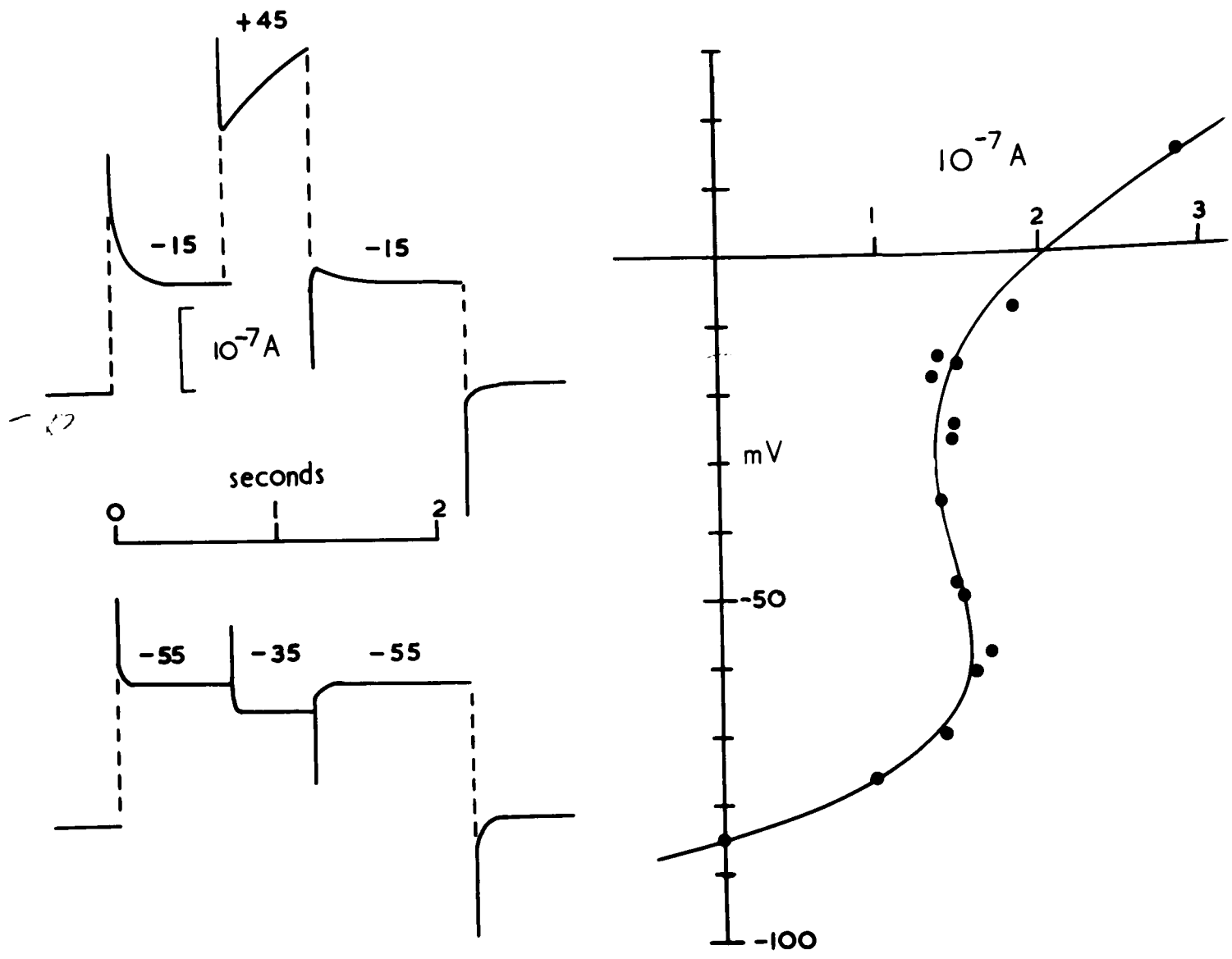


Figure 6 : Left : tracings of currents recorded in a Purkinje fibre in Na-free solution during double step changes in clamped membrane potential. Resting potential = -85mV. Potentials during steps are indicated by figures above the current records. Right : steady-state current-voltage relation, with a negative slope between -20 and -60 mV.

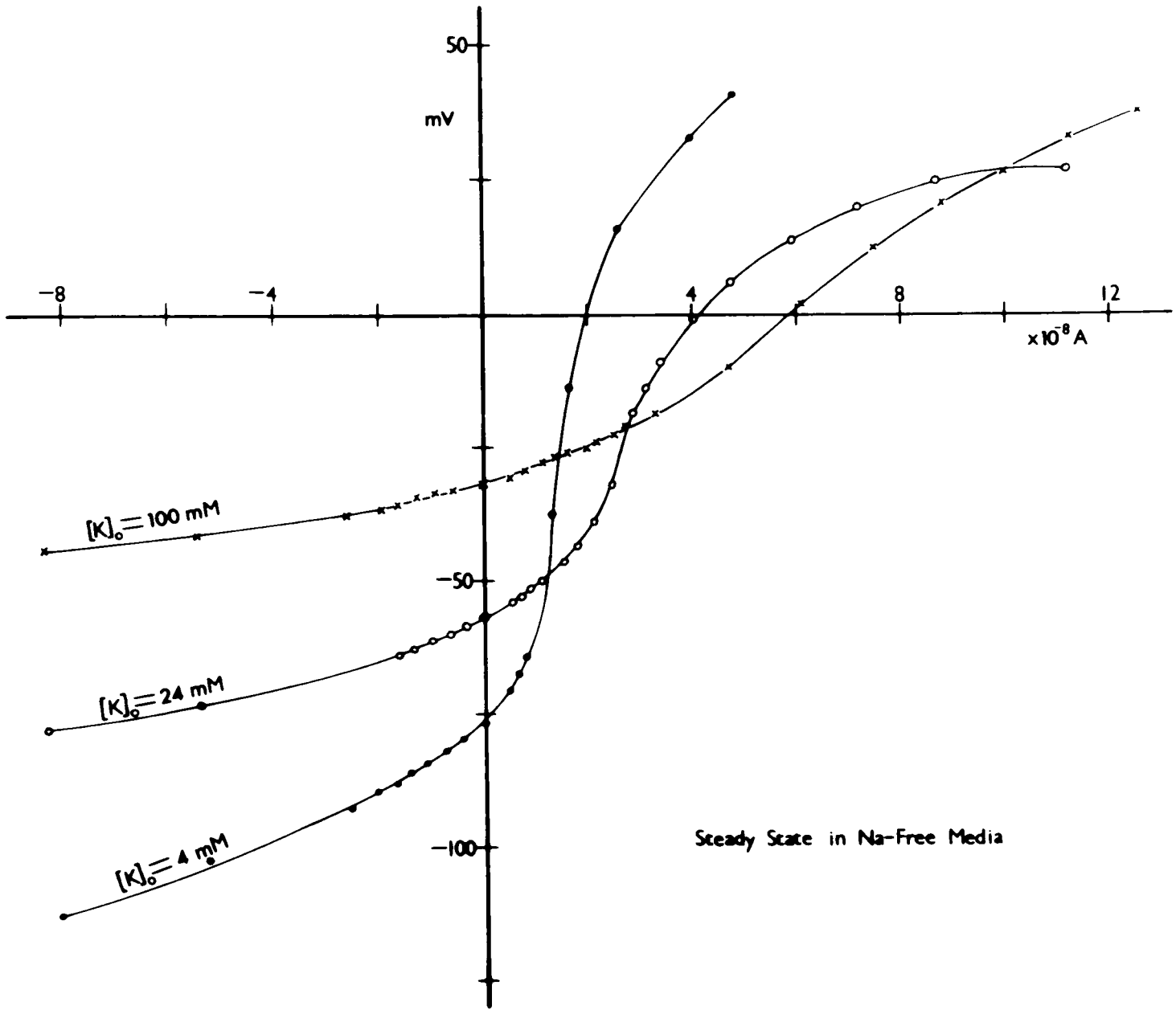


Figure 7 : Steady-state current-voltage relations in different external K concentrations, measured with long constant-current pulses. Na-free choline solutions were applied in order of increasing K-concentration.

indication that negative membrane conductance is present (a smooth curve has been drawn through the points). These steady state curves agreed with those of other workers (Hall, Hutter & Noble, 1963; Deck & Trautwein, 1964; ~~Weidmann, 1962~~), for each of the eight experiments performed.

The slow decline of the potential response to a constant current above a certain threshold is interpreted as the onset of a delayed outward rectification for potassium currents. Thus, as g_{K2} increases, the membrane potential tends to drift closer to E_K. This effect is clearly seen in Figure 8, where the applied current is increased in equal steps. The first response is small and constant; doubling of the current sends the membrane potential through a negative-conductance region to a much greater steady value; and the next two current steps both switch on a portion of the delayed rectification, so that the membrane potential declines from its peak values. The lower picture of Figure 8 shows the same effect; a doubling of the current sends the membrane beyond the threshold voltage for g_{K2}, and a slowly-declining response occurs. Moreover, g_{K2} also returns to its initial value slowly: for on return to the sub-threshold level of membrane current, the potential under-shoots and only slowly returns to its steady state value as g_{K2} declines. The equilibrium potential for the ion involved in this effect is clearly more negative than -40mV. Voltage clamp studies to be described in Section 3.2 will show that the same effect occurs at much more negative levels of membrane potential when ordinary Tyrode solution is used, and that the ion involved is certainly potassium.

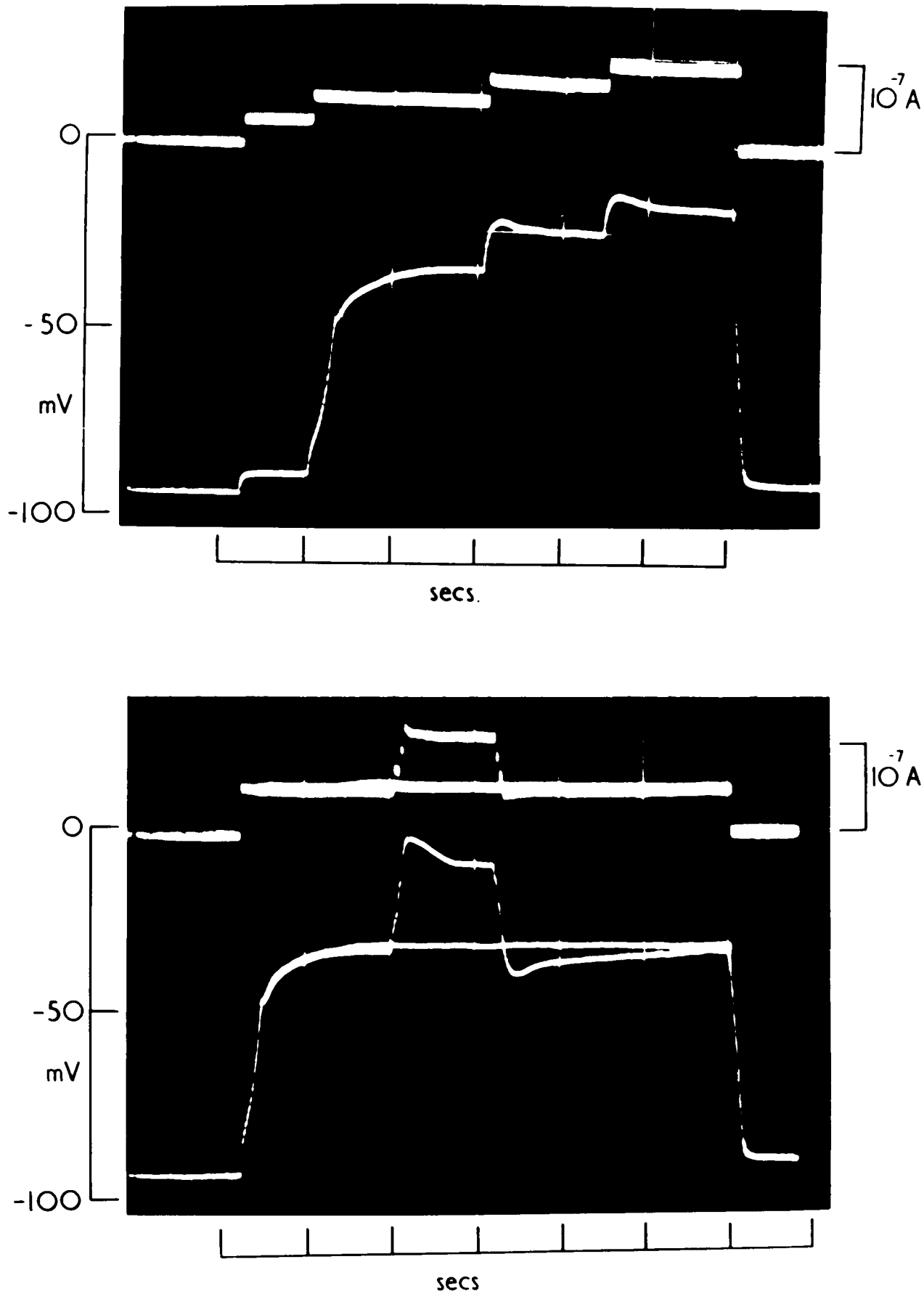


Figure 8 : Effect of a 'staircase' current on a short Purkinje fibre in Na-free solution. The current was increased in nearly equal steps and held at each value long enough for a steady state to be achieved. Membrane potential (below) increases in very unequal steps, and shows a time-dependent decrease in response to the two largest currents. Bottom: effect of a short pulse (0.06μA) superimposed on a longer pulse (0.05μA). The short pulse was produced by rapidly movingthe switch on a decade resistance so that it rises in 3 very short steps. The small change in current during the pulse only accounts for about 20% of the decline in potential.

2.2b Experiments with Increased External K Concentrations

The steady state current-voltage relations were similar to those described by an empirical equation in Noble's modification of the Hodgkin-Huxley equations. Hall, Hutter & Noble (1963) found that the magnitude of the resting-g_K change on depolarization in high $[K]_o$ was as predicted by the constant field equation (equation 16); this equation has P_K as a constant, whereas the observed anomalous rectification shows that this is not usually the case. Noble (1965) therefore assumed that, since for depolarizations in high $[K]_o$ the K-equilibrium potential changes to about the same extent as the membrane potential, the K permeability may be a function of the electrochemical potential gradient $(e-E_K)$ rather than of e alone. When this expression replaces e in his anomalous-rectification equation, the current-voltage relations predicted for different external K concentrations cross over at some potential above the resting potential, as shown in the right side of Figure 9 (from Noble, 1965). It therefore became imperative that this ad hoc hypothesis be tested by measuring these current-voltage relations experimentally.

Solutions with K concentrations ranging from 4mM to 100mM were prepared by substituting equal amounts of KCl for ChCl in the Na-free solutions (Table 1, A,B,C,K,L and M). Six experiments were carried out with external K concentrations of 4 mM and 24 mM, and similar results were obtained in every case. Figure 7 shows the results of one of these, the only one in which 100mM K was also applied. The crossover occurs as predicted by Noble's equation in $(e-E_K)$. The curves may also cross at a more positive potential. Because of a well-

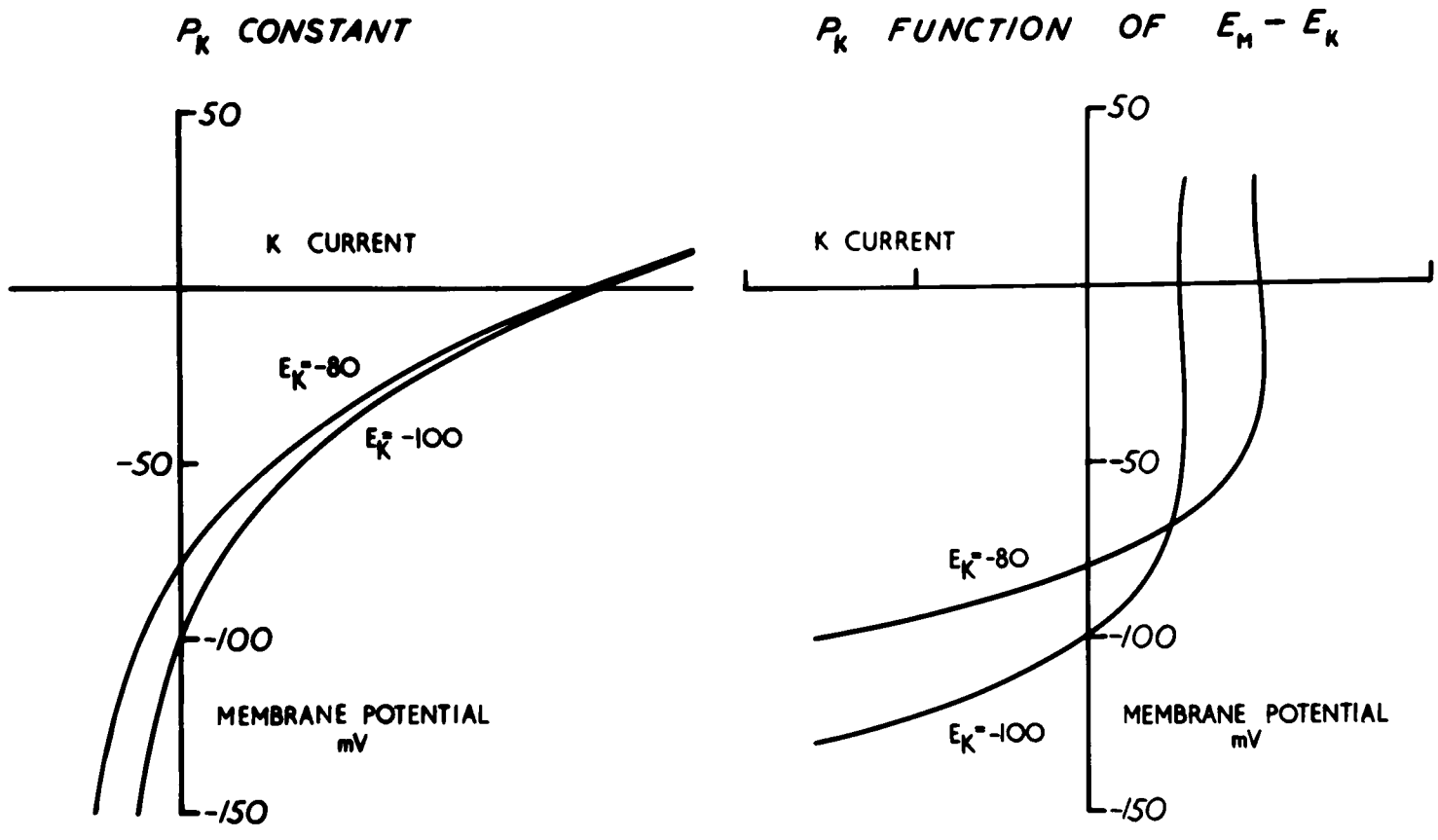


Figure 9 : Left : calculated K current-voltage relations obtained from the constant-field theory with P_K constant. The relations for E_K = -100mV and E_K = -80mV are shown; both show outward-going rectification and never cross each other. Right: calculated current-voltage relations for the same values of E_K. These relations show inward rectification and cross each other in the region of outward current.

established constant drift of baseline during this long experiment, a correction of -2mV has been added to the curve for 24mM K, and one of -12mV to that for 100mM. This fibre had been in Na-free solution for 55, 94 and 55 consecutive minutes when the 4mM, 24mM and 100mM curves (respectively) were measured.

The general shape of the current-voltage relation is unaltered except for the increase in the tangent slope of the resting potential level - the resting conductance - with higher external K concentrations. The resting conductance is plotted against membrane potential and against deflection from normal (4mM K) resting potential in Figure 10A and B. Hall & Noble (1963) found that the resting conductance dependence on external K concentration was as predicted by the constant field theory if the resting potential is assumed to be very close to the K equilibrium potential and $[K]_i$ remains constant; in this case, from equation (16),

$$\left(g_K\right)_{E_K} = P_K \frac{F^3}{(RT)^2} E_K \frac{[K]_o \quad [K]_i}{[K]_o - [K]_i} \quad . \qquad (21)$$

$[K]_i$ is determined by assuming a value for E_K in 4mM solutions (-100mV is indicated by voltage clamp measurements, and is used in these calculations). As measured in the present experiments, the ratios of resting membrane conductances in different external K concentrations has no direct dependence on either deflection from normal resting potential (Figure 10A) or on actual membrane potential (Figure 10B). In plotting the observed ratios against those predicted by equation 21

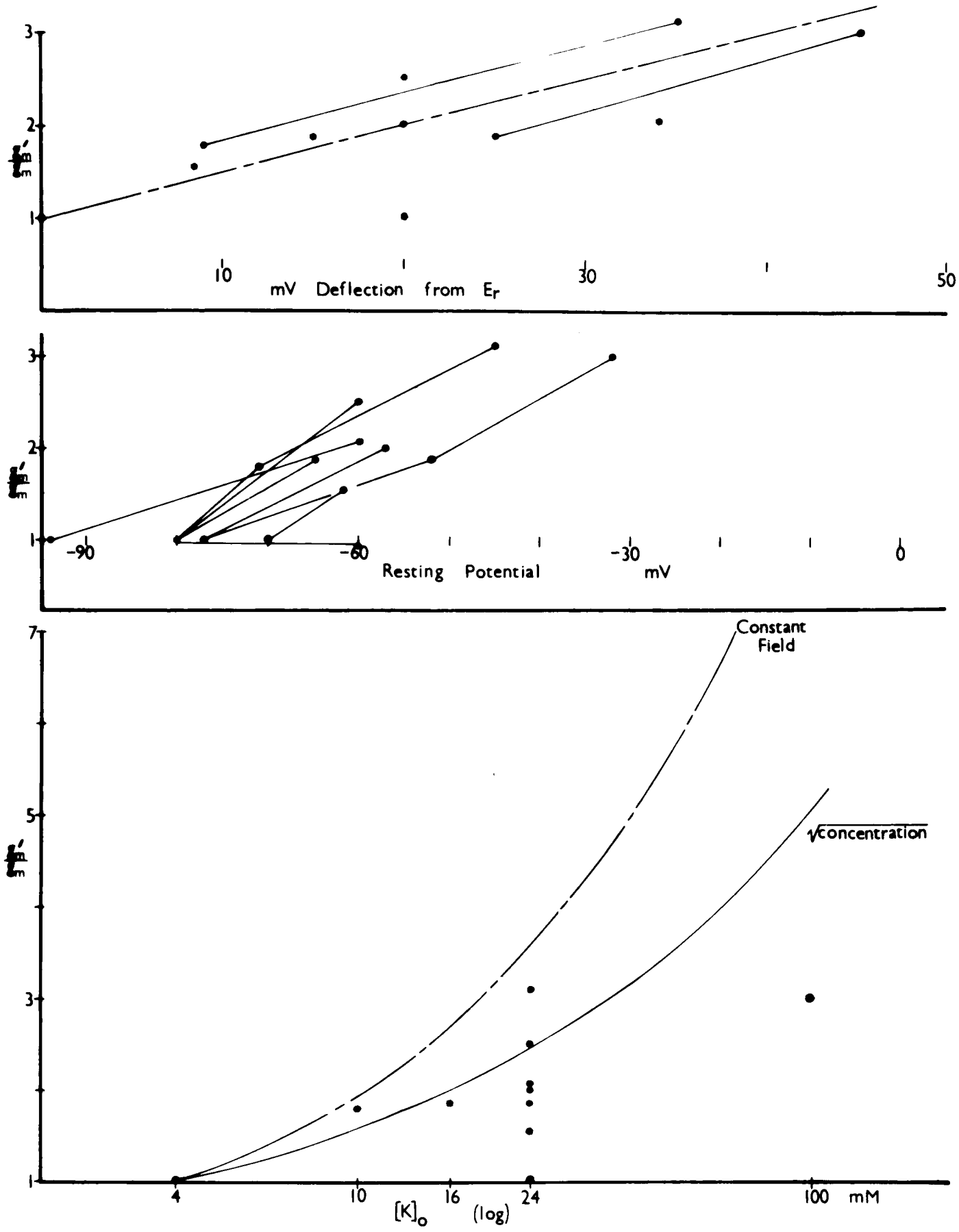
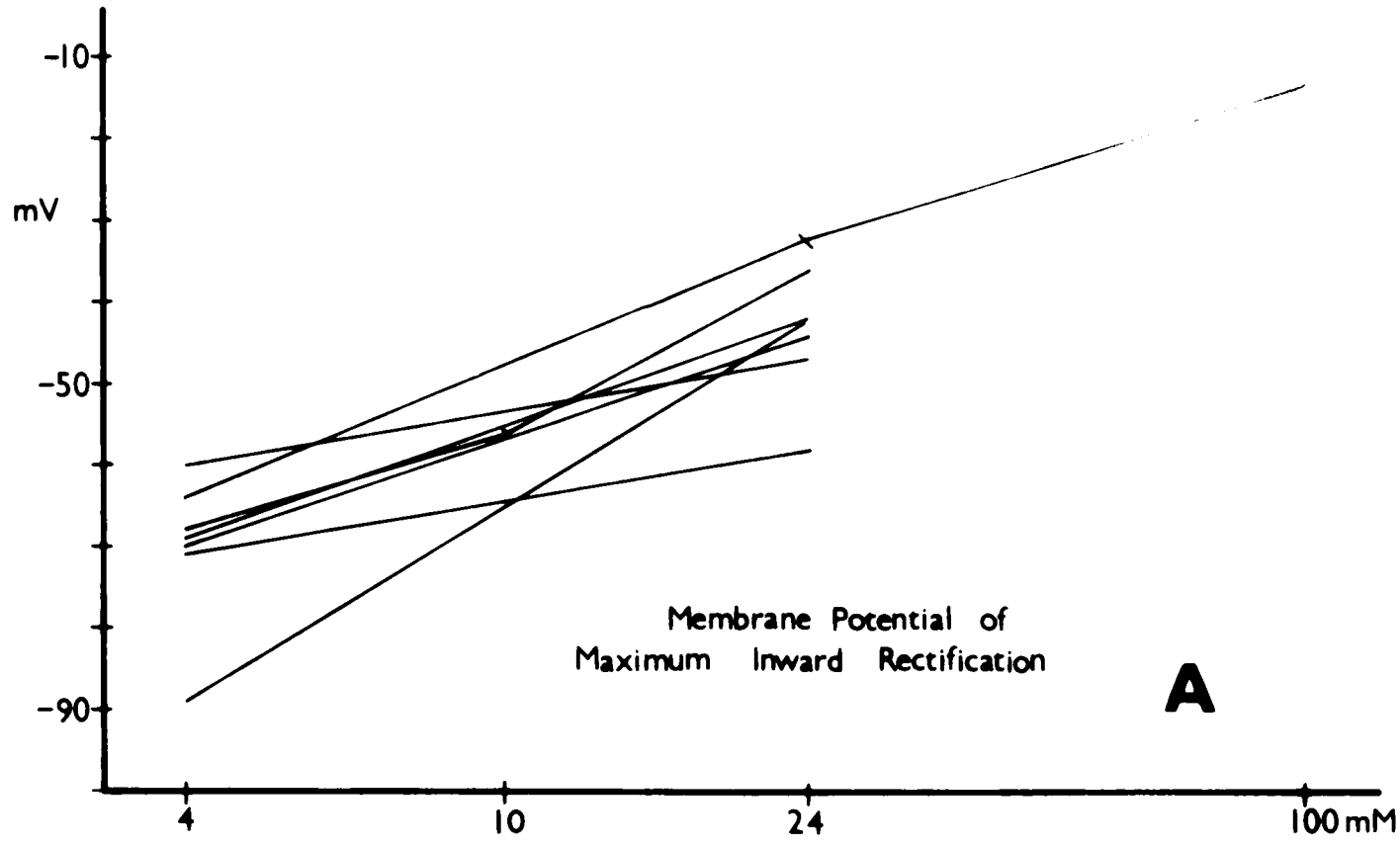


Figure 10 : Top : ratio of resting conductance in high-K solution to that in 4mM solution, plotted against shift in resting potential. Dashed line indicates trend. Centre : the same ratio plotted against resting potential in the high-K solution. In this and the top figure, lines join measurements made on the same fibre. Bottom : the same ratio plotted against log K_o. The dashed and solid curves indicate values expected according to different theories. All solutions were Na-free.

(Figure 10C), it is seen that the latter are too high; Adrian (1965) has also found this for frog skeletal muscle. Since the present experiments were not designed with these measurements given a high priority, insufficient values are available to permit accurate curves and deductions to be drawn. Noble (unpublished) has suggested a model giving rise to a conductance ratio dependent on $\sqrt{[K]_i\ [K]_o}$; the predicted values from this model are shown as a dotted line in Figure 10c.

The voltage dependence of inward rectification at various external K concentrations is given in Figure 11. The values plotted were obtained by inspections of the steady-state current-voltage relations arising from seven experiments; as reference point the point of maximum upward curvature was taken - that is, the point of maximum inward rectification. Lines join measurements made on the same fibre in different external K concentrations, and the abscissa is proportional to the logarithm of the concentration. The value of the membrane potential at which inward rectification appears is clearly concentration dependent (upper graph), whereas the deflection from resting potential required (lower graph) remains essentially constant. The deflection from resting potential approximates the electrochemical potential gradient for potassium ions.

The existence of the crossover and the inward rectification's dependence on electrochemical potential gradient give experimental confirmation to Noble's choice of voltage parameter, at least for inward rectifications. In plotting the voltage dependence of outward rectification, the only suitable reference point on the current-voltage curves was the initial point of ~~curvature~~ inflection in the outward-



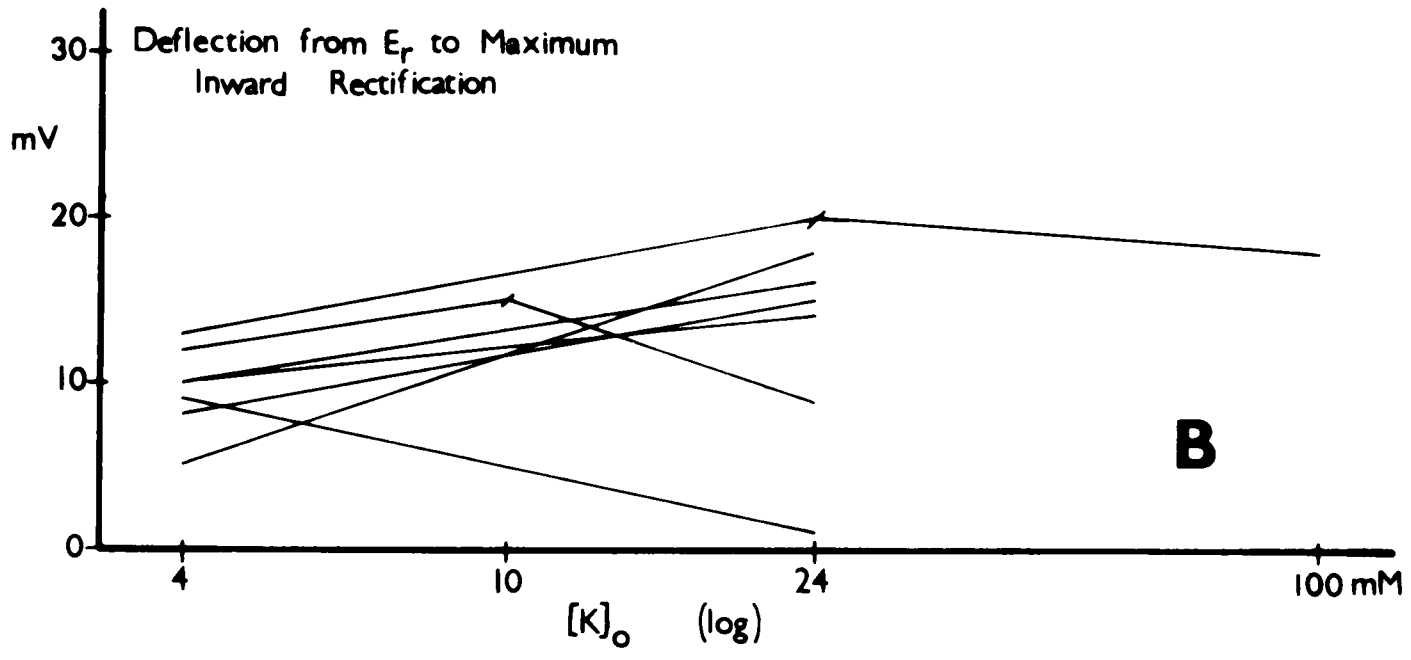
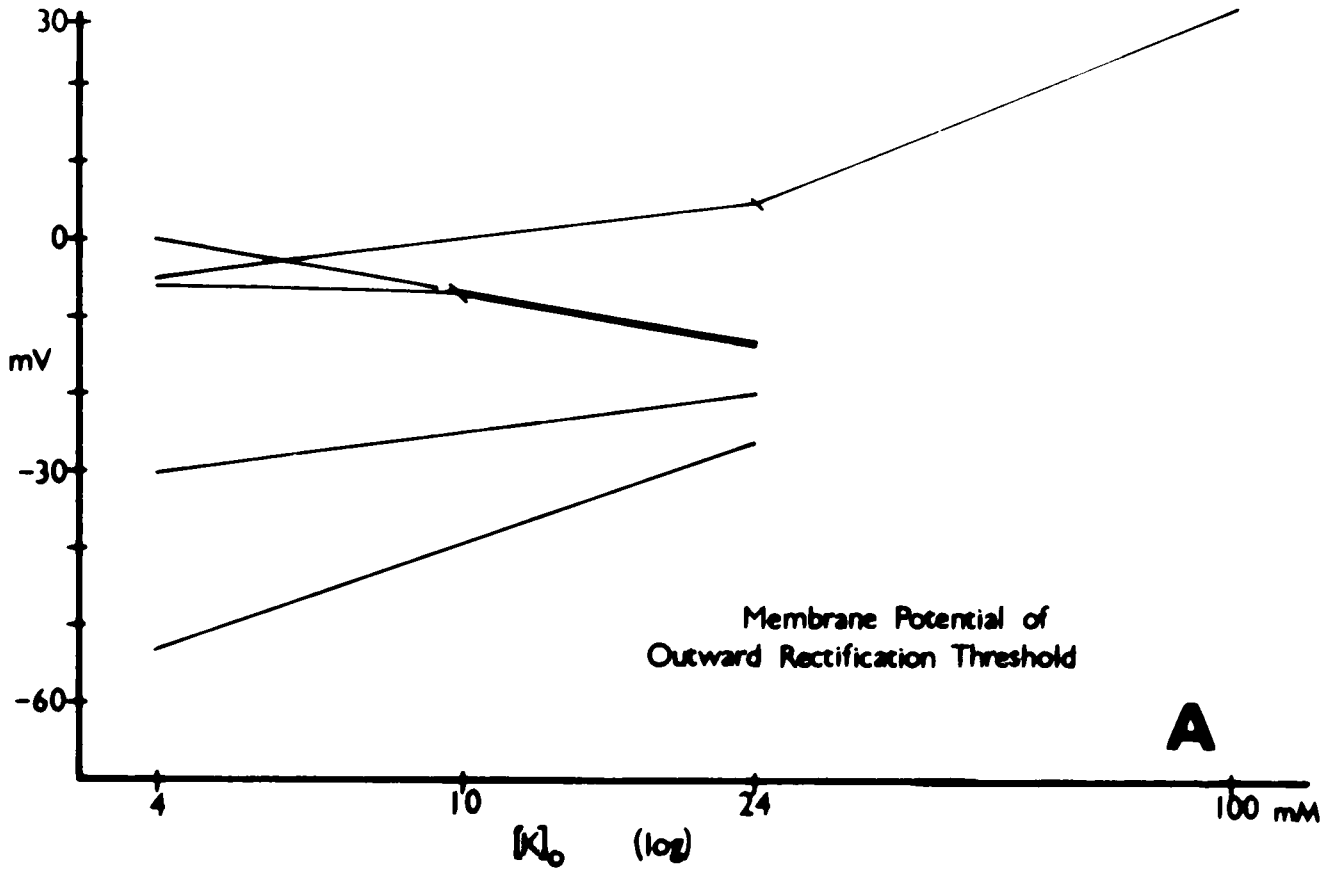


Figure 11 : A : membrane potential for maximum inward rectification versus log K_o. B : deflection from resting potential to maximum inward rectification versus log K_o. All solutions were Na-free.

rectifying direction - i.e. the threshold point; this was because, although the curves all showed outward rectification, the slope in the region of large depolarizations was very variable. Figure 12 has been plotted using this point, and both membrane potential and deflection from resting potential have been used as ordinates. With the data to date, it is not possible to establish a strict dependence on either of these variables. The depolarization from resting potential required to reach threshold was in every case decreased in high extracellular K; the actual membrane potential of the threshold, on the other hand, could conceivably be constant on average.

At this stage in the experimentation a paper by Miller (1965) appeared which suggested that graded depolarization and repolarization brought about by changes in external K concentration gave rise to a discontinuous curve of resting potential versus extracellular [K]: i.e., that a greater than expected depolarization occurred on increasing [K] from 13mM to 16mM, whereas otherwise the relation was linear versus log [K] with a much lower slope. Three experiments were performed to test this observation, all yielding similar ~~(contradictory) results~~ and strictly linear relations. Na-free solutions with varying K concentrations were prepared by substituting potassium methyl sulphate for an equal amount of choline chloride (Table 1, solutions B and D to J). The ionic strength of the bathing solution was thus kept constant, so that the activities of the ions could be considered constant; and the concentration of impermeant ions was also held constant (since choline and methyl sulphate ions are both considered relatively impermeant), in an attempt to minimize osmotic effects and consequent cell-volume changes. The membrane



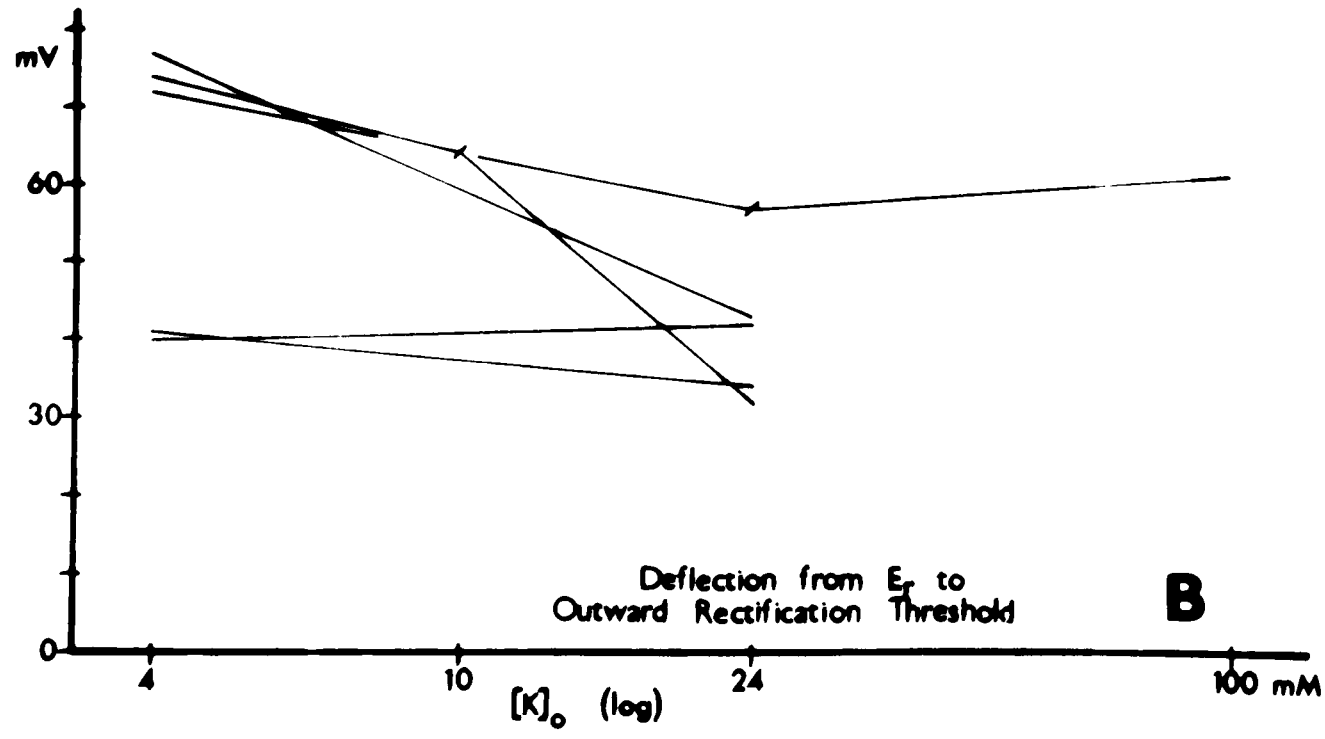
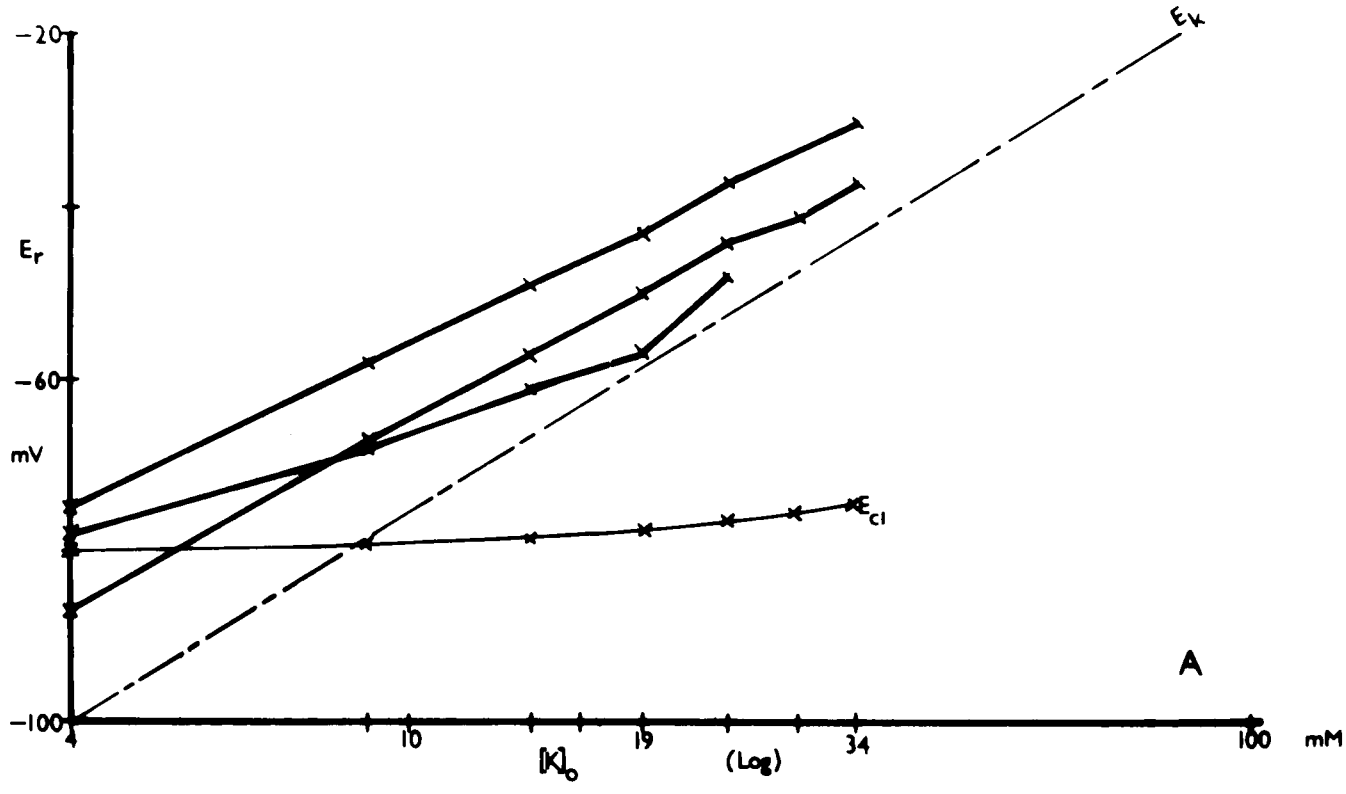


Figure 12 : A : membrane potential of outward rectification threshold versus log K_o. B : deflection from resting potential to outward rectification threshold versus log K_o. All solutions were Na-free.

resting potential after these changes was plotted versus log $[K]_o$ in Figure 13A, and is practically linear for each experiment. Bathing in each solution was continued until no further changes in membrane potential occurred, normally about 10 minutes. The order of application of the various solutions was varied - e.g., 4mM followed by 24mM, followed by 9mM, etc. - to indicate any cumulative effect, but none was detected. Recovery of action potentials on return to Tyrode solution occurred in every case. The dotted lines in Figure 13 indicate the K equilibrium potential as predicted by the Nernst equation, assuming internal K concentration is constant.

Figure 13B is a similar plot of the membrane potentials observed in the experiments described earlier, i.e. those demonstrating the crossover of the current-voltage curves in different external K concentration. These values were taken from fibres which were usually in the various solutions for longer periods than those used to plot Figure 13A, and which had intracellular currents passed at various times; however, as no progressive depolarization was observed in these experiments, the resting potentials are believed to be as reliable as those in Figure 13A. The resulting curves are again linear, but the slope is very different (about half that in Figure 13A). The only other difference between the two experiments is that K-methylsulphate is substituted for choline chloride in Figure 13A, and K-chloride is substituted for choline chloride in Figure 13B; all solutions have the same ionic strength. The membrane resting potential is more negative than the assumed K equilibrium potential when external K concentration is greater than 15mM.



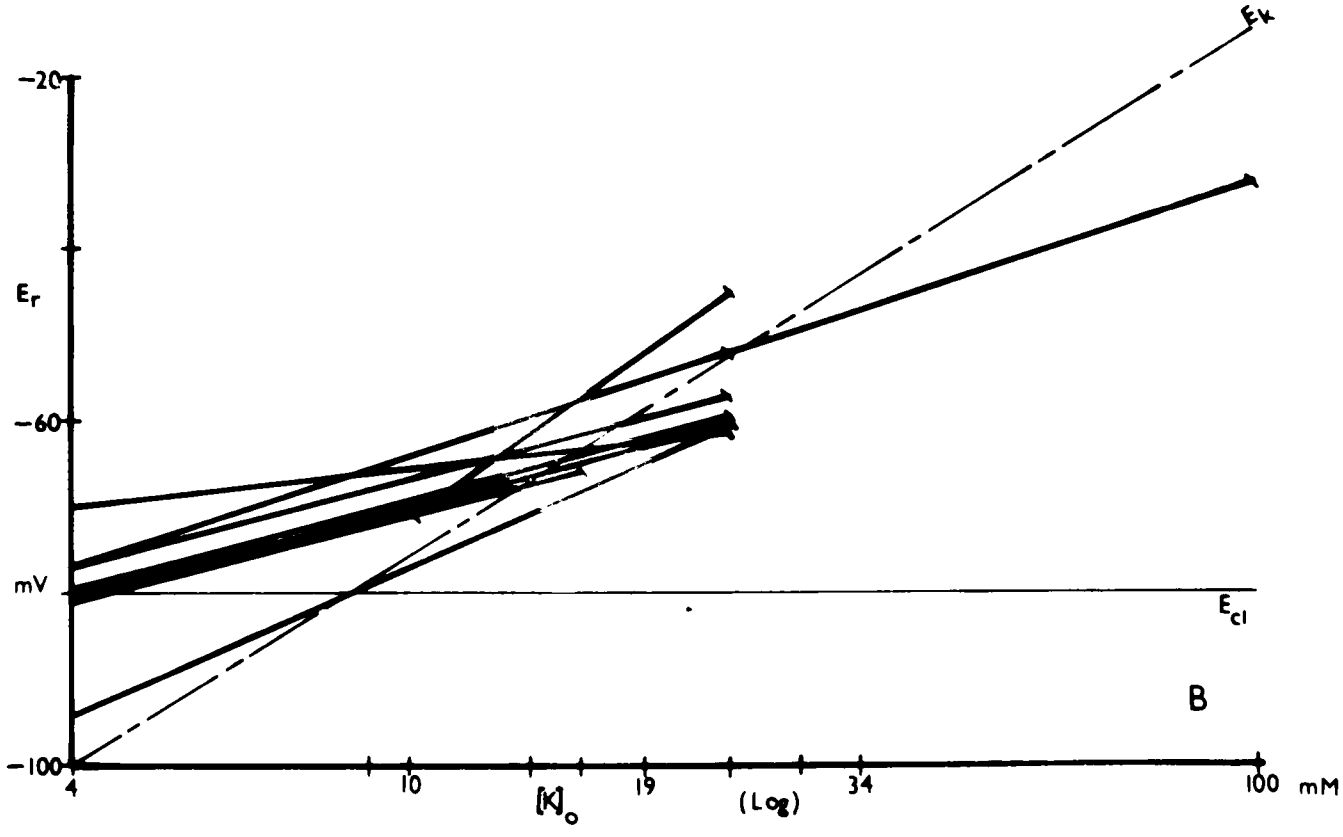


Figure 13 : A : membrane resting potential plotted against log K_o, when KCH_3SO_4 was substituted for ChCl. B : the same relation, obtained when KCl was substituted for ChCl. All solutions were Na-free. Measurements are indicated by a short diagonal line.

The failure of the membrane resting potential to vary in approximately equal amount to the K equilibrium potential as predicted by the Nernst equation is at first puzzling, since the K conductance of the resting membrane is known to be high and other components of conductance are relatively low. Even Cl, which has a maximum conductance of 30% of the total membrane conductance at the resting level and may be passively distributed (Hutter & Noble, 1961) cannot be dominating the resting potential even transiently, for E_{Cl} changes very little in Figure 13A and not at all in Figure 13B (dashed lines) if internal concentrations are assumed constant; it cannot therefore account for the halving of the slope between Figures 13A and 13B. Flux measurements indicate that the internal concentration responds only very slowly to changes in external concentration, in times of one hour or more (de Mello & Hoffman, 1960); it seems, therefore, that bulk movements of ions across the cell wall cannot give rise to the observed rapid changes of membrane potential.

Hodgkin & Katz (1949) found that the squid axon membrane resting potential could be approximated by the relation

$$e = \frac{RT}{F} \ln \frac{[K]_i + a[Na]_i + b[Cl]_o}{[K]_o + a[Na]_o + b[Cl]_i} , \qquad (22)$$

where a and b are respectively the ratios of P_{Na} and P_{Cl} to P_K. Hutter & Noble's (1961) results give b as no greater than about 0.4 for Purkinje fibres. The sodium contribution to the resting potential in the present experiments will be negligible as a first approximation, since the fibres were all in Na-free solutions for one hour or more.

Inserting the appropriate values of the concentrations in equation 22, the expected resting potentials for Figure 13 can be calculated: the results do not account for the large difference in slope in Figure 13B unless the value of b instantaneously becomes more than an order of magnitude larger than measured.

It is clear that if E_K does not undergo the changes predicted by the Nernst equation, then one of two situations must exist: either the internal K concentration must increase with increasing $[K]_o$, or else the external K concentration at the excitable membrane is less than that in the bathing solution. The former could occur as a result of an efflux of water, occurring because of some osmotic imbalance; the latter could occur if there were an extracellular space which equilibrates only slowly with the bathing fluid.

Burgen & Terroux (1953) have varied the bathing solution for cat's auricle by substituting KCl for NaCl; since P_{Na} is relatively very low in the resting state, this corresponds to the experiment plotting in Figure 13B. They found the straight-line relation of e_r versus log $[K]_o$, with a slope of 38mV for a ten-fold increase of external K concentration. The slope in Figure 13B is 26mV, and that in Figure 13A is 52mV. De Mello & Hoffman (1960) have investigated rabbit atrial and SA nodal fibres by adding KCl to normal Tyrode solution, experiments more closely resembling those plotted in Figure 13A; they found a slope for the atrial fibres of 35mV, and a variable slope for the SA nodal fibres (22mV at K concentrations less than 8, gradually approaching the slope for atrial fibres at higher concentrations). In similar experiments on rabbit atria, but only extending to

a $[K]_o$ of 11mM, Vaughan Williams (1959) found a slope of 56mV. Trautwein & Dudel (1958) found a slope of 35mV for dog auricular fibres, gradually increasing toward 45mV at K concentrations above 25mM. This wide range of results contributes little toward a better understanding of the phenomenon.

It is striking that the slopes in Figures 13A and 13B differ by almost exactly a factor of two; i.e., while Figure 13A obeys the Nernst equation quite well, Figure 13B will do so equally well if the square root of $[K]_o$, rather than the first power, is used as the numerator in the logarithmic argument. Such an expression does arise if two assumptions are made: (1) a Gibbs-Donnan equilibrium always exists across the membrane in the steady state; and (2) when the osmotic balance is upset, only water flows across the membrane. A Gibbs-Donnan equilibrium arises across a passive semi-permeable membrane if one ion of a 3-ion system is impermeant; e.g. the simplified cell, which has A^-, Cl^- and K^+ within, and K^+ and Cl^- without. Equilibrium will then occur when the diffusion potentials for K and Cl are equal, or, when $[K]_i [Cl]_i = [K]_o [Cl]_o$ (from the Nernst equation). The second condition is approximated for a few score minutes after a concentration change, until the fluxes of K and Cl cause significant changes in internal amounts. Before the latter happens, the internal concentrations will all change by the same factor solely on account of the volume change, and the Gibbs-Donnan relation requires that this factor be proportional to $\sqrt{[K]_o [Cl]_o}$. If, then, the replacement of KCH_3SO_4 for ChCl leaves the bathing solution osmotically unchanged (as is reasonable, choline and methyl sulphate being impermeant rather

strong electrolytes, and K and Cl having practically identical osmotic properties in aqueous solution), water would not enter or leave the cell and the K equilibrium potential would be given by the usual Nernst relation. If, on the other hand, substitution of KCl for ChCl upsets the osmotic balance (ChCl at the concentration used has about 7% less osmolarity than NaCl at the same concentration (Hodgkin & Katz, 1949) so one-for-one substitution would promote water influx; then KCl substitution for ChCl would provoke a somewhat greater water efflux, KCl having a higher osmolarity than NaCl), the cell volume might change and a new value of $[K]_i$ $[Cl]_i$ be produced causing e_r to vary with log $[K]_o$ only half so rapidly as in the first case.

Admittedly, such a teleological argument is hardly defensible, particularly on the basis of the few experimental results of this study. A most vexatious condition is that the osmotic flow of water must cease when the new Gibbs-Donnan relation has been satisfied, for no apparent physical reason. However, other mechanisms do not yield even a remote explanation for the phenomenon. A slowly-equilibrating extracellular space should equilibrate at different rates for different external concentrations, and therefore produce a non-linear e_r versus log $[K]_o$ relation; and a relatively small change in the extracellular concentration of impermeant ions would be unlikely to affect it substantially. A genuine bulk ionic flow across the membrane would not achieve a steady-state in 3-5 minutes, as does the

membrane potential after a concentration change. It is not surprising that Müller (1965), who found a slope relation of 25mV for a ten-fold change of $[Rb]_o$ and one of 55mV for a similar change of $[K]_o$ (impermeant ion concentration unchanged), was forced to suggest active transport of K as a tentative yet still unsatisfactory explanation.

Slight departures from the theoretical Nernst relation are much less troublesome to explain. The resting potential is not really the K equilibrium potential, since some small components of conductance to other ions still exist; the resting potential is therefore given by the equation

$$g_K\ (e-E_K) + g_{Na}\ (e-E_{Na}) + \ldots\ldots + g_{An}\ (e-E_{An}) = 0\ . \qquad (23)$$

This can be rearranged to give

$$e = \frac{g_K}{G} E_K + \frac{g_{Na}}{G} E_{Na} + \ldots\ldots + \frac{g_{An}}{G} E_{An}\ , \qquad (24)$$

where G is the total membrane conductance. The K conductance is very much the dominant one, however, since the resting potential is much nearer E_K than any other equilibrium potential. Figure 13A is fitted very well by $e = 0.85\ E_K$ over the whole range of concentrations, so that the resting K conductance is about 85% of the total: this is in good agreement with Hutter & Noble"s (1961) results for ion substitution. (Since g_K is such a large fraction of the total, this fraction will change very little as g_K is increased; therefore the increase in resting conductance with $[K]_o$ shown in Figure 10 would not be expected to alter the linearity of the results in Figure 13A).

The conclusions of the other sections of this thesis will not be affected by the failure to quantitatively analyse the results of this section.

2.2c Effects of Prolonged Current Pulses

A close examination of Figure 5 reveals a phenomenon that appears to contradict the delayed outward rectification hypothesis as an explanation of the slow changes in membrane potential response to constant current. When the currents are cut off, the membrane potential does not return immediately to its resting value; it drops quickly to a value a few millivolts above the resting level (increased g_K would send it to a lower level), and then declines very slowly (for tens of seconds) until it regains its resting level. Figure 14 shows such a response, with the voltage scale greatly magnified; the level during the current pulse is off the top of the picture.

This response was often, and only, seen when currents were passed across the membrane for several seconds. A more detailed study produced results as shown in Figure 15; the amplitude of the after-depolarization could be varied both by increasing the duration of the applied current and by increasing its amplitude, and the effects of doing either were practically identical. Thus, the size of the after-depolarization appeared to be a function only of the total charge transferred. Since, in these Na-free solutions, the K conductance is largest, therefore a substantial quantity of K will be leaving the cell during each current pulse. If some or all of these ions were temporarily being prevented from mixing with the extracellular solution - i.e., were being trapped in a region between the outer surface of the membrane and the bathing solution - then the apparent extracellular K concentration could become very high. Such an effect has been suggested by Adrian &

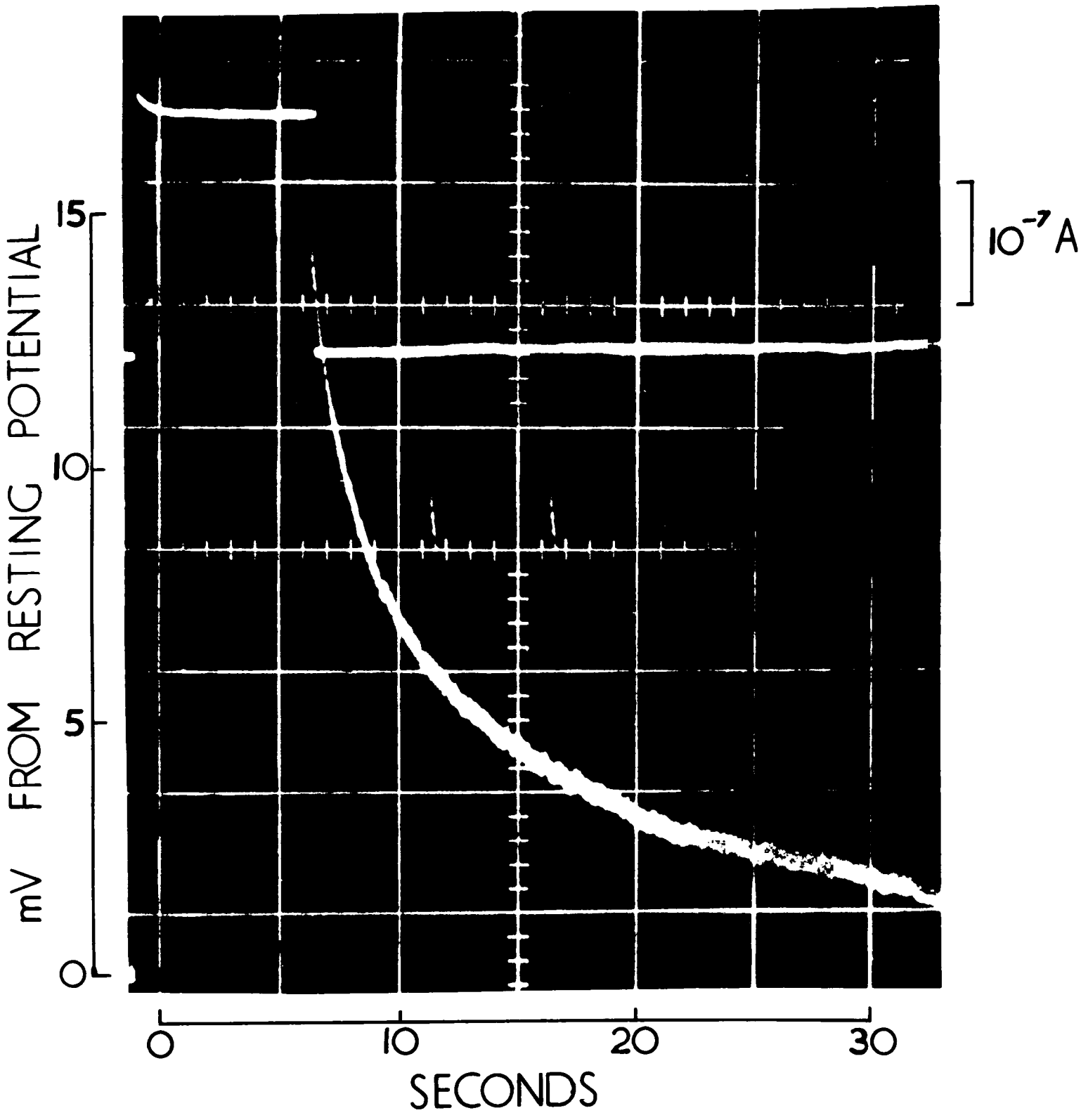


Figure 14 : Recovery of membrane potential following prolonged depolarization of a Purkinje fibre in Na-free solution. Top record shows the current passed through the membrane, sufficient to depolarize it by about 100mV. Bottom record shows membrane potential returning to the resting level. In drawing the curves of Figures 15 and 16, it was assumed that the capacitive recharging of the membrane was complete at the point at which the oscilloscope trace appears (about 16mV in this case).

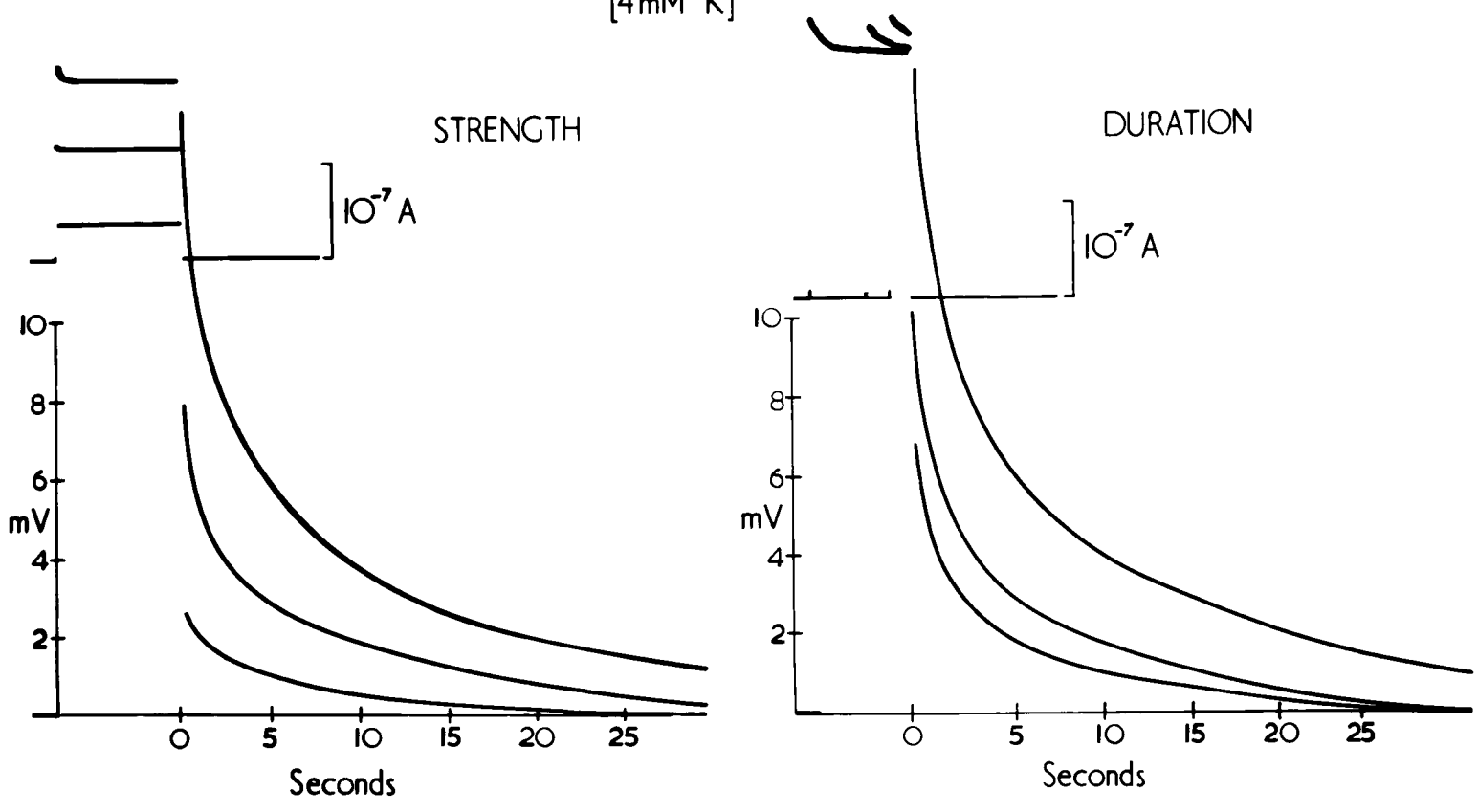


Figure 15 : Left : superimposed tracings of recovery of membrane potential following depolarizing currents of constant duration but variable strength. Right : recovery curves following currents of nearly constant strength but varying duration. The tracings begin at the point at which the oscilloscope trace appears (the potential changes too rapidly to be recorded during the capacitive recharging - see Figure 14). Note that strength and duration are approximately interchangeable.

Freygang (1962) for skeletal muscle. As a result, E_K would become more positive and the resting potential would do likewise. The time course of this effect would depend on the time taken for the trapped ions to diffuse away through whatever the barrier may be.

One clear way of testing this hypothesis emerges. If a discernable change in E_K is to be produced by such a locally-increased K concentration, the change in concentration in the extracellular space must be a certain fraction of that normally present - i.e., of that of the bathing solution. It is the relative increase that displaces E_K (Nernst equation). Therefore, if the normal concentration of K ions in this space is increased by bathing the fibre in a solution richer in K, the same accumulation of potassium (or amount of charge passed) will cause a relatively smaller concentration change, and so less displacement of E_K. Figure 16 shows the result of such an experiment: on bathing the fibre in 24mM K solution, the after-depolarizations produced by the test current pulses were greatly reduced, from about 15mV to about 4mV for the largest pulse. Thus, it seems clear that the 'accumulation effect' is the cause of this type of response, and that the ion involved is potassium; for the concentrations of all other ions in the bathing solutions were held constant (K-methyl sulphate was added to produce the increased K concentration; methyl sulphate is both impermeant and absent within the cell).

The locus of the recovery of the membrane potential after various current pulses, as shown in Figure 15, is not the same for the two cases; the responses for increasing amplitude at constant duration cannot be exactly superimposed on those for increasing duration at constant amplitude. They are also not simple exponential curves,

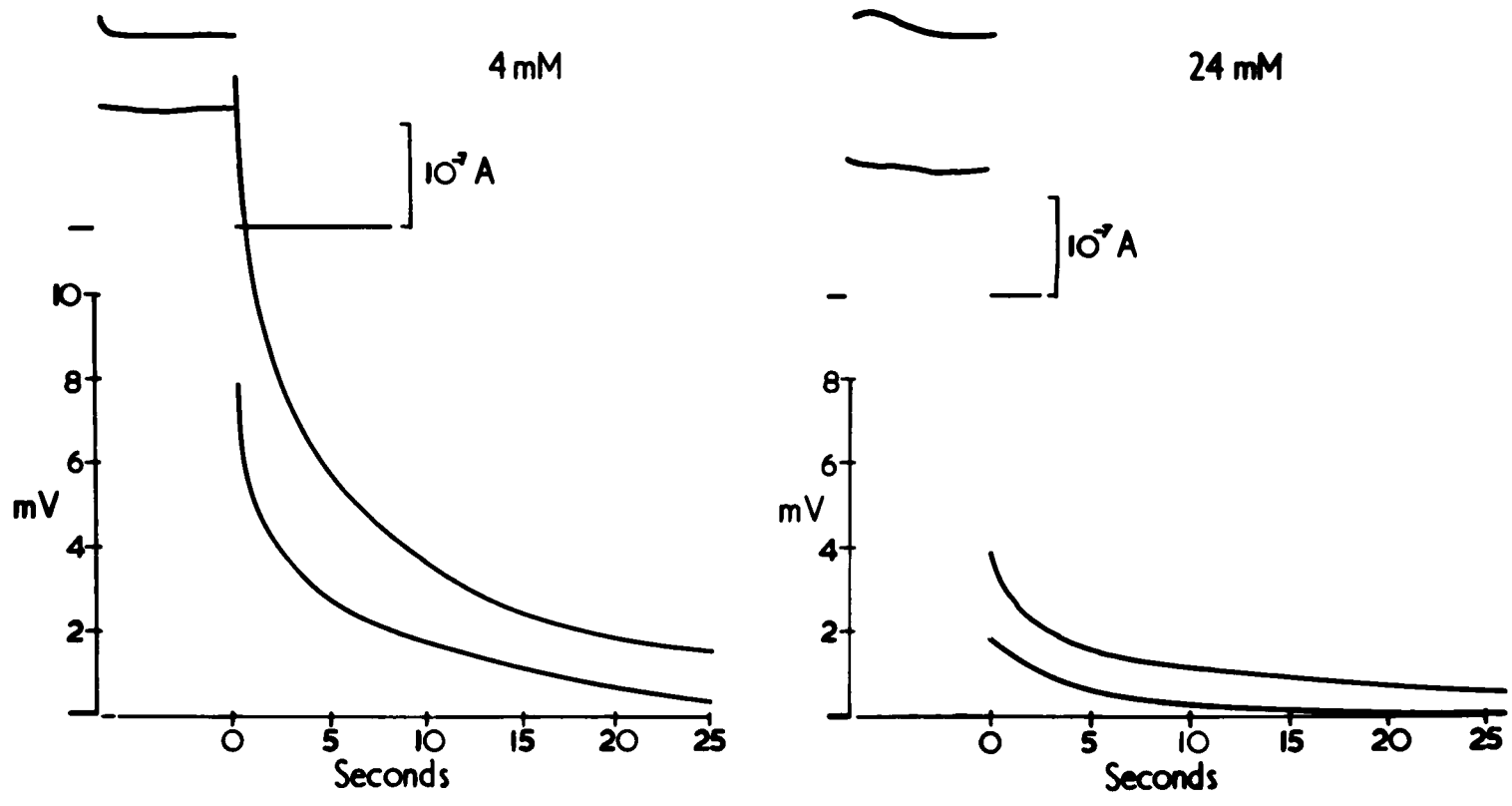


Figure 16 : Left : recovery of membrane potential following depolarizing currents applied to a fibre in a 4mM K solution (B, Table 1). Right : recovery of membrane potential following depolarizing currents applied to the same fibre in a 24mM K solution (C, Table 1). Note that, although the currents are larger, the effect on the membrane potential is very much smaller in the presence of the high-K solution.

although this is to be expected since equilibrium potential is a logarithmic, and not a direct, function of concentration. However, if the decay of the increased extracellular K concentration were due to diffusion across a single sheet barrier, then a simple adjustment of the time scales should allow the responses to be superimposed. That this is not the case is clear from a comparison of the smallest responses in the two halves of Figure 15. Therefore the K ions are not simply collecting around the cell in the adjacent space; rather, they must collect in some compartment which slows their escape with some spatially finite barrier or barriers which can account for the complex concentration decay curve.

Adrian & Freygang's (1962) suggestion for this space was an internal membrane system; the sarcoplasmic reticulum or the intercalated disc membrane could provide such a system in Purkinje fibres. These areas are known to be open to the external solution, and yet are long and narrow enough to enable local accumulations to exist transiently within them; thus the movement of the K ions toward the bathing solution could be rate-limited in a very complex manner, and transient ~~depolarizations~~ positive shifts of E_K could occur. A slow increase in the response to hyperpolarizing currents has sometimes been noted (also by Hecht & Hutter, 1965, Figure 7), which might be explained on the basis of a transient depletion of K from these same spaces and consequent increase of E_K.

2.2d Temperature Effects

A complete study of the effects of temperature on membrane

conductances could not be carried out in the time available. However, detailed records of the changes in action potential shape and response to constant-current pulses were made during one experiment, as the temperature of the bathing solution was varied between about 23°C and 38°C. Very large changes in the shape of the action potential occurred reproducibly and systematically; so much so, that some further discussion of this single experiment seems useful.

Figure 17 shows the effects of warming over a period of about ten minutes. The early action potentials were only 500 msec in duration, and were characterized by a fast positive spike and repolarization to about 34mV above resting potential (i.e. to -45mV); this repolarization was followed by a much slower depolarization, amounting to about 6mV in 100 msec, which gradually changed to the final repolarization phase which ended the plateau. As the temperature increased, the rate of depolarization during the early part of the plateau increased continuously; and the peak potential level of the plateau became slowly more positive, then rapidly changed in a positive direction by 15mV, and subsequently continued to increase slowly once more. Finally, as 34°C was reached, the deep 'notch' between spike and plateau quickly disappeared, leaving only a slight 'hump' on the early plateau of an otherwise normal action potential. Meanwhile the duration of the plateau more than doubled until the large shift in plateau peak level occurred, following which it gradually decreased back to its initial length. The temperature at any given period during the warming could not be determined, due to the long time-constant of the galvanometer in the thermocouple circuit.

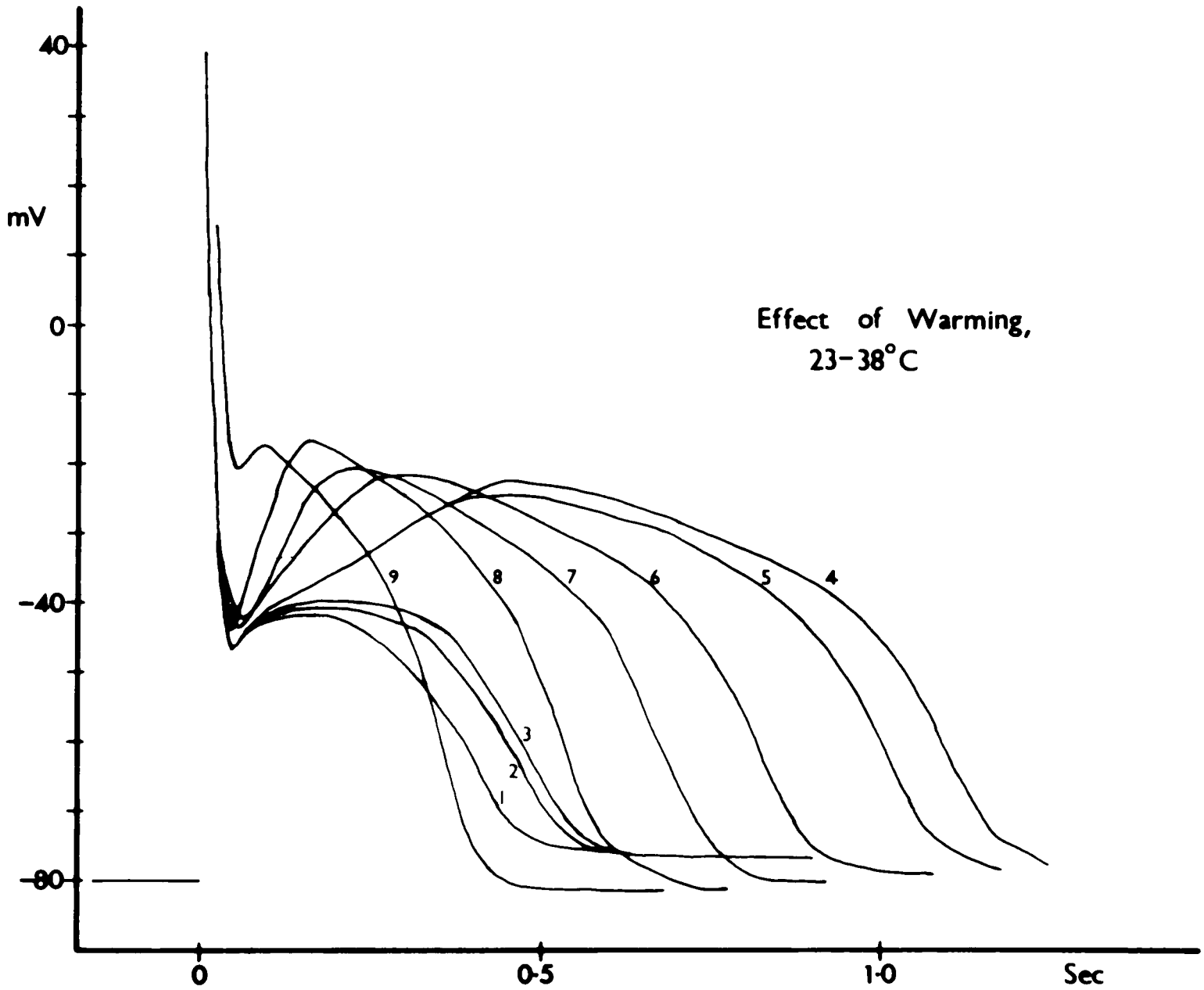


Figure 17 : Action potentials recorded when the temperature of the bathing solution (Tyrode : A, Table 1) was slowly raised from 23° to 38°C. Time lag in the temperature recording system did not permit a measurement for individual action potentials. Numbers beside the tracings indicate the order in which they were recorded.

If, as is usual, the rate of time-dependent conductance changes increases with a rise in temperature, the effects described above could be generated by a mechanism such as the following (in this case, no new components of membrane conductance need be postulated in order to obtain suitable results from the Hodgkin-Huxley equations). The course of the membrane potential in the notch suggests a conflict between two separate conductance changes. At this stage of Noble's computed action potential (10 to 50 msec after the spike peak), g_{K2} is slowly increasing, while g_{Na} decreases from its maximal value in about 5 msec (more than 300-fold) and then increases by about 100% very slowly for the next 150 - 200 msec. The anomalous rectification g_{K1} was assumed to be instantaneous. If, however, the latter were not so, then it is conceivable that at low temperatures the large decrease in g_{Na} could occur before the decrease in g_{K1} was complete (a time dependence for g_{K1} was suggested by Noble, 1962, as a possible way of overcoming the slow rate of change of membrane potential during the spike of the computed action potential). There would then be a notch where decreasing g_{Na} caused repolarization and the slower decreasing g_{K1} caused subsequent depolarization to the plateau peak. As temperature increased, the effect on the much longer-acting g_{K1} change would visibly affect the action potential shape, and depolarization to the plateau peak would be more rapid while the notch depth would remain relatively unchanged. The positive 15mV shift in plateau peak occurred spontaneously, and yet the initial rate of depolarization to this new peak occurred at about the same rate as before the change. Since the curve of g_{K1} versus membrane potential has some 'backward'

curvature - i.e. ~~it~~ current is smaller at certain levels of depolarization than at other, higher ones - the shift in plateau peak could correspond to a sudden jump across this region of low conductance to a new steady state. This is already postulated to be the cause of repolarization at the end of the plateau, as shown by Figure 18, taken from Noble (1962). In particular, if inward rectification is also time dependent, the curve labelled '0' would intersect the steady state i_{Na} curve further to the right, and the point of intersection would move left until g_{K1} reached its steady state, when a slower drift to the right would arise as g_{K2} continued to be activated. The membrane potential is given by this point of intersection, and thus would slowly climb to a peak and then decline as the plateau continued. If the '0' curve were so far to the right that intersection occurred below the peak i_{Na}, than a spontaneous shift to a new steady state would occur when the sum $(g_{K1} + g_{K2})$ became ~~great~~ small enough during the plateau to recreate an intersection above the peak of the i_{Na} curve. The qualitative effects of Figure 17 would then be explained.

Of course, the quantitative effects will not arise from the curves of Figure 18. However, the notch does not occur in all action potentials, nor does the striking effect of temperature. It seems certain that current-voltage relations can vary extensively. If, for the particular fibre of Figure 17, the steady-state Na-current curve were more like the heavy one in Figure 15 of Noble (1962) - i.e., if it had a lower value above -50mV, then was almost coincident with the solid curve of Figure 18 to -70mV, and finally curved more sharply to

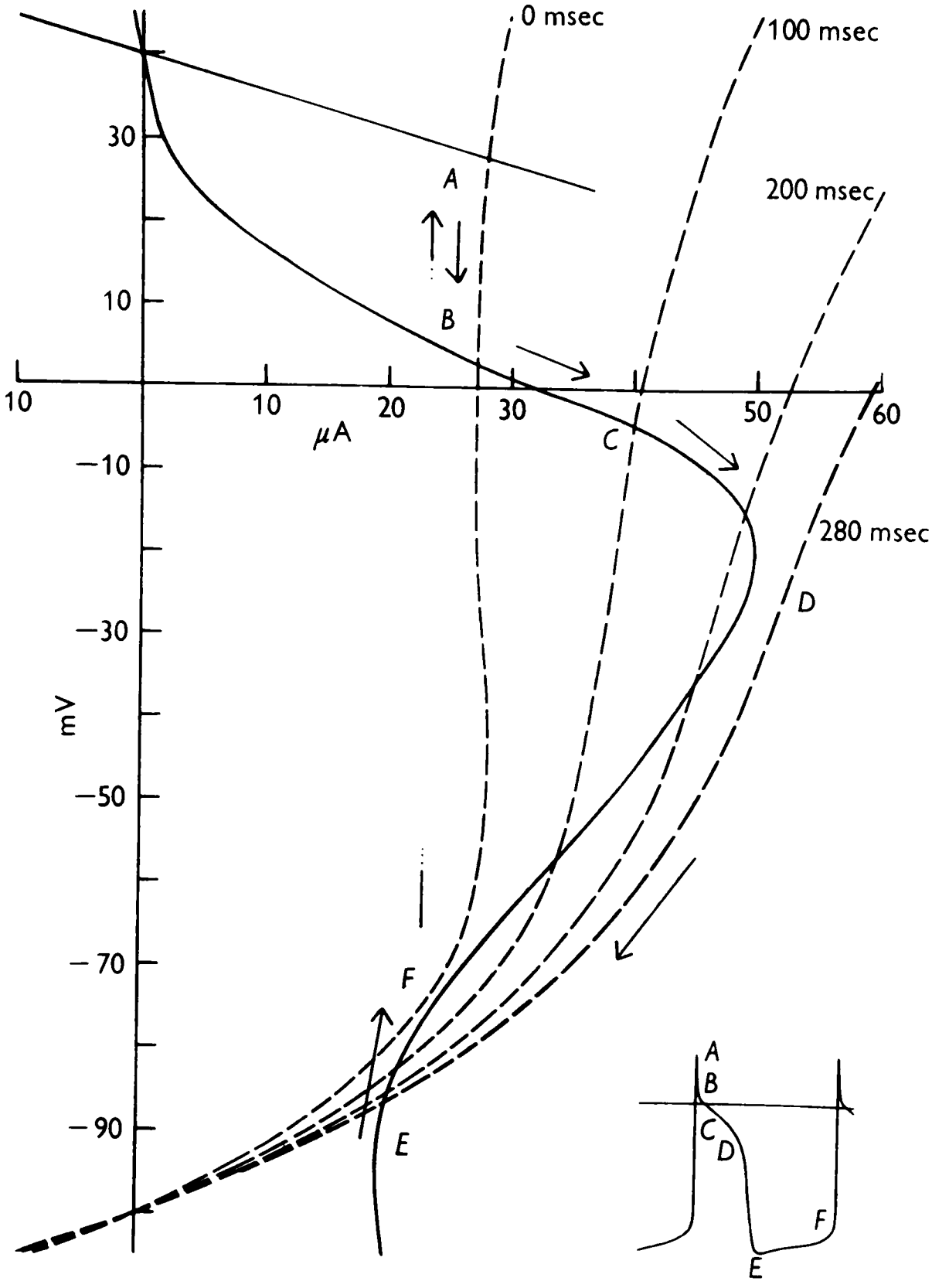


Figure 18 : Ionic current-voltage relations in cardiac muscle according to the modified Hodgkin-Huxley equations. The solid line is the negative of the Na current; intersections with the dotted curves (K current) determine the membrane potential at any time. From Noble (1962).

the right and assumed a larger value - and if the slope of the instantaneous K current-voltage relation were less than the slope of the Na-current curve in the region of -45mV, action potentials as in Figure 17 would arise.

These observations are indicative, but certainly not conclusive. Further investigation is required, preferably both by experiments on the temperature effects on the current-voltage relation, and by varying parameters in the modified Hodgkin-Huxley equation as computations are made. However, at the moment it does not seem necessary to postulate any other ionic currents because of these observations. The notches in the lower curves of Figure 5 could also be due to the mechanism postulated above, in which case only the initial fast depolarization response need be due to an as yet unidentified ionic current (e.g. calcium or choline). For example, a calcium current flowing long enough to produce the notches in Figure 17 should be very easy to detect by changing external Ca concentration; but one so brief as to be over at the end of the normal Na spike would be likely to give rise to the difficulties which have prevented many measurements of Ca current to date.

2.3 DISCUSSION

The status of choline as an impermeant ion for muscle membranes has been questioned at times. If it were not impermeant and behaved like Na, then of course action potentials would not be blocked when ChCl is substituted for NaCl. Renkin (1961) has investigated choline influxes and effluxes by radioactive tracer methods for frog sartorius

muscle, and has found that the influx is not very different from that of Na; however, active transport of choline out of the cell did not occur, so that it accumulated within the cell at a rate which gave approximately equal internal and external concentrations in 4 hours. A consequence of such accumulation would be the decrease of internal K concentration as $[Ch]_i$ rose, since if any active transport of K into the cell occurs, it is almost certainly coupled with Na extrusion and would therefore cease; Donnan equilibrium would occur, and influx of choline would be about equal to efflus of potassium. Thus, while choline would be an acceptable short-term substitute for Na, it would cause long-lasting depolarization in the long term. Boulpaep (1963) has found a doubling of radioactive K efflux from cat papillary muscle when all the external NaCl is replaced by ChCl (and also a trebling of the efflux in Ca-free solution), as would be expected from the above considerations. In the present results, Ch substitution did not continue for long enough for these effects to be noticeable in the experiments where KCH_3SO_4 was substituted for ChCl; this might explain why the K dependence of the resting potential followed a simple Nernst relation. The experiments with KCl substituted for ChCl were much longer; however, no progressive depolarization was found in any case, even after up to 12 hours bathing in Na-free solutions. The resting potential measurements in the latter experiments were made one half hour or more apart, for the different K concentrations; however, if choline were accumulating and causing a decrease of $[K]_i$ in the meantime, the potential change on raising $[K]_o$ should be greater, not less, than those for the KCH_3SO_4 - substitution experiments. Both these facts make it seem

unlikely that any substantial choline accumulation can occur in Purkinje fibres.

The possibility of a slowly-equilibrating extracellular space being the cause of the low slope found for membrane potential versus log $[K]_o$ on KCl substitution is made even less likely by the observations on the extracellular K accumulation during long outward currents. A space causing this accumulation could bein the right position to prevent rapid depolarization responses to high $[K]_o$; but the accumulation effect is reduced very markedly a few minutes after K is applied (Figure 15), so that there is apparently no more than a few minutes delay in diffusion of K to and from this space.

One other possible reason which could be advanced to explain the e_r versus log $[K]_o$ relation is a direct effect of methyl sulphate on the membrane permeabilities. This effect, if reversible, would be difficult to detect in these experiments, but seems unlikely in view of the results of Hutter & Noble (1961) in which action potentials were only slightly affected by complete substitution of $NaCH_3SO_4$ for NaCl.

The extracellular K accumulation with outward currents may be thought to cause some of the slow changes in membrane response attributed to g_{K2}. That this is not so in Na solutions is best seen by voltage clamping (see next chapter); the delayed g_{K2} increase occurs for very small depolarizations, so that the current pulses passed are much shorter and lower in amplitude than those required to significantly alter E_K. In addition, the residual current after clamping back to the resting potential level is positive, indicating that E_K (which is normally close to the resting potential) has not

been depolarized past the resting potential level. In the Na-free solutions used in the experiments described in this chapter, the currents are sometimes sufficiently long and large to have some effect on E_K. However, the slow decrease in membrane potential response to constant outward current in 4mM $[K]_o$ is also present in Figure 4 to some extent; the bathing solution here contained 24mM $[K]_o$, and if the decrease were due to an increased g_K resulting from K accumulation, it should have been largely eliminated. It seems that the accumulation effect is mainly an artificially-induced one; while it may cause some slight effect on the action potential at high rates of stimulation, it is unlikely to a significant extent in normal beating and almost certainly does not cause repolarization from the plateau, as tentatively suggested by Weidmann (1956).

The downward inflections on the upstrokes in Figure 5 (4mM K, choline solution; the fibre had been in Na-free solution for two hours) are not present in the responses of the same fibre in 24mM K solution (Figure 4), where the resting potential is depolarized by about 20mV. It may be, therefore, that some other ion is entering by the Na path, which is inactivated by depolarization; calcium or choline are possible substitutes. On the other hand, Dudel et al. (1967) have shown evidence of a fast transient chloride current on depolarization, which is inactivated with time and presumably contributes to the repolarization after the upstroke (and may be occurring prematurely in Figure 5); while a $[K]_o$ of 10mM apparently decreased this somewhat, their full findings in this regard are still in press. With ramp voltage clamps, the same authors (1966) have also obtained results suggestive of a negative non-

sodium current with about the same kinetics as the Na current; while such a current could also cause the notched upstroke of Figure 5, for the reasons outlined in Section 4.3 ramp clamp results should be considered with caution until confirmed by other methods.

The results depicted in Figure 8 argue against the hypothesis that the positive hump on depolarization is caused by a transient Ca current (Reuter, 1966). While this might be the case if the hump occurred only on depolarization, the lower figure shows that it also occurs in reverse on repolarization to a lower level. This is easily explained on the basis of a time-dependent rise and fall of g_{K2}. If permeability to Ca were to rise, no undershoot on repolarization would be expected (E_{Ca} is positive, so an overshoot would result if g_{Ca} remained high), unless there were also a time inactivation to a level lower than the original. In view of the other results presented throughout this thesis indicating g_K as the cause, it does not seem profitable to pursue this hypothesis, although it cannot be definitely excluded.

The changes in action potential shape on increasing temperature may also be caused by an effect of a resistance in series with part of the membrane capacitance; this can cause a notch before the plateau, as seen in Figure 17, and possible temperature effects on this are discussed more fully in Section 4.3.

CHAPTER 3 EXPERIMENTS WITH VOLTAGE CLAMPS

Voltage clamp experiments were begun during 1965, providing results which could be much more accurately checked against the theory of membrane behaviour, and used to improve that theory: for with the membrane potential no longer a variable, the voltage dependence of the rate constants required for equation 20 can be found. Membrane potential changes can be accomplished in normal ionic solutions without triggering the uncontrolled chain of events associated with a complete action potential. In addition, a much more direct method of measuring the equilibrium potential arises; when the membrane is held at that potential the related ionic current disappears, and when the membrane potential is pushed beyond the equilibrium potential that ionic current reverses. Such changes make identification of the particular current component involved comparatively simple. Thus all the constants required by the modified Hodgkin-Huxley equations can be directly determined.

3.1 METHODS

The experiment is carried out as detailed in Section 2.1, with the exception of the changes in electronic circuitry outlined below.

The arrangement of voltage clamp equipment is as described in Deck, Kern & Trautwein (1964). The difference between the transmembrane potential, as measured by an intracellular microelectrode,

and a preset reference potential is used to force current through a second intracellular microelectrode in a direction tending to eliminate the difference. This negative feedback is accomplished automatically by means of high-gain 'operational' amplifiers, and its speed is limited only by the amount of capacitive charging which must be accomplished in the external circuit (or more precisely, by the product of resistance and capacitance in this circuit). The cardiac muscle membrane behaves electrically as if it has a significant pure capacitance (Weidmann, 1952) and an additional capacitance in series with a resistance (Fozzard, 1966); these, together with the resistance and capacitance of the external wiring, make it impossible to completely accomplish a change in membrane potential in less than 10-30 msec. This is sufficiently fast, however, to resolve all conductance changes occurring after the initial fast g_{Na} changes of an action potential. Since the membrane potential is held constant (so that $(e-E_K)$, $(e-E_{Na})$, etc. are practically constant), the current passed is directly proportional to the conductance at any given time (equation 15).

The recording of the membrane potential and current were as described earlier. However, the amplified membrane potential, as taken from the vertical deflection plates of the oscilloscope (magnitude range of ± 40V), was fed into one of the Solartron operational amplifiers. Here it was subtracted from a bias voltage, the difference between the two being the current-generating signal. A variable feedback resistance on the amplifier allowed complete gain control from 0 to several thousand. To initiate a voltage clamp, the gain was

slowly turned up and the bias voltage was changed to bring the clamped membrane potential back to its normal level; this process was repeated until a suitable value of gain was reached, normally about 10. (The maximum usable gain in the voltage clamp circuit was limited to about 10 by the behaviour of the circuit through the electrodes and preparation: too high a value produced oscillations when a square clamp was attempted, and the oscillatory current readily became self-regenerative and ruined the membrane. A gain of 10 in the final amplifier meant a total system gain of about 1,000.). The outputs of the long-current-pulse generators described in Section 2.1d (which provided square voltage pulses of up to + 100V or - 60V) were then added to the operational amplifier input, so that a pulse provided a new reference level and the clamped membrane potential changed accordingly. The two pulse generators were connected in series, and a simple passive circuit was used to cause the end of the first pulse to initiate that of the second unit; each was of variable amplitude, duration, and polarity, and they could be superimposed if a follow-on arrangement was not required.

Voltage clamp pulses were initiated normally, when the membrane had returned to a steady state after the previous pulse; the usual time between pulses was from several seconds between short pulses to tens of seconds after long ones.

3.2 RESULTS OF VOLTAGE CLAMPS

Steady state current-voltage relations in normal phyiological solutions can be found by voltage clamp methods, since an action

potential is prevented by the clamping action. In general, these have the same shape as those found by constant-current methods in Na-free solutions. However, the negative-conductance regions cannot be examined with constant-current pulses, whereas these are particularly well-defined in voltage clamping. Figure 6, right side, shows a set of typical results: there is clearly a conductance decrease in the region between -60mV and -10mV. The top figure on the left shows a normal current as recorded during a square voltage clamp pulse, with a smaller but similar pulse superimposed midway; the bathing solution in this case is Na-free. At each change of clamp level there is the usual spike of capacitive current while capacitances in the circuitry and the membrane are charged or discharged. Following this, on the initial depolarization, there may be a fast transient of current of either inward Na or some other outward current (as discussed later). Finally the current will approach a steady state value, either immediately if the level of depolarization is below threshold for activation of g_{K2}, or slowly as g_{K2} becomes fully activated. Figure 6 shows both effects: after the first depolarization step, a steady level follows soon after the initial spike, whereas during the second depolarization to above g_{K2} threshold the current steadily increases and in this case does not reach saturation before repolarization. The steady state values are the ones plotted in the usual current-voltage relations. The lower left part of Figure 6 clearly shows the effect of the negative conductance region; initial depolarization to -55mV requires more positive (outward) current than is required to maintain the membrane potential level at -35mV, and therefore

the current decreases on the second depolarization.

Figure 19 is a closer study of the time dependent conductance changes. On theleft are shown the voltage clamps applied to the membrane, with the membrane potential during the depolarization noted above; and to the right of each is the current required to maintain it. For a small depolarization (bottom) the current during the clamp is constant: g_{Na} has not been activated, nor has the slow conductance change during depolarization. A clamp to -60mV initiates the fast conductance change which gives rise to the spike, and this appears on the current record as a large negative current at the beginning of the depolarization; a slow conductance change also appears during the clamp which does not saturate in 400 msec. Further depolarization increases both the rate and the final amplitude of the slow conductance change, and by an amount which is not directly proportional to the increase in driving force with depolarization. At the greatest level of depolarization, the rate of change of slow current continues to increase but actual magnitude does not, and there are signs of an early negative current; this latter could be an affect of membrane capacitance on Na-currents, or possibly an inward current of some other ion, e.g. calcium. The initial fast conductance change could not be studied in these experiments since adequate voltage clamping could not be obtained in the first 20 msec of depolarization; the later, slow conductance change is the main subject of this chapter.

At the end of the depolarizations of Figure 19, the clamp current does not always return to zero at the resting level. This can only mean that some component of conductance has a different value

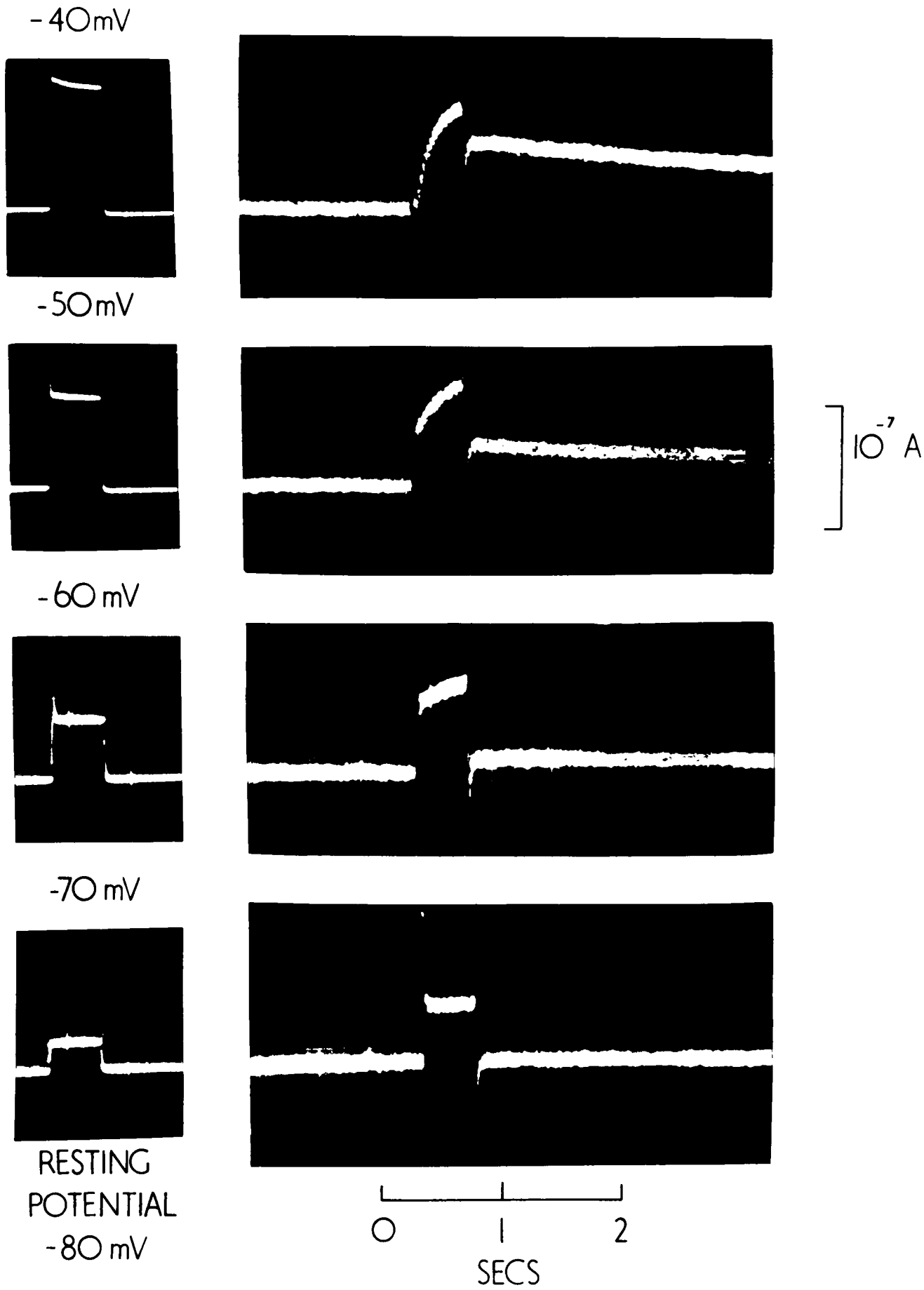


Figure 19 : Effects of a depolarizing voltage clamp on the membrane conductance. Left : membrane potential. Right : current passed through the membrane. Note the time-dependent changes.

after the end of the depolarization than before it, since the driving force is the same in both cases. The initial amplitude of this positive after-current increases with the amplitude of the previous depolarization, and then declines slowly back to zero with a time course of seconds; this suggests the possibility that the slow conductance changes during depolarization and the positive after-current may be due to the same voltage - and time-dependent mechanism. Such a mechanism was described by Hodgkin & Huxley (1952b) to account for K current in squid nerve axons, and was described mathematically in terms of their parameter 'n' by equation 19. The slow current in Purkinje fibres has a very much longer time constant, and a much smaller amplitude relative to the initial Na current: but since the action potential of Purkinje fibres is correspondingly longer than a nerve action potential, such a mechanism could play a similar role in bringing about repolarization. If this were the case, then the peak magnitude of the slow current should be proportional to both amplitude and duration of depolarization; and the positive after-current should be proportional to this peak amplitude, and should reverse if the membrane is hyperpolarized to beyond the equilibrium potential for potassium.

Deck & Trautwein (1964) have already shown that the positive after-current reverses if the membrane is hyperpolarized to beyond -100mv following a depolarizing pulse, and these results have been confirmed during the present experiments. Since the K equilibrium potential is at about this level when the cell is in Tyrode solution - and no other ion is believed to have an equilibrium potential within

60mV or more of this level - the ion involved in this current is assumed to be potassium. Whether this component of conductance is mathematically analogous to the g_{K2} assumed in Noble's (1962) modification of the Hodgkin-Huxley equations depends on the effects of duration and amplitude of depolarization on its magnitude.

For various levels of depolarizing clamp, pulses of varying duration were applied and the current was recorded both during and after the depolarization. For each level the change in current from the earliest stable value during the depolarization and the peak after-current were plotted versus duration of the pulse, with results as exemplified in the lower part of Figure 20 (the left ordinate is the amplitude of the current during the clamp, where 8×10^{-8}A arose almost immediately). Since the driving force after the pulse is different from that during it, the after-currents had to be scaled before plotting. The scaling factor required for each set of results was not simply the ratio of the driving forces; whereas the latter was 4.7 in Figure 20 (assuming $E_K = -100$mV), the ratio of currents was only 1.7. The ratio of conductances (current/driving force) during the depolarized and repolarized states was therefore 0.36, and varied between 0.3 and 0.6 in other experiments. Thus some form of inward rectification seems to govern the maximum amplitude of the slow current on depolarization. It is not inconceivable that g_{K1} and g_{K2} correspond to a fast and a slow rate of change of the same basic mechanism, but further experiments will be required to ascertain this.

However, once the correct scaling factor has been found, the curves for maximum current before and after repolarization practically

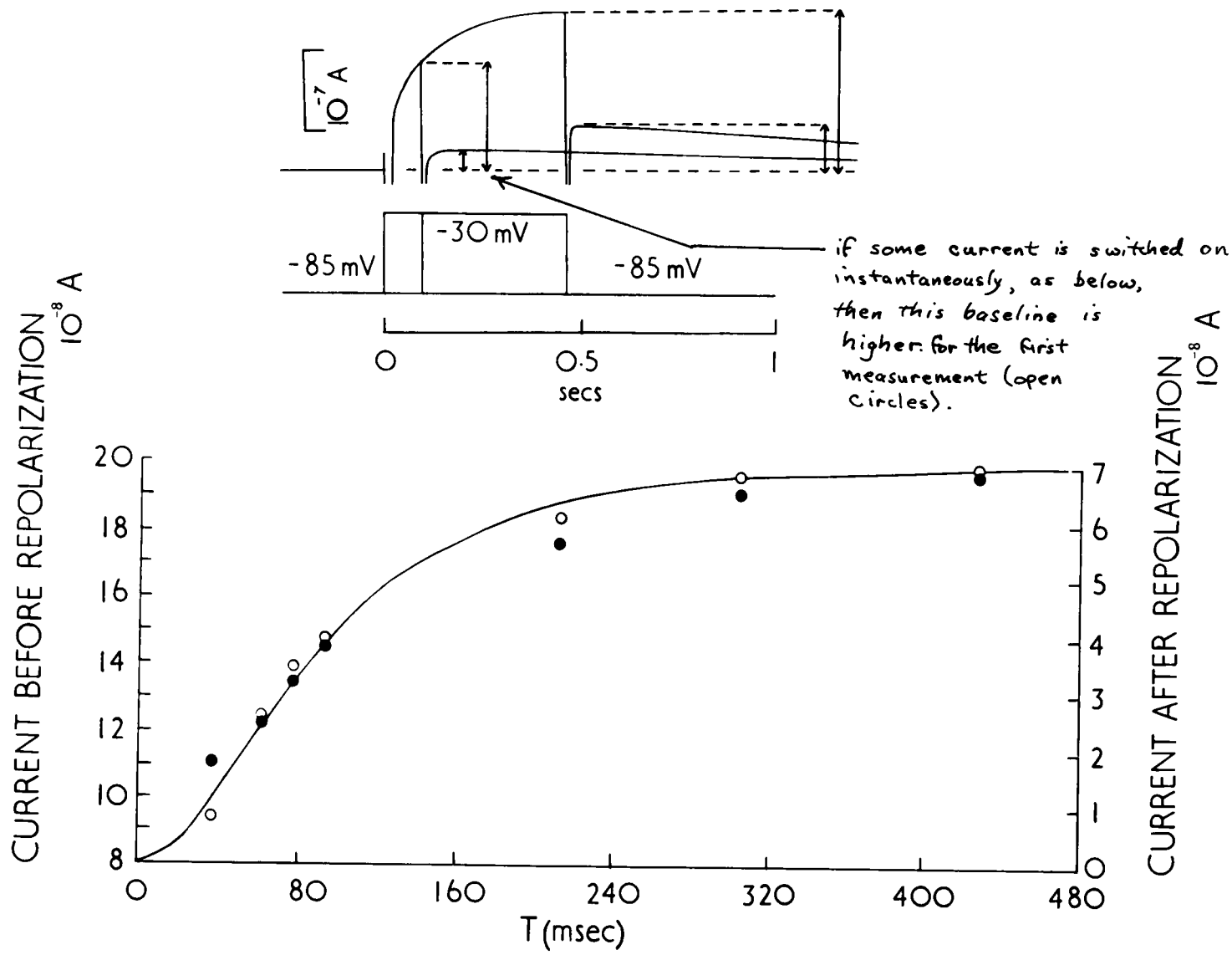


Figure 20 : Comparison between time course of slow change in current during depolarization, and the relation between peak outward current following repolarization and clamp pulse duration. Top : superimposed traces of two current records illustrating measurements made. Bottom : filled circles show peak current on repolarization, open circles show current change during depolarization. The continuous curve is proportional to the square of 1 - exp (-t/tn), where tn = 70 msec.

coincide. This was confirmed in other experiments. A new method of measuring the slow conductance was therefore adopted, and this is indicated in the top half of Figure 20. Since the decay time of the after-current is much longer than the time of onset of the slow conductance during depolarization, it is much easier to separate the former from the spike of capacitive current which occurs on changing the membrane potential. Also, on depolarization the active Na current is superimposed on the capacitive current, whereas on repolarization no active currents are triggered (e.g. in Figure 19, the spike on repolarization is the same whatever the previous depolarization). Therefore the peak after-current was taken as the measure of the degree of activation of g_{K2} at the end of the depolarization. An added advantage of this method is that the driving force $(e-E_K)$ is constant, and the nonlinearity of the 'instantaneous' value of conductance need not be taken into consideration.

Figure 21 is a typical set of results showing both the voltage dependence and the pulse-duration dependence of the slow conductance. The upper trace of the figure shows the development of the positive after-current for a depolarization of 16mV lasting for the number of msec indicated above, and the second trace shows the same effect for a depolarization of 38mV etc. The amount of g_{K2} activated by a 16mV depolarization lasting 800 msec is nearly the same as that resulting from a 38mV depolarization lasting only 100 msec. Such results are summarized in Figure 22, 23 and 24, where the abscissa is pulse duration and the ordinate is proportional to the peak after-current, or fraction of maximum g_{K2}. The membrane potential during each depolarization is

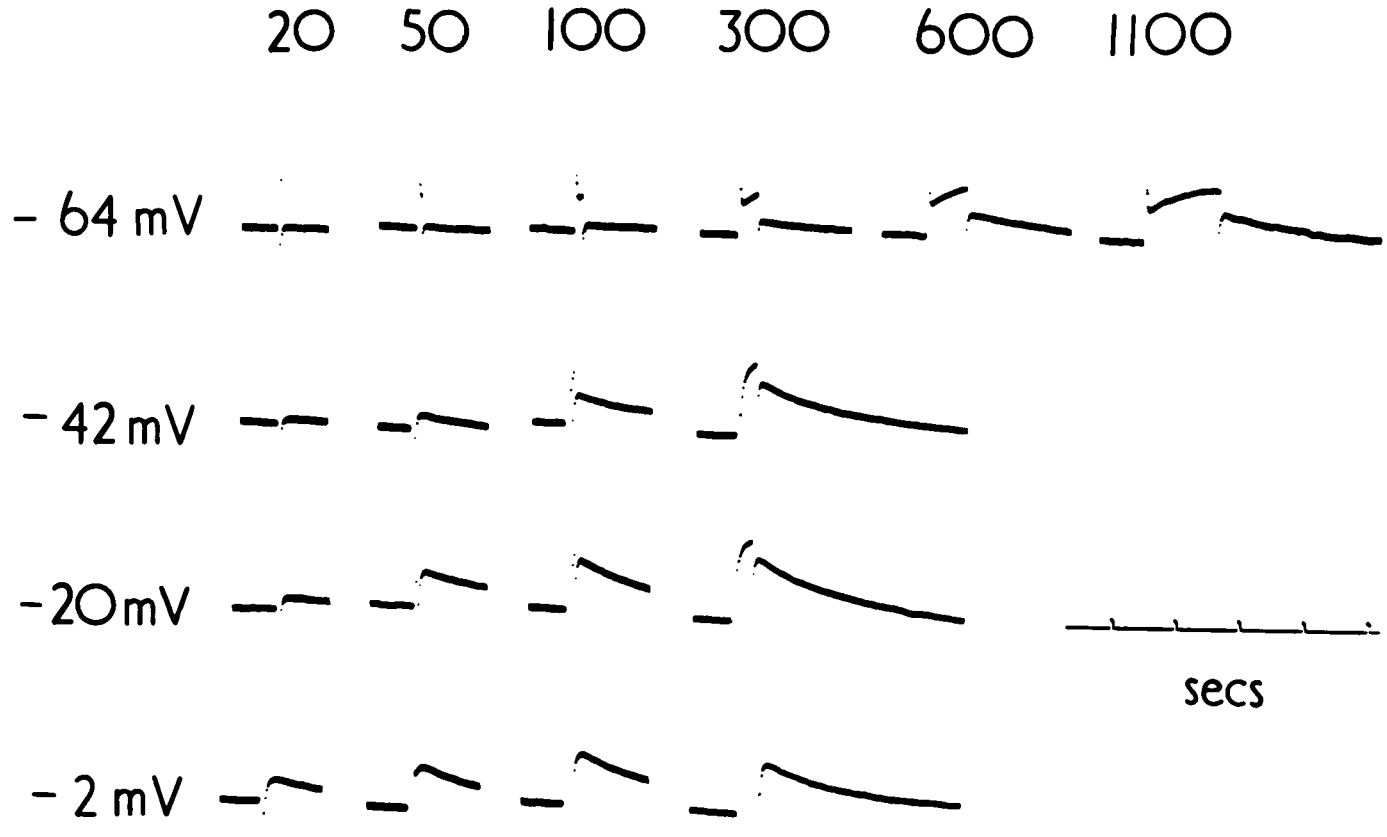


Figure 21 : Currents recorded during depolarizations of various durations (indicated in msec, top) and four magnitudes (from a resting potential of -80mV to the level indicated on the left).

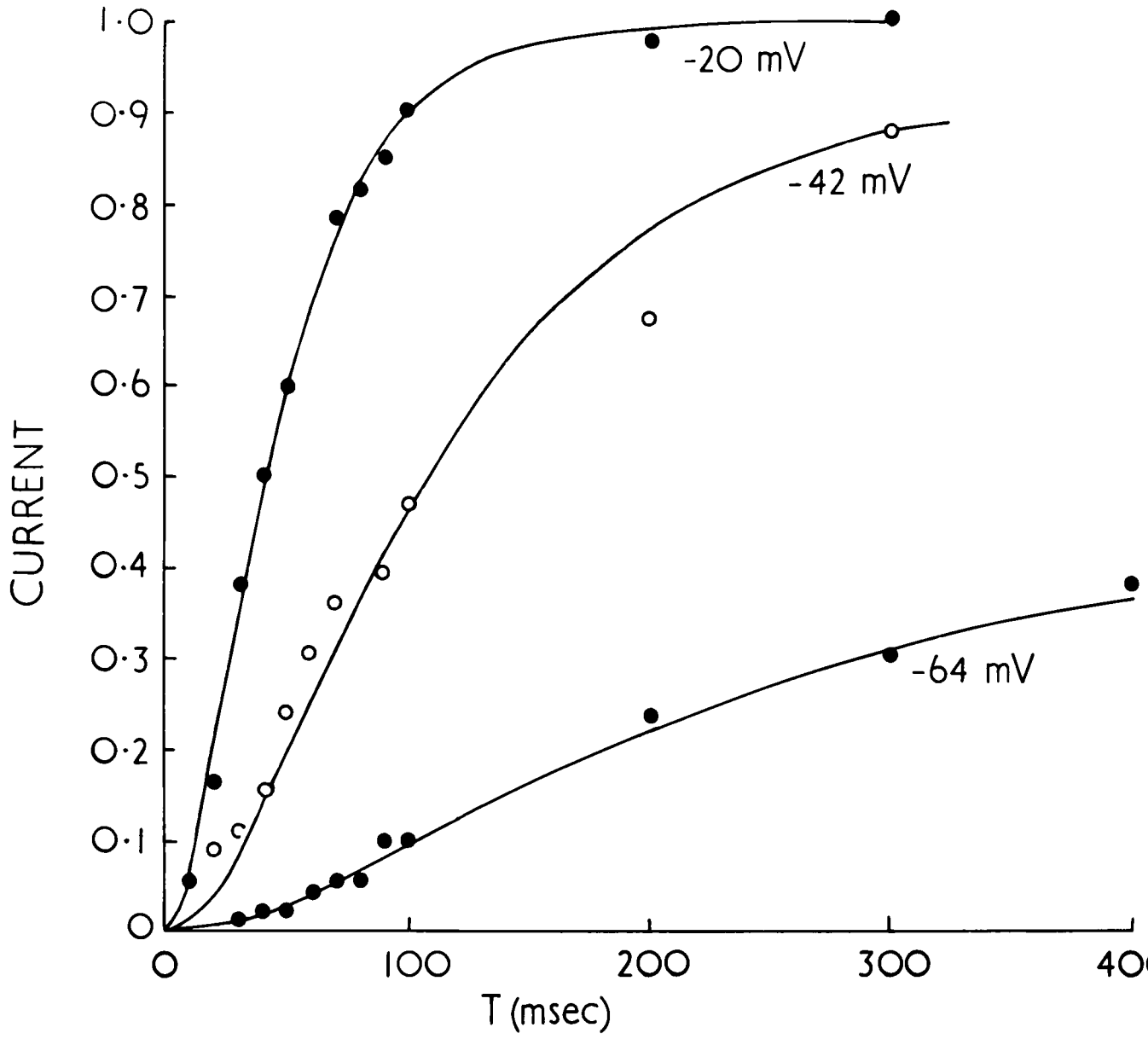


Figure 22 : Relations between peak outward current following repolarization and the duration of the depolarizing clamp pulses. The ordinate has been normalized in terms of the maximum current following the strongest depolarization. The continuous curves are calculated from the square of (1-exp(-t/tn)), with time constants (tn) equal to 160, 81 and 34 msec. Resting potential approximately -80mV.

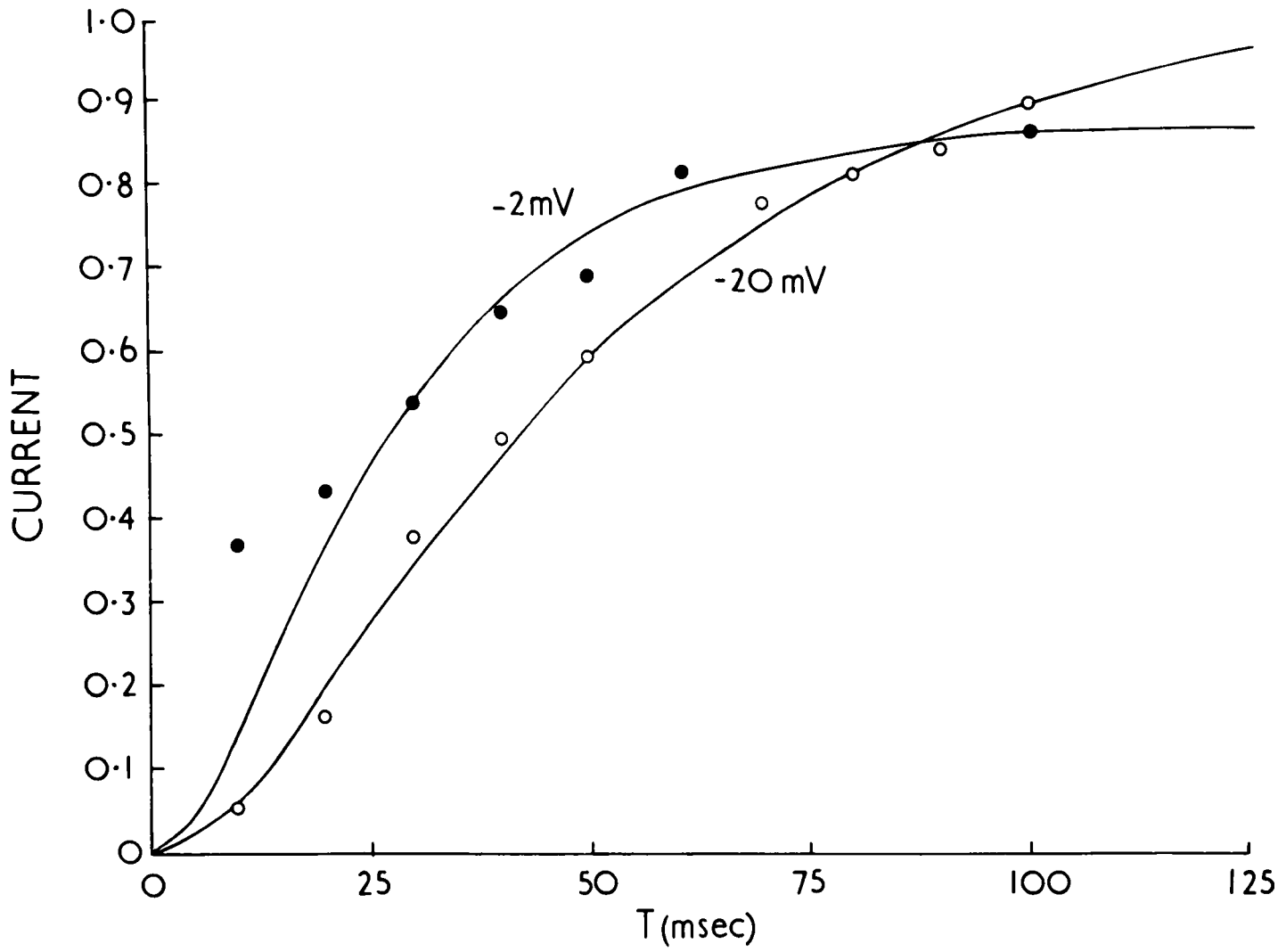


Figure 23 : Relations between peak outward current following repolarization and duration of clamp pulses depolarizing the membrane to -20mV and -2mV, from a resting potential of approximately -80mV. Same fibre as Figure 22. Time constants are 34 and 19 msec.

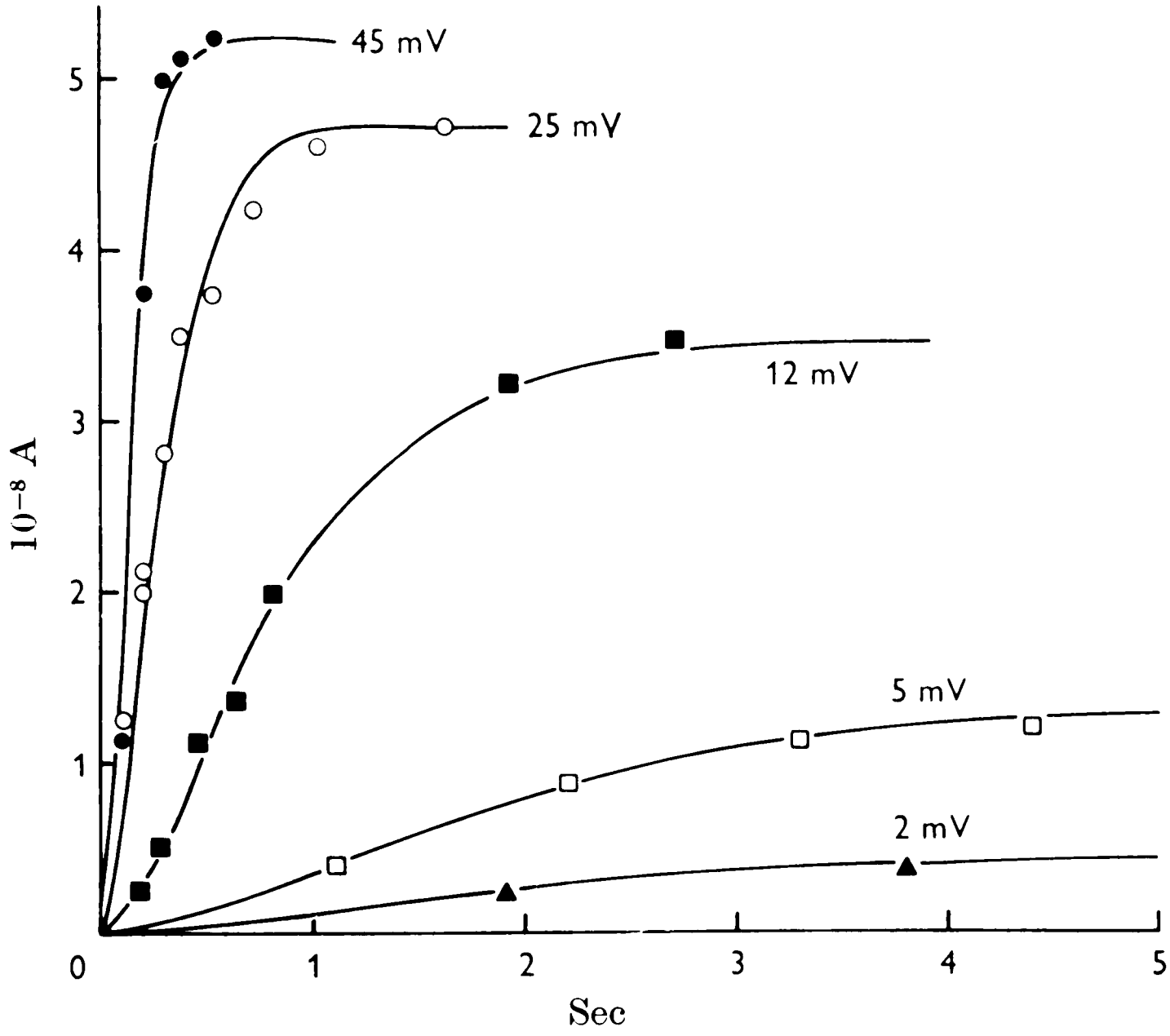


Figure 24 : Time courses of onset of slow outward current at subthreshold (2, 5 and 12 mV) and suprathreshold (25 and 45 mV) levels of depolarization. The currents were measured after repolarization to the holding potential (approximately -80mV) from the depolarization level indicated. The continuous curves are calculated ones for time constants of 90, 190, 600, 1,400 and 1,750 msec.

indicated beside each curve, except in Figure 24, where degree of depolarization is shown.

Figure 25 indicates the dependence of the maximum fraction of g_{K2} activated on the level of depolarization employed, for three experiments. If the amount of activation genuinely reaches a maximum and then declines with further depolarization, then the Hodgkin-Huxley expression for the conductance parameter will clearly be inadequate, since no power of n will fit this curve. However, the evidence for this decrease is inconclusive, and the curve for n^2 (see below) does seem to agree with the general trend of the experimental values in most cases. Therefore, no attempt has been made to alter the theory.

Hodgkin & Huxley found that the time-dependent K conductance change in the squid axon membrane varied as the fourth power of the parameter n: i.e. curves analogous to Figure 22 were quite sigmoid in shape. In the case of Purkinje fibres, the curves for large depolarizations can be fitted fairly well by using the first power of n - i.e. a simple exponential (equation 18). However, the curve for the smallest depolarization in Figure 22 has certainly some sigmoid curvature, and it was found that a second power of n could account for this satisfactorily as well. As a result, the solid curves of Figures 21 to 24 have been calculated on the basis of an n^2 relationship; and except in the case of very short pulses (for which it is difficult to establish a steady clamp level), the fit is quite good. The time constant for the activation of g_{K2} decreases sharply with greater depolarization; the time constants used in plotting Figures 22 and 23 were 160, 81 and 19 msec in order of increasing depolarization. Since

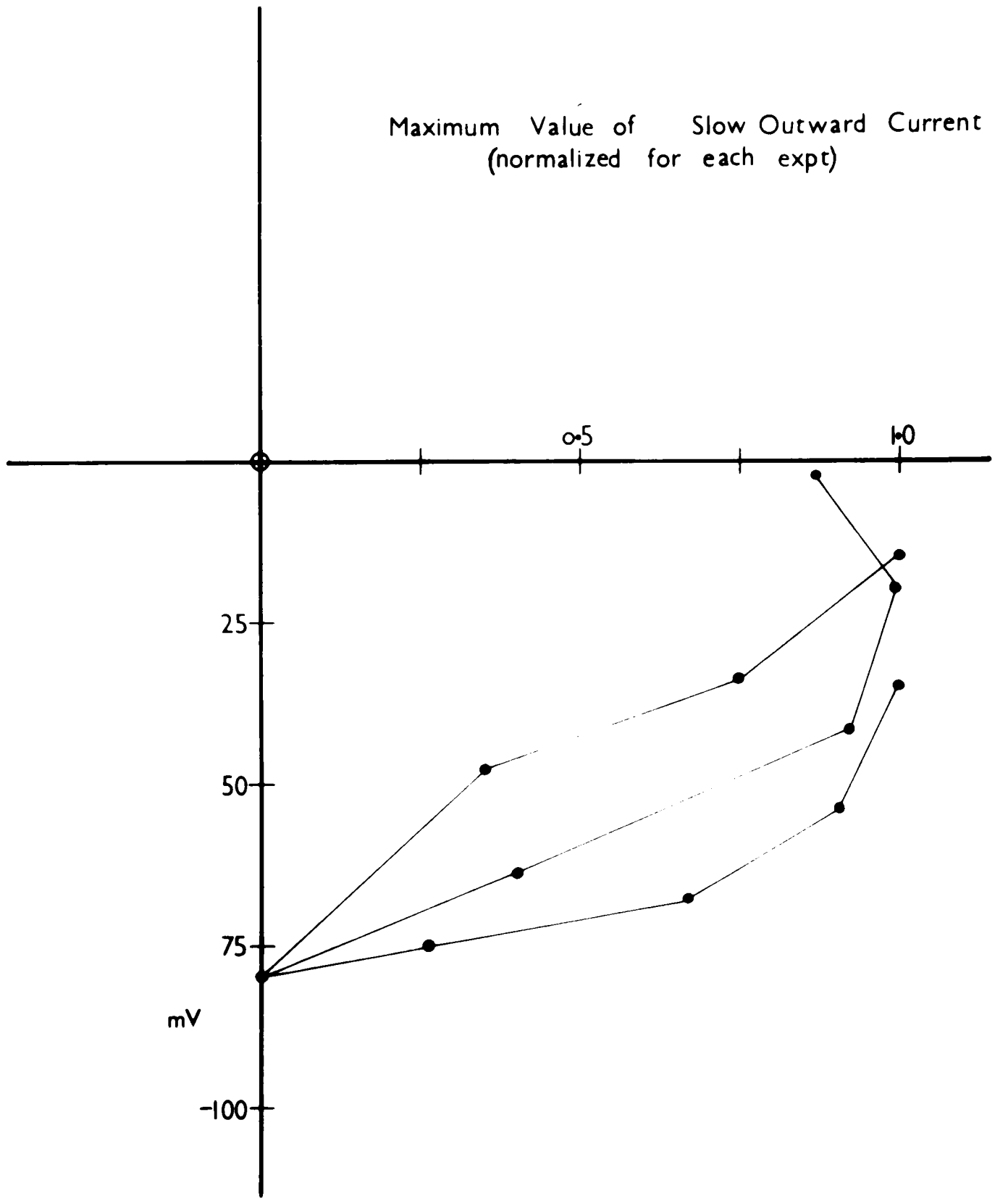


Figure 25 : Normalized maximum slow outward current as a function of the level of the depolarizing clamp, for three experiments.

depolarization increases both amplitude and rate steeply, clearly the rate constant a_n will also be voltage dependent; for

$$a_n = \frac{n_\infty}{t_n} \quad \text{and} \quad b_n = \frac{1 - n_\infty}{t_n} , \qquad (25)$$

where n_∞ is proportional to the square root of the normalized steady state current at each voltage level. Figure 26 gives the results of calculations for a_n and b_n, based on the experiments yielding the lower two curves of Figure 25. The hatched lines are the tentative values used in Noble's (1962) solution of the Hodgkin-Huxley equations for cardiac muscle. Clearly some major adjustments in these parameters will be required, although the general trend of the functions seems satisfactory. As a first approximation, Noble's function for a_n could be multiplied by 5 to 10, and b_n could be divided by 5: this would bring about the correct order of magnitude. (The value of b_n calculated for -2mV is assumed dubious, and ignored here; two very small numbers were divided to obtain it). Other constants in the Hodgkin-Huxley equations will then have to be modified to bring the various components of conductance into correct proportion again, since the major effect of such changes in a_n and b_n would be seen in faster rises and falls of g_{K2}; but such modifications are best done empirically with the aid of an electronic computer. Although the shape of the computed pacemaker and plateau regions will probably be slightly altered, the general features of the computed action potential are unlikely to be seriously affected.

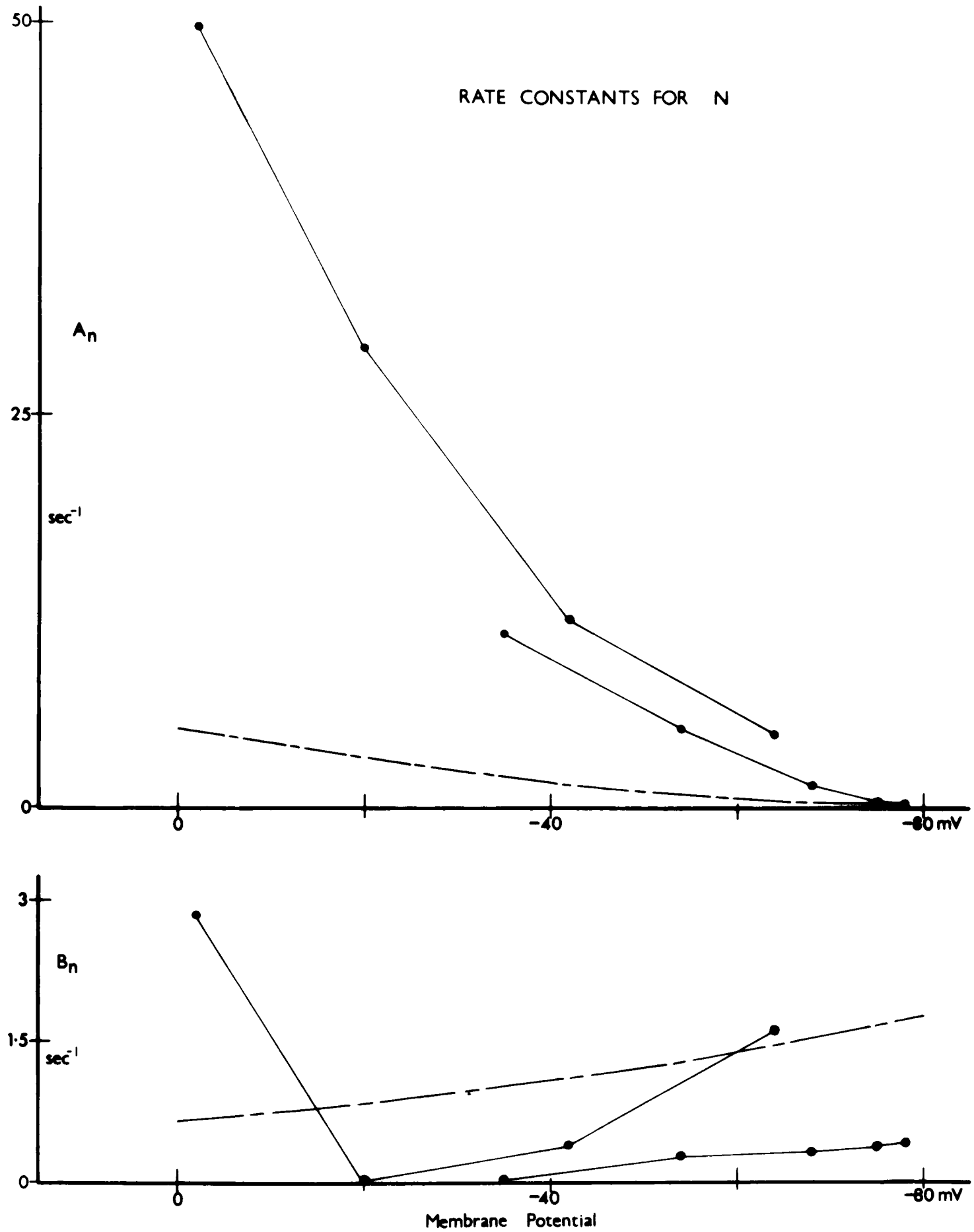


Figure 26 : Rate constants a_n and b_n plotted against membrane potential. The solid lines join points calculated from two of the curves of Figure 25; the interrupted lines are the relations used in Noble's (1962) computations.

The curves of Figure 25 meet the voltage axis at the resting potential at a very sharp angle. Notably, slow outward current is switched on for even the smallest departures from the resting level in Tyrode solution: the high threshold for this effect in Na-free solutions (Figure 12), therefore, provides strong evidence that substitution of choline for sodium does not leave the membrane unchanged, and so invalidates measurements of Na-current by simple subtraction of Na-free results from those in Tyrode. In Tyrode solution, it is possible that some g_{K2} is activated even at the resting level; perhaps up to 25% could be 'on', although a greater amount is unlikely since removal of sodium and consequent increase of g_{K2} threshold do not appreciably affect resting conductance. Various degrees of g_{K2} activation can be assumed in calculating n_∞ as a function of voltage; but fortunately, a_n and b_n remain relatively constant as assumptions of 0 to 25% are tried. Figure 22 was plotted assuming 20% active at -80mV. Experiments have not yet been attempted to accurately determine the actual amount of g_{K2} activation at the resting level; however, the good fits of the n^2 curves in Figures 22 to 24, where no activation was assumed, also suggest that it is not large.

3.3 DISCUSSION

Indications of a possible negative transient current, discussed in Section 2.3 in relation to the notch sometimes seen in the upstroke of the membrane potential response to constant-current stimuli, may also be seen in some of the voltage clamp records; the currents required for the two larger depolarizations of Figure 19 are an example.

The magnitude of the final outward current no longer increases, but the earliest current after the depolarization starts at a lower level which may even be negative in the uppermost picture. Such an early current is not uncommonly seen for large depolarizations (see also Deck & Trautwein, 1964). Rather than a transient inward current, it could also be due to a large initial fall in outward current conductance - i.e. very strong inward rectification - superimposed upon the g_{K2} rise; a stronger g_{K1} would be expected where the membrane was depolarized somewhat (increasing $e_m - E_K$), and depolarization has been found to have an effect in this direction. That the current-voltage relation of g_{K1} may also describe the instantaneous one of g_{K2} has already been discussed (Section 3.2); however, this mechanism alone will not account for the notches of Figure 5.

On the other hand, in the upper left tracing of Figure 6 there is a slow transition from the initial capacitive spike to the steady current level required for polarization to -15mV. While some of this is probably due to the slow current through that part of the membrane capacitance in series with a constant resistance (Chapter 4), it lasts much longer than such a current alone. Further depolarization to +45mV did not evoke a second such current, indicating that there may be some voltage-dependent inactivation as seen for Na currents. The records in Figure 6 are from a fibre in Na-free solution. In response to very ~~very~~ large depolarizations, a slowly-decaying outward current is often seen, rather than the increasing one associated with g_{K2} increase. Probably this marks the initiation of a new ionic current, and not a change in the properties of g_{K2}; for in response to depolarizations to

around -10mV, the declining outward current sometimes gives way to a slower increasing one: the implication being that the former can mask the latter at more positive levels of polarization. Another possible source of this fast transient outward current could be a third form of time and voltage dependent K conductance, a 'g_{K3}', which is rapidly activated at high levels of depolarization and then inactivated more slowly. At threshold level for such an effect, g_{K2} could be expected to take precedence over g_{K3} with time, but perhaps not so at higher levels. There is no further information on such a conductance change at the moment, except that it does not affect the positive after-current on repolarization (Figure 23) within the resolution time of the voltage clamp (i.e. 15-20 msec after the potential change) and so must be quite distinct from g_{K2}.

Na removal has previously been found to decrease the outward current seen after a depolarizing clamp (Deck & Trautwein, 1964; and, for myelinated nerve nodes, Frankenhaeuser, 1962), and this has been confirmed in these experiments. With ChCl replacing NaCl, out of 19 experiments definite slow outward rectification for strong depolarizations has been seen in 11; in 4 experiments there was no such effect, and in the other 4 the current for large depolarizations was too unsteady to give a reliable indication. In the eleven positive experiments, the threshold for g_{K2} was very variable, and always much higher than in Na-containing solutions (Figure 12). In Tyrode, the slow outward current was usually fully activated before -20mV (Figure 25), whereas in choline solutions the threshold was generally more positive than -30mV. In the case of Figure 6, the slow current was not switched

on until the membrane was depolarized to +25mV or beyond (top left). The threshold in Tyrode solutions is very much lower. Initially it was believed to be about 20mV below resting potential, but further experiments showed quite the contrary: not only is the threshold not very far in the depolarizing direction, but it may in fact be below the resting potential. As seen from Figures 22 and 23, The time constant for activation of g_{K2} increases greatly at more negative membrane potentials, from 19 msec for a 78 mV depolarization to 160 msec for a 16 mV depolarization in this case. When longer voltage clamps were applied, it was found that the progression continued (Figure 24), so that g_{K2} was activated with a time constant of 600 msec for a 12 mV depolarization, increasing to 1,750 msec for a 2 mV depolarization. When the level of maximum activation is plotted versus depolarization as in Figure 25, the steepness of the intersection with the resting potential suggests that some g_{K2} is activated even at the resting potential; the amount is almost certainly less than 25% as discussed in Section 3.2.

The effect of Na removal on the magnitude of g_{K2} may possibly arise from an antagonism between Na and Ca ions; if these were competing for the membrane sites which determine the conductance parameters (n, m and h), raising the concentration of one may cause the same effect as a decrease in the concentration of the other. Orkand & Niedergerke (1964) have suggested that the conductance at the peak of the frog ventricular AP is constant if $[Ca]_o/[Na]_o^2$ is kept constant. Weidmann (1955) has shown that increased Ca concentration acts by shifting the relation for the steady state of h in a positive direction on the membrane potential axis, so that the threshold for changes in h is

higher. If the same effect occurred for n, and if the ratio $[Ca]_o/[Na]_o^2$ should actually be the controlling factor, then a decrease in $[Na]_o$ would also shift the threshold for g_{K2} activation higher - as is observed. Should such a hypothesis hold, it might explain some of the variability of results for the kinetics of g_{K2} obtained by different groups working on Purkinje fibres in Na-free solutions, since $[Ca]_o/[Na]_o^2$ would be highly sensitive to any remaining Na when $[Na]_o$ is reduced toward zero. Reuter (1966) has shown that more outward current occurs at a given depolarization in low Ca solution; this is consistent with a lowering of g_{K2} threshold. His finding that the slow fall in membrane response with time is abolished when Ca is removed may indicate simply a shift in the same direction of the time constant, as might be expected. Dudel, ~~et al.~~ Peper, + Trautwein (1966) have shown that the slow outward current declines much more quickly on repolarization when $[Ca]_o$ is zero in Na solution, so that in Reuter's experiments it may have switched on very rapidly as well. However, at the moment this hypothesis is little past the speculative stage.

The outward current seen following repolarization declines much more slowly than it switches on (during the depolarization). This is quite in keeping with the Hodgkin-Huxley theory, however; equations 25 may be rearranged to show that n changes exponentially at any given voltage, with a time constant $tn = (a_n + b_n)^{-1}$. The rate coefficients a_n and b_n are quite strongly voltage dependent; if the suggestion from Figure 26 is taken and Noble's rate coefficients a_n and b_n are multiplied by 8 and 0.2 respectively, tn becomes 39 msec

at -20 mV and 630 msec at -80 mV. The time constants are longer than these in the fibre of Figure 19, but their difference at the two voltage levels is very plain.

The role of g_{K2} in the normal cardiac action potential is now becoming quite clear. It appears to be the main cause of the initiation of repolarization, as it rises during the plateau; and it is almost certainly the sole cause of the pacemaker potential, as it declines during diastole. Vassalle (1966) has confirmed this mechanism by clamping back to the resting potential at various times during the action potential, and has also identified the ion concerned as K by clamping to the K equilibrium potential. The slow time course and low threshold of g_{K2} also help to explain the effects of small changes in membrane potential and frequency on the action potential duration.

The modified Hodgkin-Huxley equations as proposed by Noble (1962) will require some further modification in order to account for these effects. In particular, the results presented in Chapters 2 & 3 suggest some possibilities, although certain of the results - e.g. the temperature effects, and the transient outward current on large depolarizations in Na-free solutions - are not yet sufficiently well known for any mathematical analysis to be attempted:

(1) The rate constants for n must be changed; the threshold for g_{K2} is at or below the resting level.

(2) The exponent of n in the equation for g_{K2} should be reduced by a factor of at least 2. A first power of n may even prove preferable, according to more recent results.

(3) Some allowance must be made for the non-linearity of

the instantaneous g_{K2}; a profitable line of approach here might be to incorporate g_{K1} and g_{K2} into one function, so that the total g_K is given by

$$g_K = \overline{g_K}\ (a + n^2)\ f\ (e - E_K) \quad ,$$

where $f(e-E_K)$ is the present equation describing g_{K1}, and a is a suitable constant.

(4) Changes in the threshold for g_{K2} when Na is removed from the solution must be included. A factor including the ratio $[Ca]_o/[Na]_o^2$ may be of use here.

(5) Where responses to long current pulses are to be described, some allowance for the K accumulation effect, such as a linear or other change in E_K with time, should be included. This will not be necessary for normal action potentials.

CHAPTER 4 COMPUTATIONS

Noble's (1962) modification of the Hodgkin-Huxley equations to provide a mathematical model for Purkinje fibre action potentials was highly successful despite the lack of detailed information on certain relevant properties of the membrane, particularly the voltage- and time-dependence of the rate constants and outward potassium conductance. A consideration of the results presented in the previous two chapters has led to modifications in some of the constants and parameters of these equations, and new computations have therefore been performed, using some of these, for the sake of comparison. In addition, evaluation of the technique of applying a voltage clamp with linear time-dependent amplitude (a ramp) to the cell membrane in order to obtain an instantaneous plot of a current-voltage relation, which is becoming more common in the literature, has been attempted by computing solutions to the membrane equations under these conditions.

Noble's computations were performed in 1960-62 on the London University 'Mercury' digital computer, using a Runge-Kutta numerical approximation method. This computer was slower by a factor of ten than present-day models, and some economy of machine time was required; to achieve this, the step length of integration was increased by a factor of ten, from 0.1 to 1.0 msec, during the slowly-changing phases of the action potential. The programming language used was 'Autocode'.

The computer presently available in Oxford is a modern English

Electric-Leo-Marconi KDF-9 machine, for which the main programming language is Algol. The starting-point in the present mathematical analysis, then, was the writing of a program in Algol which would reproduce the earlier results. Because of the greatly increased speed of computation, it was also decided to attempt to make the integration step length more flexible. The complete and annotated program is given in Section 6.1.

Ramp-shaped voltage functions have been applied to the excitable cell membrane by several workers in recent years in the form of 'ramp' voltage clamps'; the object has been to obtain a much faster impression of the membrane current existing at each of a whole range of values of membrane potential. The procedure takes only a few seconds or minutes at most, as compared with the half-hour or more required to plot a current-voltage relation by constant-current pulse analysis; as a result, there is the possibility of ~~reducing~~ minimizing any deterioration of the membrane caused by the test currents and the time taken to obtain the data. Also, the current through the pure membrane capacitance is reduced to a constant, leaving as variables only those through the conductances (or so it is often assumed). However, there are two very real disadvantages which affect these apparent benefits. At any particular membrane potential, the slower time-dependent conductances are still at values governed completely by earlier values of potential, whereas the 'instantaneous' components of the conductances and the electro-chemical gradients are determined completely by the latest value. The resulting confusion gives rise to unavoidable errors in the measured voltage dependence of the membrane currents; the

differing time constants of activation and inactivation of the variable conductances mean that only a very slow ramp function can yield data subject to analysis without the prior assumption of a membrane model, and such a ramp will provide no information on the time dependence. In addition, it is unlikely that at least part of the membrane capacitance is without some series resistance, which would give rise to serious transients. However, the results of fast ramp-voltage clamps are being described (Dudel, Peper, Rüdel & Trautwein, 1966; Bennett & Grundfest, 1966) and interpretations attempted, as discussed in Section 4.3; no computed responses to a ramp voltage clamp have as yet appeared to check these interpretations.

4.1 METHODS

4.1a The Computed Membrane Action Potential

The method used was different from that of Noble in two ways: Runge-Kutta approximations were not used to obtain the values of the conductance parameters n, m, and h; and the step length of integration could be increased or decreased automatically during the calculation to obtain desired accuracy in a minimum of computer time. Rather than apply the Runge-Kutta (RK) methods to equation 17, the new values were obtained by using equation 18 with t set equal to the integration step length, dt; thus a good approximation to the new value of the parameter was obtained in only one computational step, rather than the five of the RK method. The step length of integration was changed by performing a routine check of the membrane potential value after a set number of integration steps had been completed (usually five); the same end-

values were computed over a doubled step length, beginning from the values current two steps previously, and any discrepancy between the two values outside set limits caused a changing of step length (and recalculation, if the step length was found too large). An absolute rate of change of membrane potential greater than a specified limit also caused reduction of step length and recalculation.

The Runge-Kutta method (e.g., Hawgood, 1965) was used to calculate new values of membrane potential, e. This gives four approximate values from four complete compuations, which are averaged with appropriate weighting to produce the final new value. Each of the approximate values generated new values of the rate constants and conductance parameters, which were used in the next approximation. The main steps in the operation of the program were as follows:

(1) Initial values of membrane potential, time, and conductances fed into computer store, along with values of operation-controlling variables.

(2) Rate constants, g_{K1}, and time constants and end-values of conductance parameters calculated as a function of the current value of e, using Noble's empirical equations.

(3) Values of conductance parameters and time-dependent conductances calculated, using equations 18 and 19.

(4) First extrapolation to a new value of e is calculated, using the RK method on equation 20 with $I_m = 0$.

(5) Steps 2 to 4 are repeated for this new value of e and steplength dt/2, giving the second value of e.

(6) Steps 2 to 4 are repeated for this 2nd value of e and

step-length dt/2, giving the third value of e.

(7) Steps 2 to 4 are repeated for this 3rd value of e and step-length dt, giving the fourth value of e.

(8) A weighted mean is taken and the final, new value of e is obtained.

(9) Time is advanced one step, and control returns to step 2.

The final computed action potential reproduced that of Noble exactly; the result is shown by Figure 27 from his paper (the results of his computations were available, and there was exact agreement with his numerical values to the required number of significant digits). One complete action potential was computed by the 'Kalgol' method (i.e. using the Kidsgrove algol compiler, the more efficient system of the two available in Oxford) in about six minutes, covering 830 msec of real time in about 500 steps of integration varying from 0.03 to 1.0 msec in length.

Because the results of the last two chapters suggested that the exponent of n in equation 13 should be 2 rather than 4, new computations were performed in the same manner as above, with a view to finding the required changes in the various constants.

Once these programs had been established, modifications were made to enable computation of the effects of a series resistance-capacitance (series-RC) component in the membrane in parallel with the pure membrane capacitance. This required a modification of equation 20 to include the current through this part of the membrane as an added

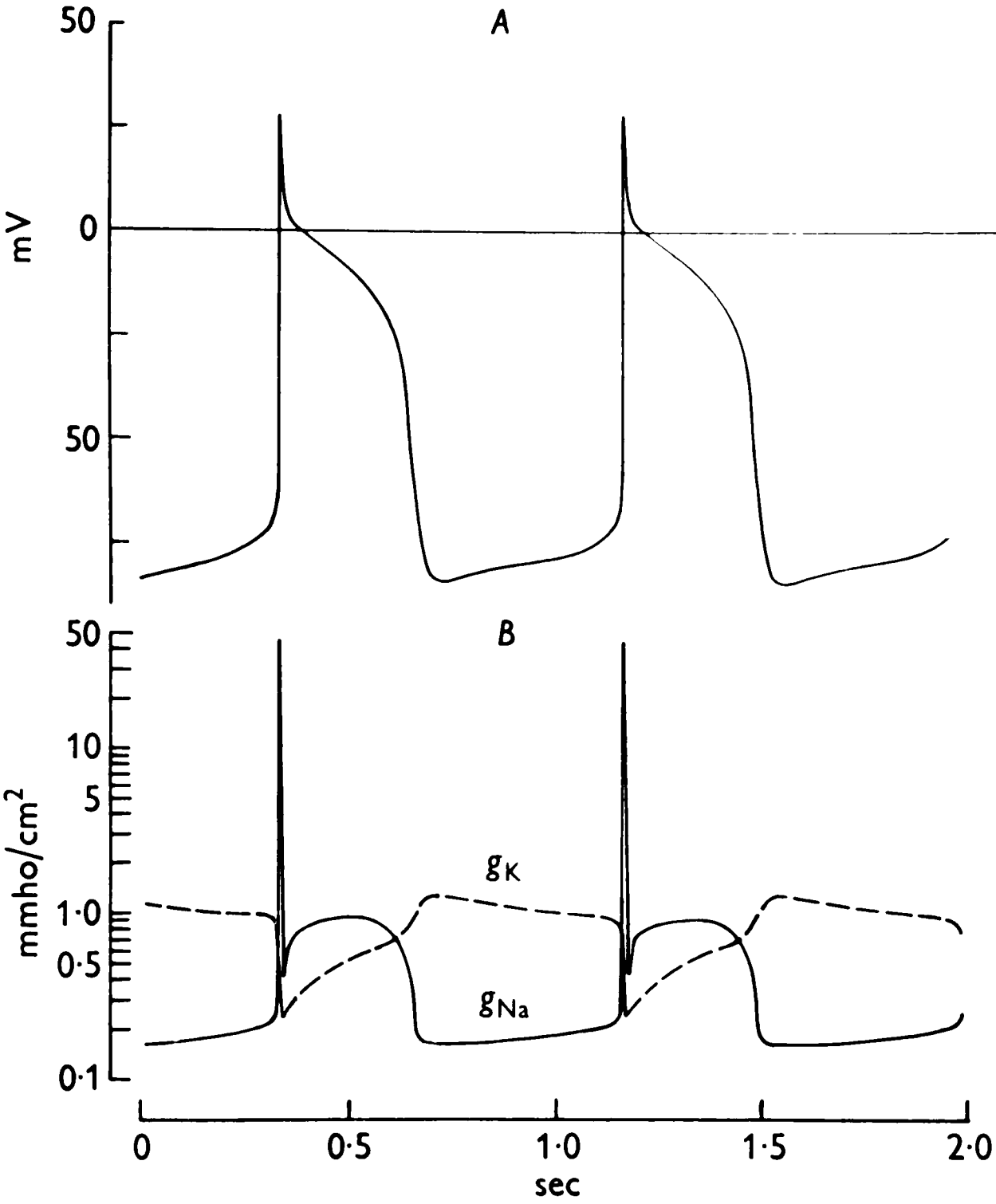


Figure 27 : Cardiac action potential and conductance changes computed from Noble's modification of the Hodgkin-Huxley equations. From Noble (1962).

term on the right side:

$$I_m = \left[c_m + c_s(1-\exp(-t/r_s c_s))\right]\frac{de}{dt} + \bar{g}_K n^4 (e-E_K) + \bar{g}_{Na} m^3 h (e-E_{Na}) + \bar{g}_L (e-E_L) \quad , \qquad (26)$$

where c_s and r_s are the in-series values. The method of computation was similar to that outlined above, but with the following differences:

(1) An initial value, io, of the current through the series-RC branch of the membrane equivalent circuit was read into the computer. This need not be a very accurate value, since any error in this term would be eliminated after one action potential has been computed. The initial value was usually chosen by multiplying the rate of change of voltage in a slowly-changing part of the diastolic depolarization phase, by the value of the series capacitance (i.e., by assuming that io had reached its steady-state value for an applied, slowly-changing ramp voltage).

(2) The RK extrapolations were made from equation 26, rather than equation 20.

(3) When the new value of e at the end of the step was found, de/dt over this step was also computed, then the new value of io was found from the equation

$$io = c_s \frac{de}{dt}\left[1 - \exp(-dt/r_s c_s)\right] + io \exp(-dt/r_s c_s) \; ; \qquad (27)$$

this is the theoretical expression for the current at the end of the step dt, when the initial current was io.

This cycle was repeated as many times as was required to

generate a complete action potential.

4.1b The Ramp-shaped Voltage Clamp

The computations for a ramp voltage clamp were performed on Noble's (1962) membrane model; this was for reasons of convenience (the computations preceded the complete analysis of the experiments of Chapters 2 and 3), and continuity with the established literature. Any changes which would arise in the computed results because of the modifications of this model must be small, since the modifications were confined to relations governing the variables with slower time dependence, and it is fast ramp voltage changes that are being chiefly considered here.

Two different Algol programs were written. One used the Runge-Kutta method to arrive at new values for the conductance parameters [illegible], as did Noble; the other was based on the method of computing the action potential described in Section 4.1a. The first produced results identical with the second, and provided a check on the method; however, it required more than twice as much computer time to calculate each current-voltage relation, and was therefore discarded. Only the second program will be described, and an annotated copy is included in Section 6.2.

The method is basically the use of equations 18, 19 and 20 to calculate I_m for a given value of e. The value of e is then changed in steps, a new I_m being calculated for each new value of membrane potential. The calculation is simpler than that of the action potential, since e is no longer a free variable. The step size was chosen

small enough so that further decrease caused no detectable change in the computed current-voltage relation; for example, a step of 0.3mV gave a current-voltage relation indistinguishable from those for steps of 0.03 and 0.015mV. Larger steps than 0.3mV did give rise to an error, underestimating the magnitude of the fast current changes; steps of 0.1mV were always used. The basic operations of the program were as follows:

(1) Calculate the new value of e, according to the rate of rise or fall being considered.

(2) Calculate the rate constants, and time constants and end-values for the conductance parameters for this e.

(3) Calculate the conductance parameters and conductances.

(4) Calculate the membrane current and its ionic components.

(5) Repeat from (1).

Parts of this program were taken directly from that for the computation of the action potential. It was arranged that once the rate of change of e had been specified, the current-voltage relation would be calculated for a change at this rate from a given initial membrane potential up to a maximum (usually E_{Na}), and then down to a minimum (usually E_K); the clamp waveform was thus a 'sawtooth'.

The effects of a series-RC component of the membrane on this result was also computed. The current through such a branch, after a square-wave voltage has been applied, is given by

$$i_{rc} = i_o \exp(-t/RC) \; ; \qquad (28)$$

here i_o is the initial current (applied voltage step divided by

series resistance), and i_{rc} will become zero as the capacitance changes to the new value. The ramp voltage clamp is simulated by supposing the voltage to change in a step-wise fashion; as the size of the steps becomes very small, the solution approaches that for a true ramp. In this case the initial current i_o is given by the sum of the current i_{rc} at the end of the last step and the amplitude of the new voltage step divided by the series resistance.

The resulting solutions agree with the theoretical one arrived at by Laplace transform analysis. Given any current-voltage relation from an applied ramp-voltage clamp, the effect of adding a series-RC component to the membrane is to superimpose a transient current upon it, having the value

$$i_{rc} = c_s \left(1 - \exp\left(-t/r_s c_s\right)\right) \frac{de}{dt} \; ; \qquad (29)$$

i.e. the additional current approaches a constant value in a time determined by the size of the series resistance and capacitance.

4.2 RESULTS OF COMPUTATIONS

4.2a Results with g_{K2} as a Function of n^2

Besides changing the exponent of n in equation 19 to two, it is necessary to choose a new value for $\overline{g_K}$ (which is 1.2 when the exponent is four), since the action potential is very sensitive to changes in g_{K2}. Various values ranging from 0.01 to 1.2 were tried, beginning the computation at -80mV and with the same (almost steady-state) starting values for n, m and h in every case. When

$\overline{g_K}$ was very low, an early depolarization occurred which was much like a normal AP spike; then, when the plateau of the repolarization was reached, the rate of repolarization practically ceased and the plateau was indefinitely prolonged, just above the zero potential level (no sign of further repolarization was seen when the computation was extended for up to 1½ sec of 'plateau'; in fact, g_{Na} increased slightly at the end of this time). As $\overline{g_K}$ was raised, the depolarizing spike occurred later and the plateau level fell slightly; when values of 0.3 and 0.45 were tried, the repolarization continued during the plateau at a normal rate for a few hundred msec before the levelling-off occurred at -10 to -20 mV. Finally, a value of 0.6 caused an action potential of acceptable shape to be generated, as shown in Figure 28. It appeared that if the repolarization during the plateau could be induced to exceed about -20mV, then a normal final repolarization phase would occur. This is to be expected, because below about -15mV the steady-state Na current (which is reached very early in the plateau) begins to decrease, and as soon as the K current exceeds it repolarization will occur (see Figure 18); i_K will not exceed i_{Na} until $\overline{g_K}$ is given a sufficiently large value. Larger values of $\overline{g_K}$, up to 1.2, only caused a later occurrence of the spike and an earlier and faster repolarization (see Figure 13 of Noble, 1962, for the effects of increasing g_K). Figure 28 compares the effects of fourth and second powers of n, and also in the latter case of decreasing the membrane capacitance from Weidmann's (1952) value of 12 $\mu F/cm^2$ to 9.4 $\mu F/cm^2$, the total value measured by Fozzard (1966). The smallest value of $\overline{g_K}$ which would generate repetitive AP's for a second-power

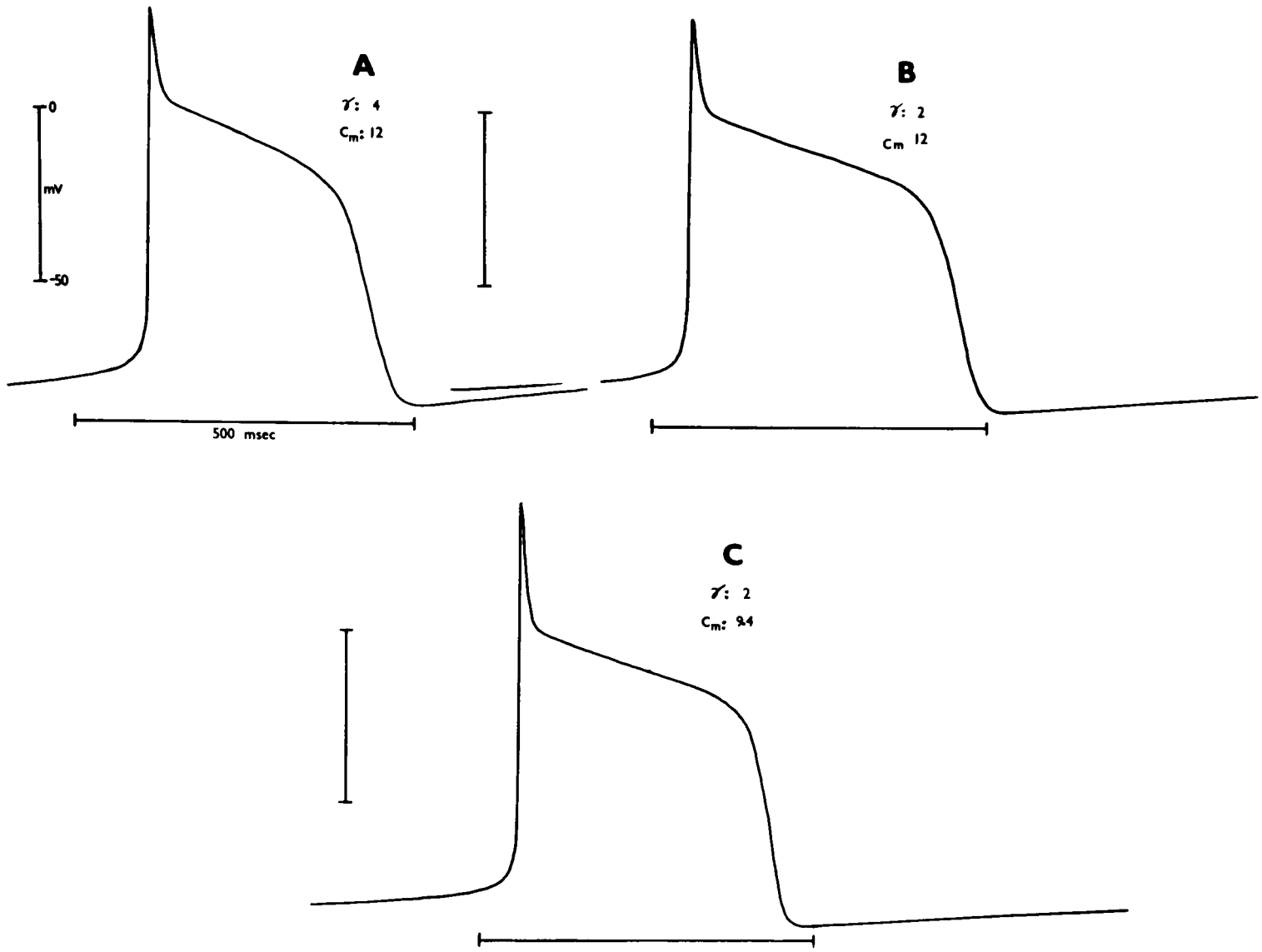


Figure 28 : Computed action potentials, with (A), $g_{K2} = 1.2\ n^4$, Cm = 12 $\mu F/cm^2$; (B), $g_{K2} = 0.6\ n^2$, Cm = 12 $\mu F/cm^2$; and (C), $g_{K2} = 0.6\ n^2$, Cm = 9.4 $\mu F/cm^2$. The starting potential is -80mV in every case.

relation of n also caused the highest frequency of firing; the smallest period with C_m = 12 was thus 1336 msec, compared with 815 msec for a fourth-power relation. This was shortened to 1253 msec when C_m was reduced to 9.4 $\mu F/cm^2$; but it is apparent that the two cases cannot be made to generate the same frequency of firing without altering some other conductance parameter, Altering the magnitude of g_{K1} would probably be the simplest solution, until more voltage clamp data is available to suggest a better one. The difference in frequency apart, there seems little reason for preferring a fourth-power-of-n relation for a computed AP, if a second-power relation is indicated by experimental data.

4.2b Results with the Series-RC Component Included

Most of the study of the effects of a series-RC component in the equivalent membrane circuit were done using the fourth-power relation for g_{K2}, since the primary aim was to get results comparable with those of Noble (1962), obtained while considering a pure membrane capacitance only. The membrane capacitance used here was normally that indicated by Fozzard's (1966) measurements; i.e. the total capacitance was usually 9.4 $\mu F/cm^2$. Figure 29, therefore, shows the effect on Noble's computation of decreasing C_m from 12 $\mu F/cm^2$ (A) to 9.4 $\mu F/cm^2$ (B); in the latter case, the frequency is about 5% higher and the maximum rate of depolarization during the spike is increased, while the overshoot increases by 10 mV. However, the shape of the action potential is very similar, and it is not unlike many which have been recorded in experiments.

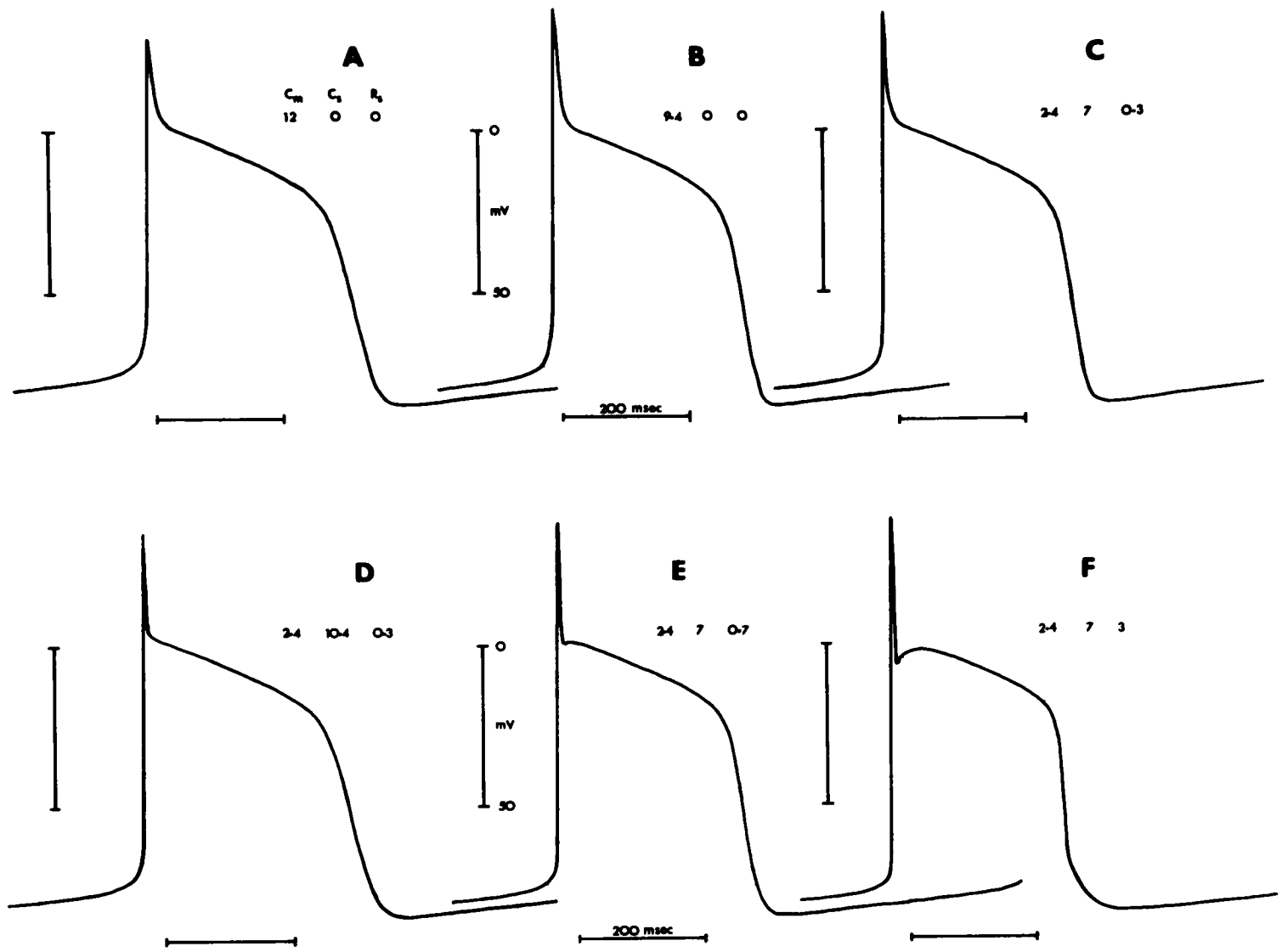


Figure 29 : Computed action potentials with $g_{K2} = 1.2\ n^4$ and a series-RC element in the membrane. Starting potential is -80mV in every case. Pure capacitance (C_m), series capacitance (C_s), and series resistance (R_s) are indicated by numbers above each AP, in $\mu F/cm^2$ and K ohm cm^2.

The rest of Figure 29 shows the effects of placing part of the membrane capacitance in series with a constant resistance. In C, the values calculated by Fozzard from the results of an experiment on a Purkinje fibre have been used: the pure capacitance (C_m) is 2.4 $\mu F/cm^2$, that in the series element (C_s) is 7 $\mu F/cm^2$, and the resistance (R_s) is 300 ohm cm^2. The shape of the AP is practically unchanged, except in one notable respect: the spike is sharper and of shorter duration, with a maximum rate of depolarization of 286 V/sec compared with 97.3 V/sec for the AP with a pure capacitance only. As a result, the frequency of firing is increased slightly, by about 1.5%. The time constant (R_sC_s) of the series-RC element is 2.1 msec, so that the potential on C_s can lag appreciably behind that of C_m if the latter is changing rapidly; in this case, when the peak overshoot potential is reached, C_s is charged only to -40mV and is therefore drawing a considerable current (the current drawn by C_s is given by the difference in potential between C_m and C_s, divided by R_s). The current drawn by C_s, (i_s), during the depolarization slows the rate of depolarization, since less current is available to charge C_m (the potential on C_m is the membrane potential); but C_m is much smaller than the 9.4 $\mu F/cm^2$ of Figure 29B, so even this reduced current will increase the rate of depolarization in Figure 29C. The depolarization itself is brought about by the rapid increase of g_{Na}, due almost entirely to an increase in the conductance parameter m when threshold is reached, occurring with a time constant of 0.1 - 0.2 msec over the range -80 to + 35mV; by the time the peak overshoot is reached, m is within 1% of its steady-state value at that level. The potential would undergo a

further slight increase as C_s is charged to the same potential and i_s disappears, except that the inward (Na) current is so reduced by the fall in electrochemical potential gradient that it cannot supply the required i_s; therefore current will be drawn from C_m and repolarization will begin even before the net ionic current reverses in sign--a phenomenon that cannot occur if none of the capacitance is in series with a resistance. At the same time but at a slower rate, the complementary parameter h is declining toward its very small steady-state value at the peak potential, so the inward current will decline with time nevertheless and cause repolarization; the time constant for changes in h varies from 8 msec at -80mV to 1 msec at +35mV. There are thus two important points to note at this stage of the analysis:

(1) The rate of depolarization is increased when C_m or C_s is lowered, or when R_s is raised.

(2) Repolarization begins earlier when the charging current i_s is greater at the peak of the spike.

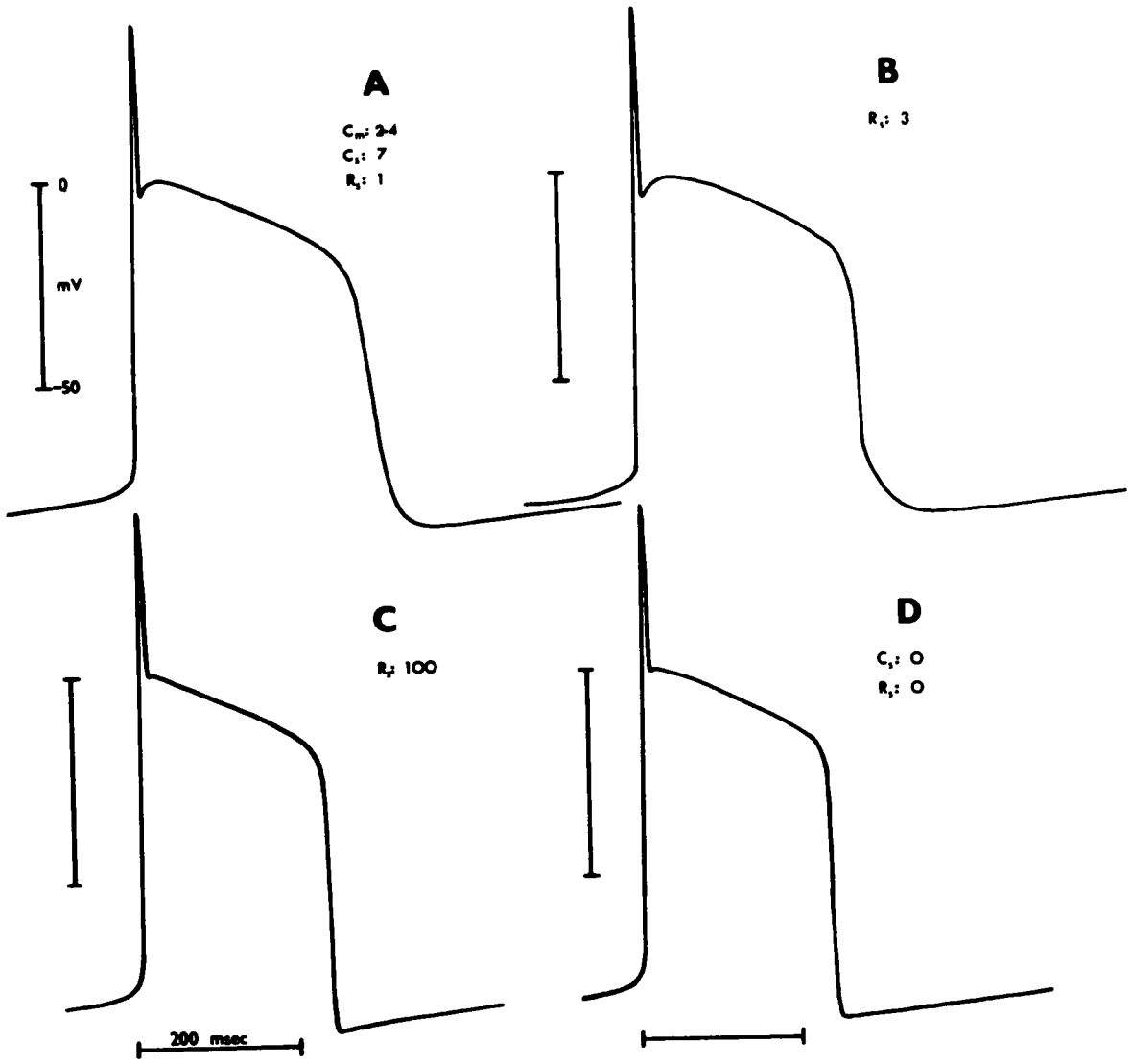
Condition (2) will be satisfied when C_s is made larger for a given C_m and R_s: compare Figures 29C and 29D, computed for capacitances of 7 and 10.4 $\mu F/cm^2$ in series with 300 ohm cm^2. It will also be satisfied when R_s is large enough to allow a fast rate of depolarization and slow rate of charging C_s, but also small enough to allow a substantial i_s to flow when potential on C_s lags behind e_m. Clearly there will be an optimal value of R_s giving the earliest repolarization for given C_m and C_s; thus in Figures 29C, E and F, all with the same capacitance, the widths of the spike at the +20mV level are respectively 4.67 msec (R_s = 300), 4.04 msec (R_s = 700), and 4.95 msec (R_s = 3000 ohm cm^2).

Once the repolarization has begun, its rate will be controlled by the interrelation between i_s and the net ionic current (through the conductances); it will cease when these are equal. Without a series-RC element, a balance between the inward Na current and the outward K current is brought about near the zero potential level by the changes in g_{Na} and the driving forces for Na and K, and a plateau begins. With an RC element, however, the repolarization ceases when a balance between the currents has been reached such that $|i_s| + |i_K| = |i_{Na}|$. Even for the briefest spikes, h declines to a level below its steady-state level for the plateau. If the repolarization occurs slowly, it will remain near its steady-state level thereafter; however, if the repolarization is rapid, it may still be below its steady-state value when the plateau level is reached. In this case, i_s decreases as C_s is charged nearer the plateau level, as usual; but also, i_{Na} increases with a time constant of about 1 msec as h rises toward its plateau-level steady-state value. In this way there arises the possibility of a significant alteration in AP shape: the appearance of a 'notch' between the spike and the plateau. The delayed increase in i_{Na} manifests itself as a decrease in the net outward ionic current. Both this and the normal decrease of i_s (as the potential on C_s rises) will tend to slow the rate of repolarization, and if their sum is sufficiently great a secondary depolarization can occur. As mentioned above, i_{Na} will increase with a time constant of about 1 msec; this must be much faster than the decrease in i_s, for such a short time constant for the series-RC element would certainly allow C_s to be practically fully-charged by the time the repolarization

to the plateau has occurred, and therefore eliminate i_s. In this way it becomes clear that the controlling factor in the generation of the notch is h, although it certainly will not have a non-steady-state value at the beginning of the plateau unless the series-RC element is present to cause a rapid repolarization to that level.

Figures 29E, 30A and 30B show computed AP's with a notch which grows deeper as the series-RC time constant approaches 20 msec. Figure 31 shows the changes in the Na current during the notch in Figure 30B, on a much increased time scale; the changes in i_s and i_K during this time are relatively very slight. If R_s is increased somewhat further, the peak of the effect is reached and it then begins to decline; the charging current i_s is reduced and the repolarization from the peak potential occurs more slowly, allowing h to approach its steady state more closely. The limit for large R_s is the case for which $i_s = 0$, i.e. when C_m is 2.4 $\mu F/cm^2$ but C_s and R_s are zero; the highest possible rate of depolarization (393 V/sec) is attained, and there is only a very slight trace of a notch left (see Figure 30C). With this low capacitance, even the final repolarization to the resting level is very rapid, and the AP takes on a very rectangular appearance. In Figure 30D a practically identical AP to that of Figure 30C is obtained even if the product R_sC_s is kept the same as for the AP with the greatest notch, Figure 30B, but C_s is reduced and R_s increased; this indicates the importance ~~for~~ *of* a large i_s, prevented in this case by the large R_s, in causing the rapid repolarization and hence the notch.

If the capacitance C_s is increased from 7 to 10.4 $\mu F/cm^2$



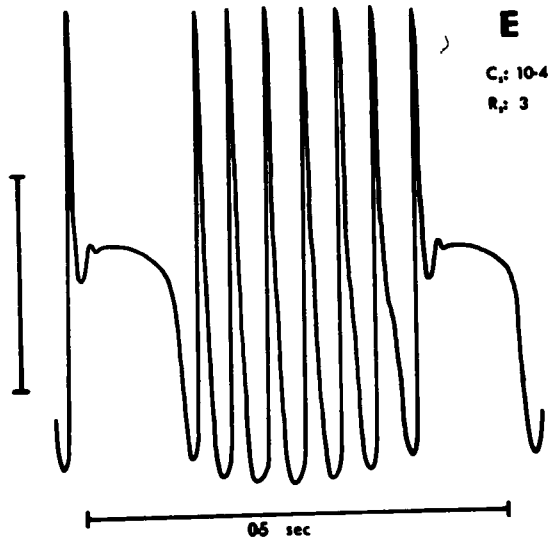
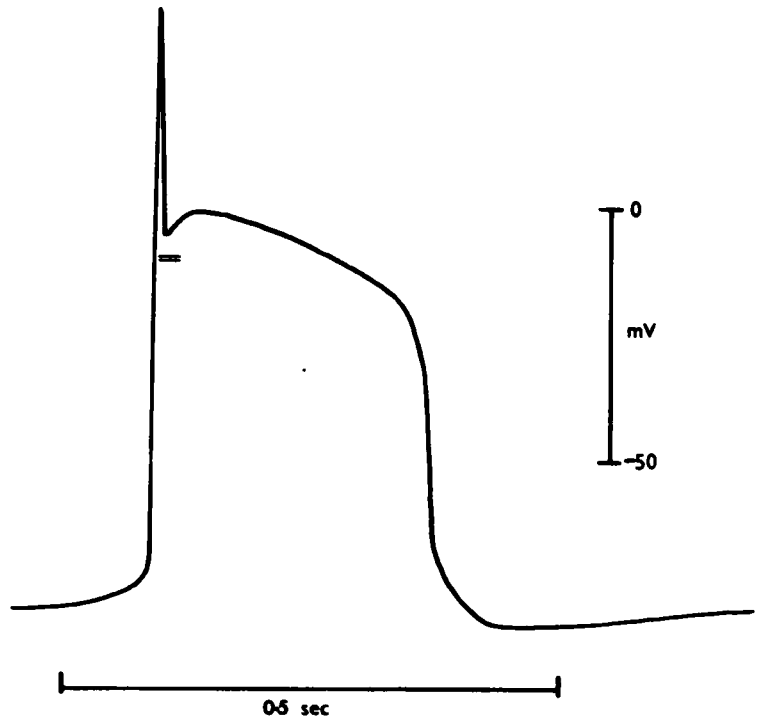


Figure 30 : Computed action potentials with $g_{K2} = 1.2\ n^4$ and a series-RC element in the membrane. Starting potential is -80mV in every case, but in E only the steady-state configuration is shown. C_m, C_s and R_s have the values indicated in A, unless otherwise noted by each AP.



C_m: 2·4 C_s: 7 R_s: 3

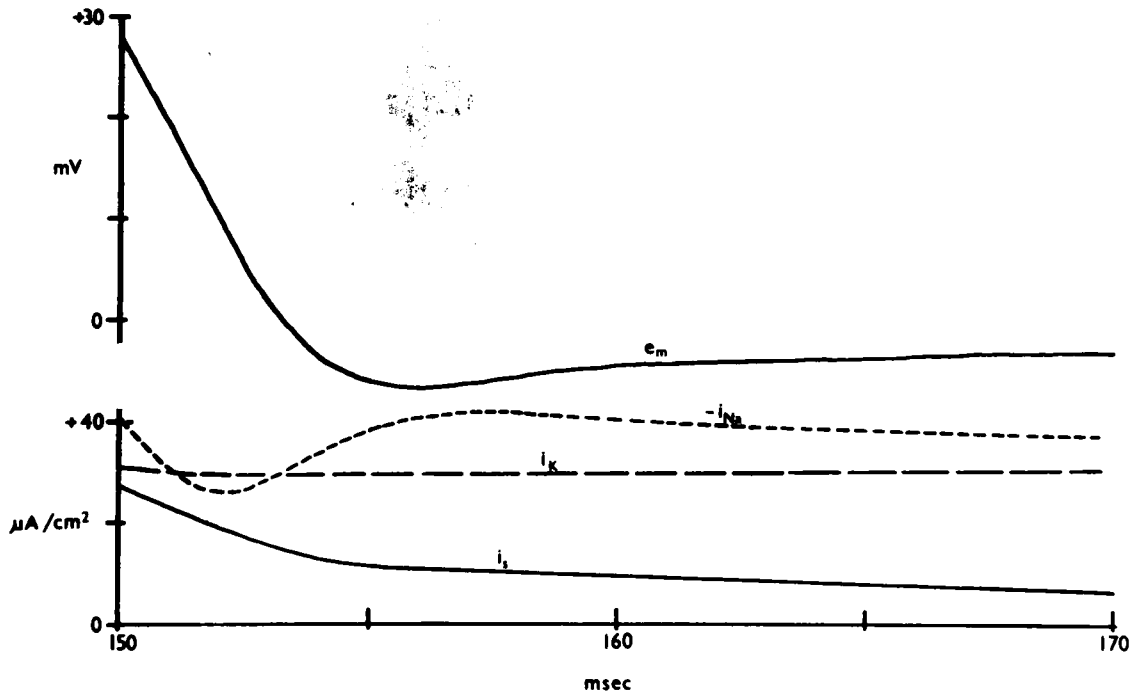


Figure 31 : Top: the AP of Figure 30B. Bottom: the currents flowing during the notch (underlined, top figure), shown on a greatly-expanded time scale. i_s is the current through the series-RC element.

and the other elements are as for Figure 30B, another interesting result is obtained as shown in Figure 30E; a repetetive train of six spikes of varying amplitude, and a seventh one resulting in a short AP, is the steady-state configuration. The notch is apparently deep enough in the other six cases to cause all-or-nothing repolarization. This configuration only occurs after g_{K2} has been increased, as during the plateau of a normal AP; once g_{K2} is sufficiently high, spike-like action potentials as computed by Noble (1962; see his Figure 13, curve a) for a membrane with high g_K occur. In the present case, after the plateau of the short notched AP, g_{K2} declines during the next six spikes because the positive excursions are of too little duration to cause a net increase. At the same time, however, C_s, is discharging from its high potential of -19mV reached during the plateau; as it does so, it provides progressively less depolarizing current, and the maximum diastolic potential rises after each of the next three spikes. Then, however, the decline in g_{K2} takes precedence and maximum diastolic potential falls again, until g_{K2} becomes so low that there is insufficient repolarizing current after a spike to turn the notch into a repolarization, and another plateau occurs. The cycle then repeats itself, and in this way Noble's spike-like action potentials become repetitive. (damped oscillations of h about its steady state level occur early in the plateaux of this figure, because the rise in h towards its plateau level carries the membrane potential far enough to establish a new steady state level for h which is lower than its current one, etc.) If C_m is made smaller the same process appears to occur, but at a much higher frequency because of the small current needed to change the

potential on C_m. Sixteen spikes have been computed in 200 msec this way when C_m is only 0.1 $\mu F/cm^2$, their envelope appearing much like that of the first three spikes of Figure 30E; however, step lengths as low as 5 μsec were needed, and too much computer time was required for this computation to be extended to cover the whole steady-state configuration. Obviously, though, at least some of the membrane capacitance must not have a resistance in series with it, if the Hodgkin-Huxley model is valid.

A notch also occurs when g_{K2} is a function of the second power of n, as would be expected because of the relatively insignificant part played by g_{K2} in its generation. However, the repolarization at the end of the plateau becomes very sharp as R_s is increased to 3000 ohm cm^2, and it is preferable to assume a larger value for C_s (e.g. 10.4 $\mu F/cm^2$) in order to decrease this to a more normal value.

4.2c Ramp Voltage Clamp Results

The results illustrated in Figure 32 are for a membrane with pure capacitance only, and for ramp speeds of 0.001 to 10 Volts/sec. The constant current required to continually change the charge on the membrane capacitance has been omitted for the sake of clarity; it is positive during the upward portion of the ramp and negative during the downward portion. It has been assumed that the membrane was clamped at -80mV for a long time prior to each ramp voltage clamp. The large negative 'hump' of current which begins to appear at -60mV for a ramp of 0.3 V/sec is the active sodium current, which in normal circumstances gives rise to the spike of the action potential. The increase in size

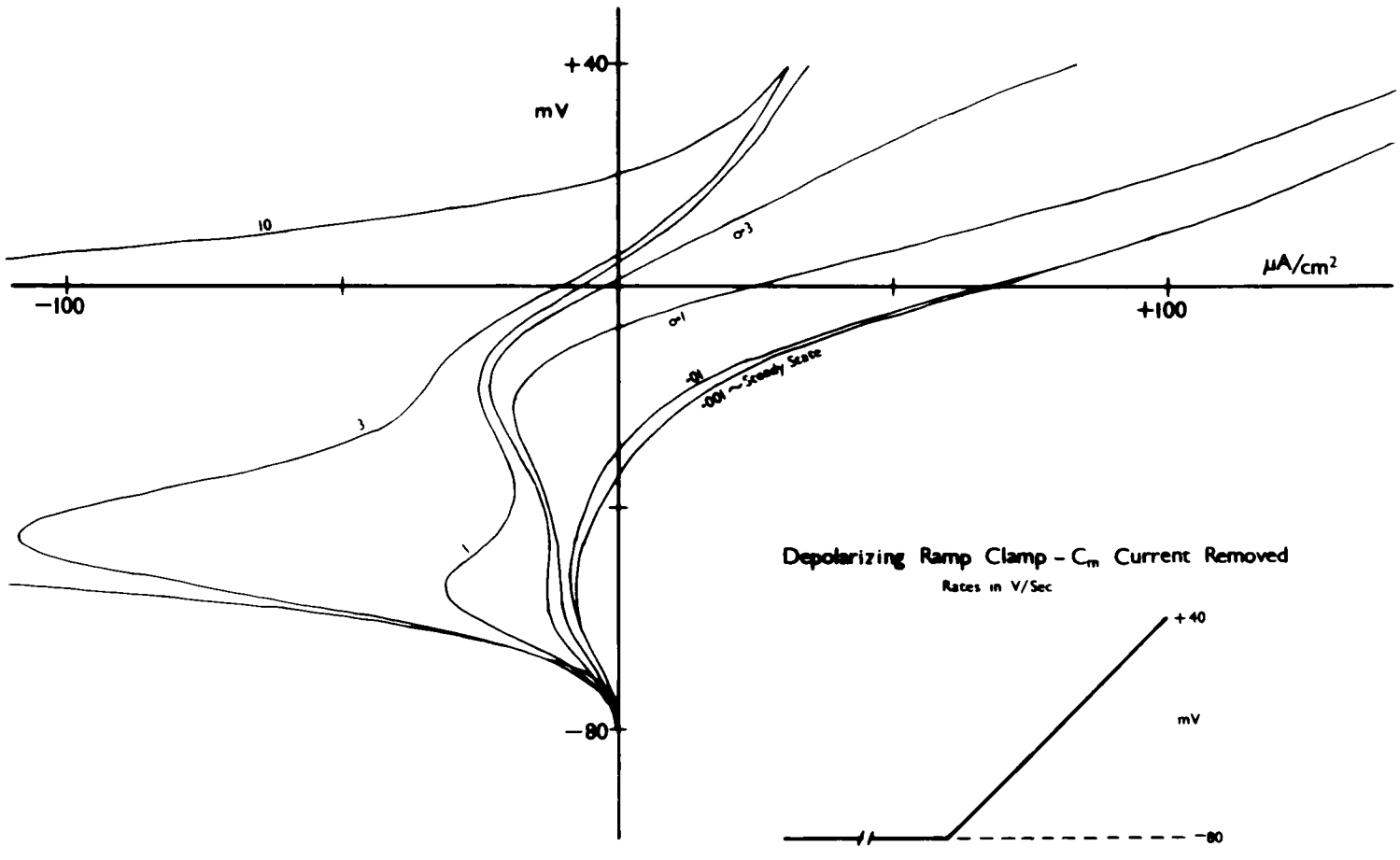


Figure 32 : Current-voltage relations for depolarizing ramp voltage clamps of various speeds, computed from Noble's modified Hodgkin-Huxley equations. The constant capacitive current has been removed. The figures beside each tracing give the ramp speed in V/sec.

of this with increasing ramp speed is to be expected, since the conductance parameters are farthest from their end-values when the potential is changing fastest, and therefore they also change faster - and, since g_{Na} has a third-power dependence on the more-rapidly changing activation parameter m, the latter's effects temporarily swamp the inactivating effect of h. The peak of the inward current occurs at more positive potentials with increasing ramp speeds for similar reasons: h lags further behind a faster-changing potential, so inactivation sets in later.

The current-voltage relation as measured by very long constant-current pulses is the same as that computed for the slowest ramp in Figure 32; at a rate of change of only 1mV/sec, the conductance parameters all achieve virtually their steady state values. The displacement to the right of the uppermost points of the curves for different rates reflects the increase in K-current due to the switching-on of g_{K2} (since at this potential, + 40mV, the Na-current is zero). Figure 33 gives the repolarizing current-voltage relations following the depolarizations of Figure 32. These are much more similar to each other, because the fast sodium conductance changes have been completed before the repolarization begins (this is not true for ramp speeds greater than 10 V/sec, when a large negative Na-current appears during the repolarization).

At speeds greater than about 1 V/sec, the amount of g_{K2} which has been activated when repolarization begins is relatively small, corresponding to the steady state value at a membrane potential not far above resting level; as a result it continues to increase during

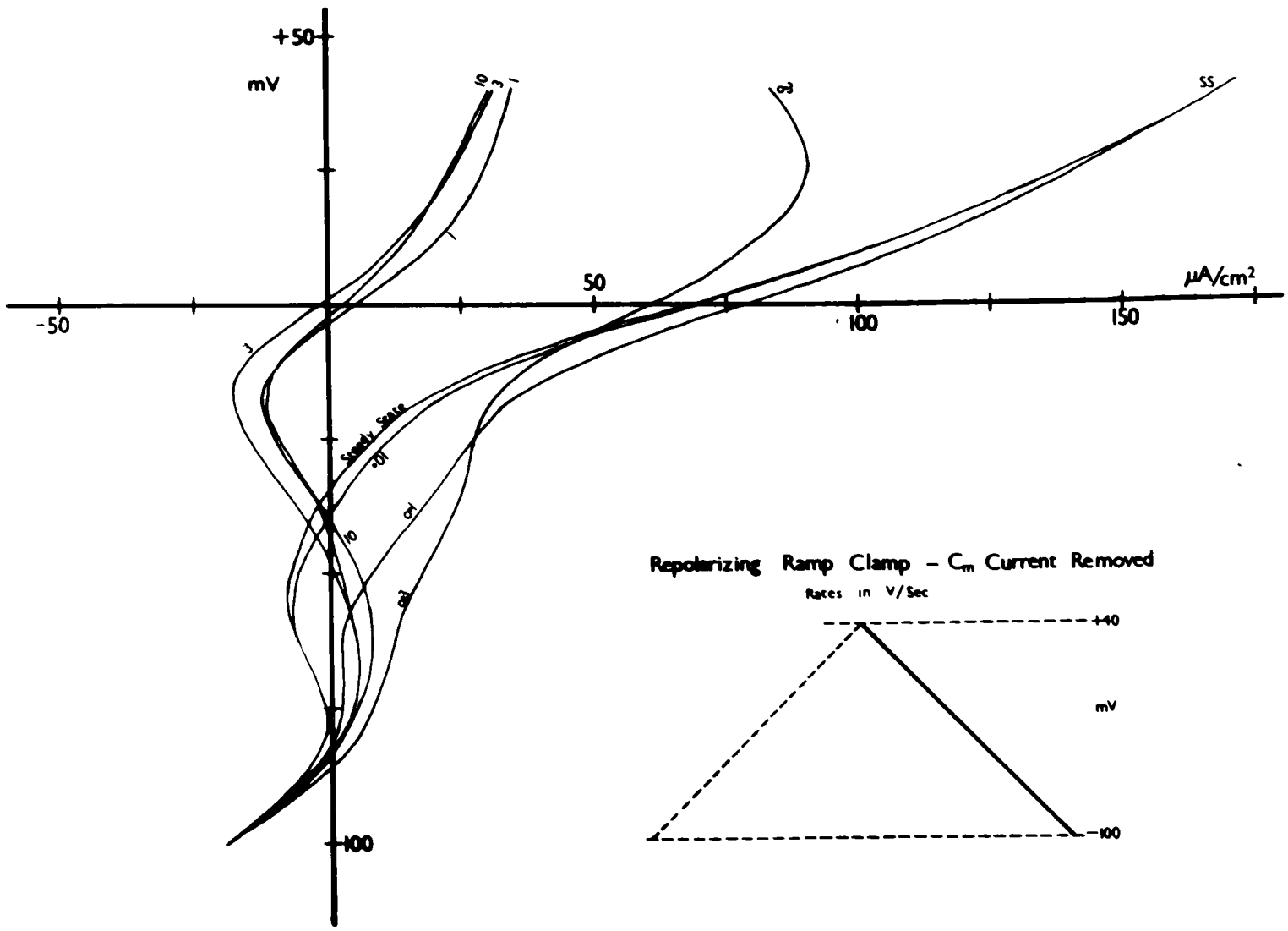


Figure 33 : Computed current-voltage relations for repolarizing ramp voltage clamps, each of which is applied immediately after the depolarizing clamp of the same speed in Figure 32. The figures beside each tracing give the ramp speed in V/sec.

part of the repolarization, and so the lower parts of the current-voltage relations bend to the right above the resting level (-80mV). At speeds slower than 1 V/sec, more g_{K2} is activated by the time repolarization begins, so the top of the current-voltage relations is displaced to the right; but most of this has decayed again by the time the membrane has been repolarized to -50mV, so that the lower parts of the relations are influenced more by the negative Na-current- and therefore shift more to the left. The intersections of several of the curves at various membrane potentials are a direct consequence of the interactions between rate of change of e and rate of change of g_{K2} at each value of e.

Figure 34 shows the effects of a series resistance-capacitance component in the membrane in parallel with the pure capacitance. The rate of change of membrane potential is 3 V/sec in every case, and the total capacitance of 9.4 $\mu F/cm^2$ is proportioned in various ways. Curve $\frac{1}{3}c$ corresponds to the values obtained by Fozzard (1966) for the Purkinje fibre. The effect of the series-RC branch is simply to add a decaying transient current and a constant current to the current-voltage relation for the pure capacitance case (curve $\frac{e}{3}$). The duration of this transient is proportional to the product of the resistance and capacitance in series, and the constant current is that which would flow through the capacitance if there were no resistance in series. Then, doubling the resistance and keeping the series capacitance constant only increases the duration of the transient, while doubling the capacitance and keeping the series resistance constant causes the same increase in transient duration and produces an additional constant shift. The

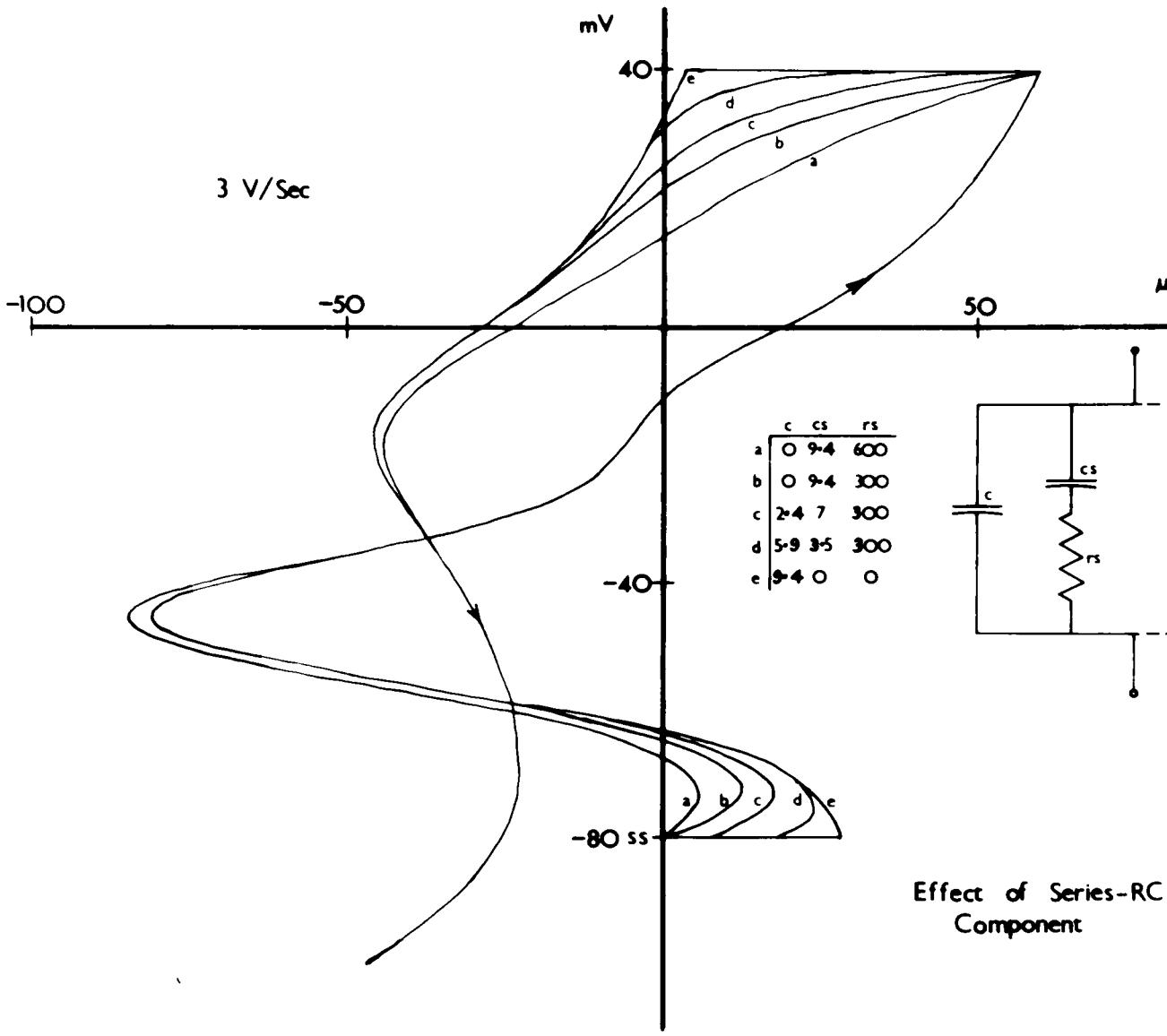


Figure 34 : Effects of a series-RC branch in the equivalent membrane circuit on the computed current-voltage relations for a ramp voltage clamp. The ramp speed is 3 V/sec in every case.

effect is the same for all other ramp speeds, except that for faster ramps the transient may not die out before the direction of the ramp is changed.

Figure 35 gives the current-voltage relations for ramp voltage clamps of 3 V/sec and 0.1 V/sec which would be obtained from the membranes generating the action potentials of Figures 29C and 29F; at the speed of 0.1 V/sec, the results for the two cases are indistinguishable (bottom), and are the same as the relation for a membrane with no series-RC element (Figures 32 and 33). The membrane giving rise to a notched AP passes less outward current, or more inward current, on depolarization, and vice versa on repolarization; but the current-voltage relations are basically so similar that the difference in action potentials would not be suspected on this information alone. It is difficult to escape the conclusion that ramp voltage clamps are of practical use only in measuring time constants of series-RC elements (and even then only if R_s and C_s prove to be constants with respect to both membrane potential and time), and relative effects during studies of fast conductance changes.

4.3 DISCUSSION OF COMPUTED RESULTS

The finding that the rate of depolarization during the spike is increased when part of the membrane capacitance is in series with a resistance - and in particular that, when the configuration is as measured by Fozzard, the maximum rate of depolarization is within the range found by Weidmann - eliminates the main discrepancy between Noble's computed AP and that found in experiments. Noble (1962)

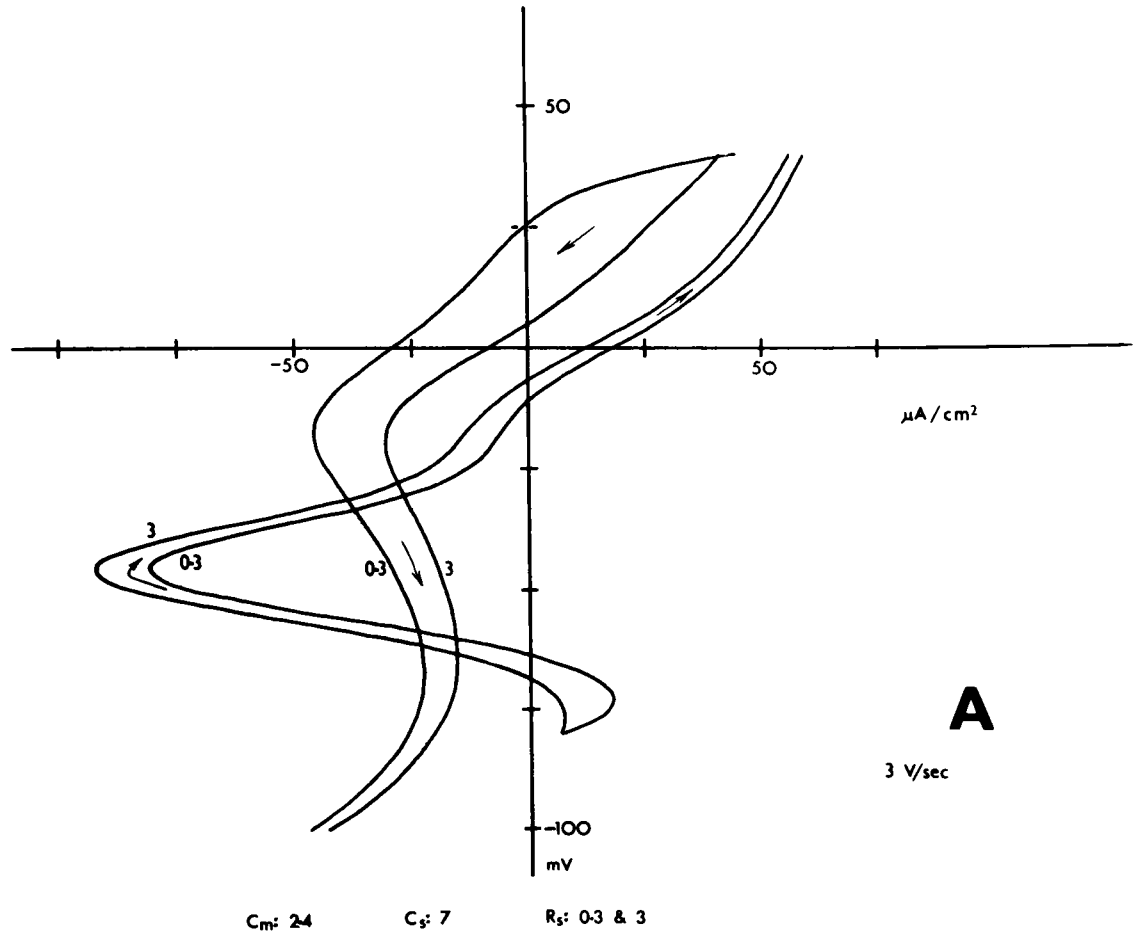


Figure 35 : Computed current-voltage relations for ramp voltage clamps at 3 V/sec (A) and 0.1 V/sec (B), for membranes generating the AP's of Figures 29C and 29F. At 0.1 V/sec, the current voltage relations of the two membranes are identical.

suggested that such a membrane circuit could overcome the difficulty, but had only the measurements from skeletal muscle with which to speculate. Another difference between his computed AP and the recorded ones was in the rate of repolarization after the spike; the reduced pure capacitance in the membrane could also account for this, as could a delayed fall in g_{K1}, which he postulated might account for the notch sometimes seen before the plateau in the AP. It has now been shown that the notch is a logical result of the equations when a series-RC circuit is considered, even when g_{K1} is (as usual) considered instantaneous.

The notch or hump early in the plateau has been recorded by almost every investigator of Purkinje fibre electrophysiology at various times (Draper & Weidmann, 1951; Trautwein, Gottstein & Dudel, 1954; Hoffman & Cranefield, 1960; Carmeliet, 1961; Johnson & Tille, 1961; Deck & Trautwein, 1964; Moore, Preston & Moe, 1965; Vassalle, 1966; Temte & Davis, 1967; Noble & McAllister, unpublished). Fozzard (1966), however, did not show such a notch or mention recording it; possibly, therefore, the series resistance and capacitance measured in his experiments were not the same as would be found for a fibre showing a notched AP. If the resistance R_s were only twice the value found by him, a notch might possibly occur; higher values of R_s would make a notch even more likely, and would not seem to be 'unphysiological' in view of the resting membrane resistance of 1900 ohm cm^2 found by Weidmann (1951). If the series capacitance and resistance reside in folds in the sarcolemma, the membrane resistance would give a guide to the permissible limits of R_s. A difficulty with this postulate,

however, is the huge decrease in R_m on excitation, which would allow C_s to charge rapidly and behave as a pure capacitance during the spike; it would be necessary also to postulate that excitation does not occur inside the 'folds' or invaginations, but short-circuits around them instead. On the other hand, if R_s and C_s resulted from the arrangement of transverse tubules and sarcoplasmic reticulum (see Figure 1), the continued high R_s would be less surprising; in this case excitation of the tubule walls would probably be delayed, if it occurred at all (Girardier, 1965, suggests that it does not), but a significant constant resistance would occur anyway because of the small diameter of the current path. Caesar, Edwards & Ruska (1958) have seen a poorly-developed reticular system in Purkinje fibres, and Muir (1957) has also seen one. Rayns, Simpson, & Bertaud (1967) have provided a convincing demonstration that the transverse tubules are open to the extracellular fluid in cardiac muscle, although this would not be necessary to permit current passage providing any closing membrane is not of high resistance. If either the folds or the reticulum were the source of the series-RC behaviour, differences between individual fibres could be easily explained on the basis of geometrical changes resulting from osmotic effects, stretch, or deterioration.

The basic requirements for a notch are an overshoot of membrane potential lasting long enough for h to decline to near its steady-state value, and a repolarization at the end of this time too fast for h to follow. With the equations as used, this can only occur for normal values of membrane capacitance when there is a resistance in series with some of the capacitance. The equations for h adopted by Noble

were related to Weidmann's experimental values, and so should not be far in error; thus the only factors directly involved in creating a notch, i.e. h, R_s, C_s and C_m, are all experimentally determined. If some other mechanism or agent were to assist in the repolarization, it could supplement the role of the series-RC in generating a notch (the series-RC would probably still be necessary in order to achieve a sufficiently fast depolarization); a possibility here is some other ion whose equilibrium potential is at or below the plateau potential, such as the passive anion current included in some computations by Noble (1962), or the active chloride current suggested by Dudel, Peper, Rüdel, & Trautwein (1967) on the basis of their observations.

It is tempting when considering the result shown in Figure 30E to suppose a role for the series-RC, together with an increased g_{K2}, in cardiac fibrillation. Cooling is known to increase the tendency to fibrillation, and might also be expected to slow changes in h and hence possibly cause a larger notch in the AP. Decreasing h with drugs or depolarizing with high external K concentrations, are both known to stop fibrillation; so is a large electric shock, which might have the effect of reducing g_{K2}. It would presumably be possible to reconstruct Figure 30E by other means than increasing C_s, if C_m and R_s are suitably varied, and possibly to reduce the frequency of occurrence of plateaux (but not eliminate them, if the train of spikes is to continue for long). This has not yet been attempted, so any further speculation by this means on fibrillar mechanism seems premature. In any case, it is not yet certain what membrane potential changes occur during fibrillation. Pillat (1967), however, has obtained spike-like

responses from sheep ventricular fibres in the extended relative refractory period, after a normal action potential, produced by quinidine-like drugs. He has suggested that the drugs may cause a blocking of g_{K2} in the fully-activated state, since rate effects on AP duration are abolished. Toward the end of the relative refractory period, the spike potentials changed to normal action potentials with a very deep notch.

The action potential exhibiting the temperature-dependent effects of Figure 17 was notched at normal temperature, and much more so at low temperature. Rather than postulate a delay in the decrease of g_{K1} on depolarization to explain the observed behaviour, as was done in Section 2.2d, it could also be explained if the increase in h which generates the hump after repolarization to the plateau were temperature dependent. Then, the solid curve of Figure 18 ($-i_{Na}$) would be initially further to the left, and would move slowly to the right as h increased to its steady-state level. This would cause a secondary depolarization, as the point of intersection with the curve marked 'o' rose, to be followed by the normal repolarization as g_{K2} rose. Increasing temperature would then increase the rate of rise to the plateau peak by hastening changes in h. As h lagged behind its steady-state value less and less with increasing temperature, the repolarization from the peak overshoot might be slowed and the notch depth vastly changed; the repolarization at maximum temperature did appear much slower, although why it should slow so suddenly at high temperature is not known.

Finally, many AP's are recorded in a cable-like preparation

yet still show a notch, whereas the present calculations have been for an AP occurring uniformly over the entire fibre. In the cable, some current is diverted along the axis of the fibre, changing the charging rate of the capacitances. This will slow the rate of depolarization and repolarization, but not so greatly that a notch need not occur by the mechanism described here; for with a conduction velocity of 1-2 m/sec along the fibre, even during the fastest conductance changes one or more millimetres of fibre will have practically the same membrane conductance at a given time (except when m is changing rapidly during the upstroke, and that does not directly concern the notch). On the other hand, a series-RC element in the cell membrane is advantageous to the organism by increasing the AP conduction velocity and safety factor.

Ramp voltage clamps were introduced by Trautwein, Dudel & Peper in 1965 in an attempt to quickly obtain current-voltage relations over a wide range of potentials. The idea was to relate currents observed in response to ramps of different speeds to those obtained at various times after a step clamp: e.g. the ramp relation for a speed of 100 mV/sec was compared with that measured 100 msec after the beginning of square clamps, etc. During these studies they particularly noted a hysteresis effect, in that the depolarizing current-voltage relation was not the same as the repolarizing one; the latter was shifted to the right in the region of -50mV in Tyrode solution, and the depolarizing relation was on the right in Na-free solution. Time-dependent conductance changes were believed excluded, because the hysteresis occurred for ramps of 0.1 and 0.01 V/sec, and even slightly

at 0.001 V/sec; and the negative current which they observed on depolarization did not appear on repolarization even when the ramp speed was increased to 3 V/sec. However, they underestimated the time constant of h, the Na inactivation factor. Figures 32 and 33 show that hysteresis is to be expected from the processes described by the modified Hodgkin-Huxley equations even for ramp speeds of 0.01 V/sec, and it increases and shifts to the left when ramp speed is increased just as the relations measured by Trautwein et al. It arises because the excitatory Na current is both voltage and time dependent; its maximum occurs near -50 mV but it is almost completely inactivated by the time the repolarizing ramp begins unless the ramp speed is greater than 10 V/sec. In addition, g_{K2} rises throughout the clamp, so that slower ramps produce a shift of the hysteresis loop to the right. If Na-free solution can be assumed to change E_{Na} to a value of about -90mV (Dudel, Peper, Rüdel & Trautwein, 1966), then the positions of the depolarizing and repolarizing relations reverse in the computed case also; this is very marked if g_{Na} is assumed unchanged by $[Na]_o$ changes, and still occurs, though greatly diminished, even if P_{Na} is reduced according to the Goldman constant-field relation (which is probably an excessive reduction). Some of Trautwein et al.'s measured hysteresis may also be due to the accumulation of K ions outside the membrane during the long periods of polarization for slow clamps (see Section 2.2c), in particular when they stopped the clamp midway for one minute to look for time-dependent changes; they found none, but accumulation and increasing g_{K2} must have been causing changes in opposite directions, perhaps so as to compensate one another's effects.

In the same study they noted a negative current at around -40mV in Na-free solutions, attributed to an as yet unidentified ion. A slight negative current also occurs in the computed relation for low $[Na]_o$ on account of the anomalous rectification g_{K1}, and the fact that Trautwein et al.'s current required low $[K]_o$ suggests that K may be involved (high $[K]_o$ would degrade the anomalous rectification's effect). However, the 'figure-8' type of current-voltage relation seen with this current does not occur in the computed results unless E_{Na} only falls to between 0 and -60mV in Na-free solution; and even then, the depolarizing and repolarizing traces are reversed in position. Possibly some other ion is involved here, as the authors suggested.

Because of the strong voltage and time dependence of the Na and K conductance, it does not seem a profitable avenue of approach to try to relate ramp voltage clamp results to the currents measured during an action potential. However, in 1966, Dudel, Peper, Rüdel & Trautwein used the ramp clamp at a much faster speed to study the fast conductance changes connected with the AP spike. Although the only completely satisfactory way of measuring time and voltage dependences of the membrane conductance is by instantaneously clamping to various potential levels, The capacitive current following such changes masks all the rapid conductance changes in Purkinje fibres. As explained earlier, a ramp clamp reduces this capacitive current to a constant plus a transient, which is much less of a hindrance. Dudel et al found a non-sodium current-voltage relation by locating E_{Na} for different extracellular Na concentrations; they then plotted g_{Na} against membrane potential and found its magnitude varying greatly in proportion

to ramp speed. They were unable to decide whether P_{Na} differed substantially from that in other tissues in its dependence on membrane potential, or rather that the Na inactivation was very fast (1-2 msec). The computed current-voltage relations of Figure 32 are similar to their recorded ones in most respects, even to the second, smaller negative current hump near 0 mV and the shift in the depolarizing direction of the maximum negative current with increasing ramp speed. These computations show that the Na inactivation as measured by Weidmann and formulated by Noble are quite adequate to reproduce most of the experimental observations under ramp voltage clamp conditions. The equations in their present form do not, however, account for the unidentified large negative non-sodium current seen at high ramp speeds (1-10 V/sec) (Dudel, Peper, Rüdel & Trautwein, 1966), or the dynamic positive chloride component seen by the same authors (1967). It is doubtful if ramp clamps will be of much use in measuring the exact time and voltage dependences of these components; but they can yield a time-integral of the active current flowing, and therefore show how the total amount is affected by experiments designed to alter it.

A possible further use of the ramp clamp technique would be in observing relative changes in C_m, C_s and R_s; this has not yet been attempted. However, as explained in Sections 4.1b and 4.2c, the constant and transient currents flowing during a ramp clamp can be separated easily, providing the transient has time to decay to zero. In this case, changes in C_m are reflected in shifts of the (non-transient) ramp current-voltage relation only; C_s changes shift this relation and also prolong the transient current; and R_s changes prolong the transient

only. This might lead to some indication whether R_s and C_s reside in the transverse tubule system of the cell; such tubules are known to swell in hypertonic solution (Girardier, 1965) and would probably be affected by this much more than simple folds in the membrane, thus causing large changes in R_s and C_s.

5 SUMMARY OF THE RESULTS OF THIS STUDY

Experiments with long constant-current pulses on Purkinje fibres in Na-free choline solutions have reproduced the S-shaped current-voltage relations measured by others, and voltage clamp studies have confirmed that there is often a negative conductance region at intermediate levels of depolarization. Experiments in solutions with increased K concentration have shown that resting membrane conductance increases logarithmically with K increase, but with a slope only 60% of that predicted by the constant-field relation. The depolarization of the resting potential in high-K solutions was about 85% of the theoretical depolarization of the K electrode potential, considered independent of other ions, if the concentration of relatively impermeant ions in the external solution was held constant. When this was not done the depolarization was much less, for reasons which are not yet clear; it is possible that osmotic changes have increased $[K]_i$. However, the resting conductance rise for this case is predicted even less correctly by the constant-field relation if $[K]_i$ is assumed changed so that the observed resting potential remains 80% of E_K; this argues against the large osmotic changes required. The current-voltage relations in increased-K solutions (impermeant ion concentration not constant in these experiments) crossed each other as would be expected if the value of the inward-rectifying K conductance were described by a function of $(e - E_k)$ rather than e; thus, the shape

of the relation was similar in external K concentrations up to at least 100 mM, but a greater current was required for a given polarization in high-K solutions. The maximum degree of inward rectification was found for a deflection of 10-15 mV from resting potential in K concentrations of 4 to 100 mM. Outward rectification threshold was usually between 0 and -30 mV in the $[K]_o$ range 4 to 24 mM, but was too variable for any K-concentration dependence to be discerned.

Outward rectification was found to obey the Hodgkin-Huxley type kinetics when the parameter n was raised to the second power rather than the fourth. While the threshold was high in Na-free solution, it was very low - probably slightly below the resting potential - in normal Tyrode solution, so that polarizations below the threshold for an action potential could switch on an appreciable time-dependent outward current. This outward rectification current saturated near -20 mV. The instantaneous value of the outward rectification was non-linear with voltage; it is suggested that its instantaneous value is governed by the inward rectification mechanism, and that the time-dependent changes in magnitude are superimposed upon this. This delayed outward rectification, due to potassium ion movements, is probably the main cause of repolarization from the plateau end of pacemaker activity. The rate constants for n proposed in Noble's (1962) modification of the Hodgkin-Huxley equations need revision; initially, a_n might be multiplied by 5 to 10, and b_n divided by 5.

Some evidence has been found of a fast transient negative non-sodium current during large depolarizations in both normal and Na-free solutions.

Large outward currents applied to the membrane have been found to affect E_K. It has been shown that K ions probably accumulate in an adjacent extracellular space, since the affect is proportional to the amount of charge passed and is largely abolished by increasing external K concentration. Currents flowing during normal action potentials are unlikely to cause any significant accumulation. The diffusion away from this space is not limited by a single-sheet barrier.

Large effects of ambient temperature on the action potential have been noted, particularly on the plateau level and action potential duration. A strong temperature dependence of h (and thus g_{Na}) has been suggested as a possible cause.

Computations on the effect of a series-resistance-capacitance equivalent in the membrane have been performed, using Noble's modified Hodgkin-Huxley equations. The rates of depolarization and repolarization to the plateau are increased to within the experimentally-measured ranges by such a circuit; this eliminates the major discrepancies between Noble's results and those actually measured. The notch which is often seen to occur between spike and plateau is also generated under appropriate conditions. It depends upon a fast repolarization to the plateau level following a spike, and occurs because the parameter h rises to its steady state value with a delay in such circumstances. Satisfactory action potentials are also generated at a somewhat slower rate by the same equations when g_{K2} is made dependent on n^2 rather than n^4, providing $\overline{g_K}$ is halved.

Computations of the currents during a ramp voltage clamp have

also been performed on these equations. A hysteresis loop results for a depolarization followed immediately by a repolarization, and this has been observed in the experiments of Trautwein et al (1965). A series-RC element in the membrane causes a decaying transient current when the clamp is initiated or reversed, the time constant of decay being the product of the resistance and capacitance. Changing the series capacitance also causes a d.c. shift, whereas changing the resistance does not. It is concluded that little information on the time or voltage dependence of the various membrane conductances can be obtained with such a technique,although a time integral of fast currents can be observed conveniently. It may also be useful in measuring changes in membrane capacitances and series resistance.

- - - - - -

Some of the results presented in this thesis have been published in the following reports:

McAllister, R.E. & Noble, D. (1966a). Delayed rectification in cardiac Purkinje fibres. J. Physiol. 182, 36-37P.

McAllister, R.E. & Noble, D. (1966b). The time constants of the slow outward current in cardiac Purkinje fibres. J. Physiol. 183, 23-25P.

McAllister, R.E. & Noble, D. (1966c). The time and voltage dependence of the slow outward current in cardiac Purkinje fibres. J. Physiol. 186, 632-662.

McAllister, R.E. & Noble, D. (1967). The effect of subthreshold potentials on the membrane current in cardiac Purkinje fibres. J. Physiol. 190, 381-387.

6 APPENDIX

The KDF-9 Algol programs for computing the action potential and the membrane currents during a ramp voltage clamp, for a Hodgkin-Huxley membrane model with an added series-RC branch in the equivalent membrane circuit, are given in the following two sections. They have been annotated in capital letters at the end of each component part; the annotations always appear after the underlined word 'comment' placed at the left-hand margin, and are separated by several spaces from the next part of the program. Algol is a particularly convenient computer 'language', using as it does both upper- and lower-case letters and a wide range of symbols, together with certain key-words (usually underlined) which signify what their most usual English meaning would suggest. As a result, commonsense will usually suffice when an attempt is being made to understand the mathematics as expressed in an Algol program: e.g., any number of (similar) brackets may be used, the first end-bracket always corresponding to the last initial-bracket, etc. Symbols followed by a colon are merely labels attached to particular program segments. 'Procedures' are also known as sub-routines, being minor programs in themselves which are run whenever called for in the main program. The 'library' statement at the beginning of the program simply calls for a section of the computer which already 'knows' the basic operations and functions, such as 'read', 'write', 'sin', 'cos', etc. Any programmer's guide to Algol may be referred to for

information on the general structure of programs; 'KDF-9 Algol Programming', available from English Electric-Leo-Marconi Computers Ltd., Kidsgrove, Stoke-on-Trent, or the Oxford Computing Laboratory, for five shillings, is quite adequate.

6.1 KDF-9 ALGOL PROGRAM FOR COMPUTING THE CARDIAC ACTION POTENTIAL, WITH A SERIES-RC SEGMENT IN THE MEMBRANE.

The data required for each run of this program is listed below in the correct order for input, together with the symbol which represents it in the program. Typical values follow in brackets.

Program FALMC 11 :

ei : initial value of the membrane potential in mV (-80)

ti : initial time in msec (0)

a : number of steps the program advances before a check is made (5)

b : factor by which step length is reduced, when necessary (2)

c : factor by which step length is increased, when necessary (2)

d : maximum value of the rate of change of voltage, in V/sec, before step length is reduced to a value less than dtm (0.1)

cc : pure membrane capacitance in $\mu F/cm^2$ (2.4)

ek : K equilibrium potential in mV (-100)

ena : Na equilibrium potential in mV (40)

maxtol : step length is reduced if the discrepancy found on checking is greater than this (0.01)

mintol : step length is increased if the discrepancy found on checking is less than this (0.0001)

tstop : program stops when time reaches this number of msec (1,000)

spew : when this has the value 'true', the data is printed out at the end of every step. Where step-length is reduced, there will be more than one set of data for the same time value; the last one is correct (false)

x : delayed K conductance g_{K2} is given by $xn^z + s$ (1.2)

w : Na conductance g_{Na} is given by $wm^3 + y$ (400)

y : see w (0.14)

ean : leakage equilibrium potential (0)

gan : constant leakage conductance in m mho/cm^2 (0)

f : printout line number. This is repeated 'l' times when spew = <u>true</u> (1)

noo : initial value of n (0.433)

moo : initial value of m (0.0473)

hoo : initial value of h (0.829)

continue : if this has the value '<u>true</u>', the initial values of n, m, h and the conductances are used; if '<u>false</u>', the steady-state values at the initial membrane potential are used to begin the calculation (<u>true</u>)

gktb : initial value of g_{K2} in m mho/cm^2 (0.0421)

gnab : initial value of g_{Na} in m mho/cm^2 (0.179)

gkob : initial value of g_{K1} in m mho/cm^2 (1.00)

z : see x (4)

g : maximum permissible step length, in msec (1)

l : data is printed out after every 'l' program checks, or 'al' successful steps (5)

i : if e is within this limit of the instability points (poles) of the expressions for an, am and bm, the limiting values are assigned instead (0.01)

cs : value of the capacitance in the series-RC branch, in $\mu F/cm^2$ (7)

rs : value of the resistance in the series-RC branch, in K-ohm cm^2 (0.3)

io : initial current through the series-RC branch, in $\mu Amp/cm^2$ (0.149)

s : see x (0)

v : the value of g_{K1} is multiplied by this factor (1)

maxr : if the absolute value of the rate of change of voltage is greater than this value in V/sec, spew is given the value true (25)

maxe : if the membrane potential is more positive than this value, spew is given the value true (10)

dtm : see d (0.1)

number : the number of a particular set of results, which will be printed at the head of the results (1)

fstop : when f exceeds this value the program stops, and moves on to the next set of data. This prevents computer time being wasted if a poor choice of data requires too-small step lengths (5,000)

Thus, forty-one numbers are required for each run of the program. More than one set of data may be input at one time, so that a given allocation of computer time may be fully used. The last set must be followed by one further number, a zero, in order to end the program properly and exit from the computer.

The printout will consist of eleven columns in the following order : time, membrane potential, n, m, h, g_{K1}, g_{K2}, g_{Na}, io, de/dt, and f. Thus, all the data required to carry on the computation of a

given solution at some later date is available, so that the first computation need not be repeated. All the data used for a computation is printed immediately before the results.

```
→ ESTABLISH FALMC1100APU;
EQUATIONS FOR CARDIAC AP, WITH SERIES RC;
O/PL;→

begin  library A0,A6;


comment NOBLES 1962 HH EQUATIONS FOR AP, WITH SERIES RC;

integer a,b,c,f,p,u,fmax,f1,f2,f3,f4,f5,f6,f7,
        f8,f9,number;
real    an,am,ah,bn,bm,bh,gko,gna,gkt,tn,tm,th,ne,j,d,
        me,he,n,m,h,dt,cc,ek,ena,e,t,no,mo,ho,maxtol,
        mintol,ei,ti,dti,tstop,de,x,w,y,ean,gan,noo,
        moo,hoo,gnab,gktb,gkob,z,i,l,g,io,q,r,rs,cs,
        s,v,maxe,maxr,dtm;
boolean  spew,continue;
real array  ke[1:4],  ea,ta,na,ma,ha,ana,ama,aha,bna,
        bma,bha,ioa,edot,gkoa,gkta,gnaa[0:50];

comment ALL THE VARIABLES WHICH WILL BE USED IN THE
        PROGRAM HAVE BEEN DECLARED ABOVE;


procedure ratecon(en);
value en;  real en;
begin
an:=if abs(en+50)>1 then 0.000100000×(-en-50.00000)/
    (exp((-en-50.000000000)/10.000000000)-1.0000000)
    else 0.0010000000;

bn:=0.002000000×exp((-en-90.000000000)/80.000000000);

am:=if abs(en+48)>1 then 0.100000000×(-en-48.000000)/
    (exp((-en-48.000000000)/15.000000000)-1.00000000)
     else 1.500000000;

bm:=if abs(en+8)>1 then 0.120000000×(en+8.000000000)/
    (exp((en+8.000000000)/5.000000000)-1.000000000)
    else 0.600000000;

ah:=0.170000000×exp((-en-90.000000000)/20.000000000);

bh:=(exp((-en-42.000000000)/10.0000000)+1.00000)↑(-1);

gko:=v×(1.200000000×exp((-en-90.000000000)/50.0000000)
     +0.015000000×exp((en+90.000000000)/60.000000000));

tn:=(an+bn)↑(-1);  tm:=(am+bm)↑(-1);  th:=(ah+bh)↑(-1);

ne:=an×tn;  me:=am×tm;  he:=ah×th

end;

comment THIS PROCEDURE EVALUATES THOSE PARAMETERS
        WHICH ARE A FUNCTION OF THE MEMBRANE POTENTIAL
        ONLY;
```

```
procedure nmh(tt);   value tt;  real tt;
begin
n:=(no-ne)×exp(-tt/tn)+ne;
m:=(mo-me)×exp(-tt/tm)+me;
h:=(ho-he)×exp(-tt/th)+he;

gkt:=x×n↑z+s;    gna:=w×m↑3×h+y
end;

comment THIS PROCEDURE USES THE RATE CONSTANTS
        CALCULATED BY ratecon TOGETHER WITH THE
        TIME AND PREVIOUS VALUES OF THE CONDUCTANCE
        PARAMETERS TO CALCULATE THE NEW VALUES OF
        THE CONDUCTANCE PARAMETERS, ACCORDING TO
        A SIMPLE EXPONENTIAL EQUATION;


procedure k(en,a,x);   value en,a,x;   real en,x;
integer a;
begin
ke[a]:=-dt×((gko+gkt)×(e+en-ek)+gna×(e+en-ena)+
       gan×(e+en-ean)+io×x)/(cc+cs×(1-x))
end;

comment THIS PROCEDURE CALCULATES EACH OF THE FOUR
        EXTRAPOLATED VALUES USED FOR A RUNGE-KUTTA
        APPROXIMATE SOLUTION;


open(20);
open(30);
ea[0]:=e1:=e:=read(20);

repeat:
t1:=t:=read(20);  p:=u:=0;
dt:=dt1:=read(20);  a:=read(20);  b:=read(20);
c:=read(20);  d:=read(20);    cc:=read(20);
ek:=read(20);  ena:=read(20);  maxtol:=read(20);
mintol:=read(20);  tstop:=read(20);
spew:=read boolean(20); x:=read(20); w:=read(20);
y:=read(20);  ean:=read(20); gan:=read(20);
f:=read(20); noo:=read(20);  moo:=read(20);
hoo:=read(20); continue:=read boolean(20);
gktb:=read(20); gnab:=read(20); gkob:=read(20);
z:=read(20);  g:=read(20);  l:=read(20);
i:=read(20);  cs:=read(20);  rs:=read(20);
io:=read(20);  s:=read(20);  v:=read(20);
maxr:=read(20);  maxe:=read(20);  dtm:=read(20);
number:=read(20);
close(20);

comment ALL THE DATA REQUIRED FOR THE PROGRAM
        HAS NOW BEEN READ IN;
```

```
ioa[0]:=io;

f1:=format([nddd.ddss]);   f2:=format([+nd.dss]);
f3:=format([ssd.dd10-nd;]);  f4:=format([ssnddddc]);
f5:=format([nddddc]);     f6:=format([ndds]);
f7:=format([+ndd.dds]);     f8:=format([d.dddddds]);
f9:=format([ss+d.dd10-nd;]);

write text(30,[result*number]);  write(30,f4,number);

write text(30,[[c]***ei**********ti**********dti
**********a**********b**********c**********d
**********cm**********ek**********ena******
maxtol******mintol[c]]);

write(30,f9,ei);  write(30,f9,ti);  write(30,f9,dti);
write(30,f9,a);   write(30,f9,b);   write(30,f9,c);
write(30,f9,d);   write(30,f9,cc);  write(30,f9,ek);
write(30,f9,ena);  write(30,f9,maxtol);
write(30,f9,mintol);

write text(30,[[cc]tstop********spew******x**********w
**********y**********ean********gan**********f****
******noo*********moo********hoo[c]]);
write(30,f9,tstop);  write boolean(30,spew);
write(30,f9,x);  write(30,f9,w);  write(30,f9,y);
write(30,f9,ean);  write(30,f9,gan);  write(30,f9,f);
write(30,f9,noo);  write(30,f9,moo);  write(30,f9,hoo);

write text(30,[[cc]continue**gktb********gnab********
gkob*********z**********g**********l**********i
**********cs**********rs[c]]);

write boolean(30,continue);  write(30,f9,gktb);
write(30,f9,gnab);  write(30,f9,gkob);
write(30,f9,z);  write(30,f9,g);  write(30,f9,l);
write(30,f9,i);  write(30,f9,cs);  write(30,f9,rs);

write text(30,[[cc]***io**********s**********v******
****maxr********maxe********dtm*********number[c]]);

write(30,f9,io);  write(30,f9,s);  write(30,f9,v);
write(30,f9,maxr);  write(30,f9,maxe);
write(30,f9,dtm);  write(30,f9,number);

write text(30,[[cc]]);

write text(30,[program*falmc*11[cc]**time****em*****
*****n**********m**********h**********gk1********gk2
*********gna**********io**********de/dt******f[cc]]);

comment THIS SECTION PROVIDES A PRINTOUT OF ALL THE
        DATA FOR EACH RUN, WRITES THE HEADINGS, AND
        DETERMINES THE FORMAT OF THE DATA OUTPUT;
```

```
ratecon(e);
if continue then begin na[0]:=no:=noo; ma[0]:=mo:=moo;
ha[0]:=ho:=hoo;  gkt:=gkta[0]:=gktb; gko:=gkoa[0]:=gkob;
gna:=gnaa[0]:=gnab;  goto cycle end;
na[0]:=no:=ne;  ma[0]:=mo:=me;  ha[0]:=ho:=he;
nmh(0);
gkta[0]:=gkt;  gkoa[0]:=gko;  gnaa[0]:=gna;

comment PRELIMINARY CALCULATIONS HAVE NOW BEEN
        COMPLETED, AND THE MAIN BODY OF THE PROGRAM
        BEGINS BELOW;



cycle:
if rs≠0 and cs≠0 then begin
q:=exp(-dt/(2×rs×cs));  r:=exp(-dt/(rs×cs)) end
else begin q:=0;  r:=0 end;

t:=t+dt;  u:=u+1;
p:=p+1;
k(0,1,1);
ratecon(e+ke[1]/2);
nmh(dt/2);
k(ke[1]/2,2,q);
ratecon(e+ke[2]/2);
nmh(dt/2);
k(ke[2]/2,3,q);
ratecon(e+ke[3]);
nmh(dt);
k(ke[3],4,r);
de:=(ke[1]+2×ke[2]+2×ke[3]+ke[4])/6 ; e:=de+e;
io:=cs×(de/dt)×(1-r)+io×r;
edot[p]:=de/dt;

comment THIS SERIES OF CALCULATIONS AND PROCEDURES
        PROVIDES THE NEW VALUE OF MEMBRANE POTENTIAL
        AT THE END OF THE STEP;



if p<(a+1) and abs(de/dt)>d and dt>dtm
then goto decstep;
if e>ena or e<ek then goto dump;
ratecon(e);
nmh(dt);

ea[p]:=e;  ta[p]:=t;  na[p]:=n;  ma[p]:=m;
ha[p]:=h;  ana[p]:=an;  ama[p]:=am;  aha[p]:=ah;
bna[p]:=bn;  bma[p]:=bm;  bha[p]:=bh;  gkoa[p]:=gko;
gkta[p]:=gkt;  gnaa[p]:=gna;  ioa[p]:=io;

comment THIS SECTION CALCULATES THE NEW VALUES OF ALL
        THE OTHER PARAMETERS AND STORES THEM IN A
        MATRIX, AND ALSO REDUCES THE STEP LENGTH IF
        THE RATE OF CHANGE OF e PASSES A PRESET LIMIT;
```

```
if p=a then
begin  t:=t-2xdt;  e:=ea[p-2];  no:=na[p-2];  mo:=ma[p-2];
ho:=ha[p-2];  dt:=2xdt;  gkt:=gkta[p-2];  gko:=gkoa[p-2];
gna:=gnaa[p-2];  io:=ioa[p-2];  goto cycle
end
else if p=a+1 then
begin dt:=dt/2;  j:=abs(ea[p]-ea[p-1]);
if j>maxtol then
begin t:=t-axdt;  p:=0;  dt:=dt/b; e:=ea[p];  no:=na[p];
mo:=ma[p];  ho:=ha[p]; gkt:=gkta[p]; gna:=gnaa[p];
gko:=gkoa[p];  io:=ioa[p];  goto cycle
end
else  if j<mintol then
begin dt:=cxdt; if dt>g then dt:=g;    p:=a;
goto data
end
else begin p:=a;
goto data
end
end
else

print:
if spew then goto data else goto reset;

decstep:
t:=t-pxdt;  p:=0;  dt:=dt/b;  e:=ea[p];   no:=na[p];
mo:=ma[p];  ho:=ha[p]; gkt:=gkta[p]; gna:=gnaa[p];
gko:=gkoa[p];  io:=ioa[p];  goto cycle;

comment THIS SECTION CHECKS THE CALCULATIONS BY
        RECALCULATING OVER A DOUBLED STEP LENGTH
        AFTER EVERY a STEPS, AND ADJUSTS THE STEP
        AFTER COMPARING THE TWO ANSWERS.  WHEN
        STEP LENGTH IS REDUCED (AS IS ALSO DONE BY
        decstep ON COMMAND), A RECALCULATION IS DONE;


data:
if p=a then begin e:=ea[a]; n:=na[a]; m:=ma[a];
h:=ha[a];  gko:=gkoa[a]; gkt:=gkta[a]; gna:=gnaa[a];
io:=ioa[a] end;
if entier(f/l)≠entier((f-1)/l) or spew then begin
write(30,f1,t);  write(30,f2,e);  write(30,f3,n);
write(30,f3,m);  write(30,f3,h);  write(30,f3,gko);
write(30,f3,gkt);  write(30,f3,gna);
write(30,f9,io);  write(30,f9,edot[p]);
write(30,f4,f/l)  end;

if abs(de/dt)>maxr or e>maxe then spew:=true
else spew:=false;

f:=f+1;  if t>tstop then goto stop;

comment THIS SECTION PRINTS OUT THE DATA WHEN REQUIRED;
```

```
reset:
if p=a then begin p:=0; ea[0]:=e; no:=na[0]:=n;
mo:=ma[0]:=m;  ho:=ha[0]:=h;  gkta[0]:=gkt;
gkoa[0]:=gko;  gnaa[0]:=gna;  ioa[0]:=io  end
else begin no:=n; mo:=m; ho:=h end;
goto cycle;

comment THIS SECTION RESETS THE PROGRAM WITH THE
        APPROPRIATE DATA AND RETURNS CONTROL TO
        cycle;


dump:
t:=t;
write text(30,[[cc]em*runaway*at*e=....*and*
           t=....[c]]);
output(30,e);  output(30,t);
  goto stop;

comment IF THE VALUES GET OUT OF CONTROL,
        THIS SECTION STOPS THE PROGRAM AND
        PRINTS THE LAST VALUES OF
        MEMBRANE POTENTIAL AND TIME;
```

```
stop:
fmax:=f;
write(30,f5,u);
write text(30,[[c]program*falmc*11*****end*
           of*data*set*.........[cc]]);

open(20);
ei:=ea[0]:=e:=read(20);
if e≠0 then begin write text(30,[[p]]);
goto repeat end;

close(20);
close(30);

comment THIS SECTION STOPS THE PROGRAM AT THE
        COMPLETION OF ONE SET OF CALCULATIONS,
        AND EITHER CAUSES THE START OF THE
        NEXT SET OR ENDS THE CALCULATION, AS
        APPROPRIATE;


end→
```

6.2 KDF-9 ALGOL PROGRAM FOR COMPUTING CARDIAC MUSCLE MEMBRANE CURRENTS DURING A RAMP VOLTAGE CLAMP.

The data required for each run of the program is listed below in the order of input, together with the symbol which represents it in the program. Typical values follow in brackets.

Program FALMC 12 :

no : initial value of n (.0818)

mo : initial value of m (.0475)

ho : initial value of h (.826)

x : delayed k conductance g_{K2} is given by $xn^z + q$ (1.2)

w : Na conductance g_{Na} is given by $wm^3 + y$ (400)

y : see w (0.14)

z : see x (4)

ei : initial value of membrane potential in mV (-80)

ti : initial value of time in msec (0)

dt : step length to be used throughout the program, usually chosen so that s times dt equals 0.1 (1)

emin : value of membrane potential in mV at which the downward ramp should stop (-100)

s : rate of change of voltage of the ramp in V/sec (0.1)

ek : K equilibrium potential in mV (-100)

ena : Na equilibrium potential in mV (40)

ean : leakage equilibrium potential in mV (0)

gan : constant leakage conductance in m mho/cm^2 (0)

emax : value of e in mV at which the upward ramp turns downward (40)

pause : if this has the value '<u>true</u>', n, m and h are assigned their steady-state values before the ramp turns downward (<u>false</u>)

d : data is printed out after every d steps (10)

c : pure membrane capacitance in $\mu F/cm^2$ (2.4)

cs : value of the capacitance in the series-RC branch, in $\mu F/cm^2$ (7)

rs : value of the resistance in the series-RC branch, in ohm cm^2 (300)

v : the value of g_{K1} is multiplied by this factor (1)

q : see x (0)

b : if the membrane potential is within this limit of the instability points (poles) of the expressions for an, am, or bm, the limiting values are assigned instead (0.1)

Thus, twenty-five numbers are required for each run of the program. More than one set of data may be input at one time; the last set must be followed by one additional number, a zero, in order to end the program properly and exit from the computer.

The printout will consist of sixteen numbers, occupying two lines, for each step, in the following order: membrane potential, total membrane current, time, n, m, h, current through g_{K1}, current through g_{K2}, current through g_{Na}, current through g_{An}, line number, (start new line) current through the pure capacitance, current through the series-RC branch, initial current through the series-RC branch at the beginning of each step, total membrane current less capacitive currents, and total potassium current.

All the data used for a computation is printed out immediately before the results.

```
  → ESTABLISH FALMC1200APU;
RAMP CLAMP, STEPS;
O/PL;→

begin  comment  RAMP CLAMP, STEPS;
library A0,A6;

integer f,a,f1,f2,f3,f4,f5;
real t,ti,dt,emin,e,ei,s,an,am,ah,bn,bm,bh,gko,tn,
     tm,th,ne,me,he,n,m,h,no,mo,ho,gkt,x,w,y,z,gna,
     i,iko,ikt,ina,ian,ek,ena,ean,gan,emax,tchange,
     d,q,v,c,cs,rs,ic,irc,io,ig,b;
boolean pause,set;


comment ALL THE VARIABLES WHICH WILL BE USED IN THE
        PROGRAM HAVE BEEN DECLARED ABOVE;



procedure ratecon(en);
value en;  real en;
begin
an:=if abs(en+50)>b then 0.0001000000x(-en-50.000000)/
    (exp((-en-50.0000000000)/10.0000000000)-1.0000000)
    else 0.0010000000;

bn:=0.0020000000xexp((-en-90.0000000000)/80.0000000000);

am:=if abs(en+48)>b then 0.1000000000x(-en-48.000000)/
    (exp((-en-48.0000000000)/15.0000000000)-1.0000000000)
     else 1.5000000000;

bm:=if abs(en+8)>b then 0.1200000000x(en+8.0000000000)/
    (exp((en+8.0000000000)/5.0000000000)-1.0000000000)
    else 0.6000000000;

ah:=0.1700000000xexp((-en-90.0000000000)/20.0000000000);

bh:=(exp((-en-42.0000000000)/10.0000000)+1.00000)↑(-1);

gko:=vx(1.2000000000xexp((-en-90.0000000000)/50.0000000)
     +0.0150000000xexp((en+90.0000000000)/60.0000000000));

tn:=(an+bn)↑(-1);  tm:=(am+bm)↑(-1);  th:=(ah+bh)↑(-1);

ne:=anxtn;  me:=amxtm;  he:=ahxth

end;

comment THIS PROCEDURE EVALUATES THOSE PARAMETERS
        WHICH ARE A FUNCTION OF THE MEMBRANE POTENTIAL
        ONLY;
```

```
procedure nmh(tt);   value tt;  real tt;
begin
n:=(no-ne)×exp(-tt/tn)+ne;
m:=(mo-me)×exp(-tt/tm)+me;
h:=(ho-he)×exp(-tt/th)+he;

gkt:=x×n↑z+q;    gna:=w×m↑3×h+y
end;

comment THIS PROCEDURE USES THE RATE CONSTANTS
        CALCULATED BY ratecon TOGETHER WITH THE
        TIME AND PREVIOUS VALUES OF THE CONDUCTANCE
        PARAMETERS TO CALCULATE THE NEW VALUES OF
        THE CONDUCTANCE PARAMETERS, ACCORDING TO
        A SIMPLE EXPONENTIAL EQUATION;

  procedure icalc(b);   value b;  integer b;
  begin
  f:=b; iko:=gko×(e-ek);  ikt:=gkt×(e-ek);
  ina:=gna×(e-ena);  ian:=gan×(e-ean);
ig■:=iko+ikt+ina+ian;
  ic:=if t< tchange then cxs else -(cxs);
  if rs≠0 and cs≠0 then begin
  io:=if t< tchange then (irc+1000xsxdt/rs)
  else (irc-1000xsxdt/rs);
  irc:=io×exp(-1000xdt/(rs×cs)) end
  else begin irc:=0; io:=0 end;
  i:=ig+ic+irc
  end;

  comment THIS PROCEDURE USES THE PRESENT VALUES OF
          THE CONDUCTANCES, POTENTIAL, AND THE PREVIOUS
          VALUE OF THE CURRENT THROUGH THE RC BRANCH
          TO CALCULATE THE TOTAL MEMBRANE CURRENT
          AND THE COMPONENT CURRENTS;
```

```
f1:=format([ndddd.ddss]);  f2:=format([-ndd.dss]);
f5:=format([ssnddddc]);
f3:=format([ss-d.dd10-nd;]); f4:=format([-nddd.dsss]);

open(20);
open(30);

restart:
no:=read(20);  if no=0 then begin close(20); goto stop end;
mo:=read(20); ho:=read(20); x:=read(20);
w:=read(20); y:=read(20); z:=read(20);
ei:=read(20);  t:=ti:=read(20); dt:=read(20);
emin:=read(20); s:=read(20);  ek:=read(20);
ena:=read(20); ean:=read(20); gan:=read(20);
emax:=read(20); pause:=readboolean(20);
d:=read(20);  c:=read(20);  cs:=read(20);
rs:=read(20);  v:=read(20);  q:=read(20);
b:=read(20);

close(20);

write text(30,[[cc]***no**********mo**********ho***
*******x**********w**********y**********z*******
****ei[c]]);

write(30,f3,no);  write(30,f3,mo);  write(30,f3,ho);
write(30,f3,x);   write(30,f3,w);   write(30,f3,y);
write(30,f3,z);   write(30,f3,ei);

write text(30,[[cc]***ti*********dt*********emin*
*******s**********ek**********ena*********ean*****
****gan[c]]);

write(30,f3,ti);  write(30,f3,dt);  write(30,f3,emin);
write(30,f3,s);   write(30,f3,ek);  write(30,f3,ena);
write(30,f3,ean); write(30,f3,gan);

write text(30,[[cc]emax*********pause*********d**
*********c**********cs**********rs**********v***
********q**********b[c]]);

write(30,f3,emax);  write boolean(30,pause);
write(30,f3,d);  write(30,f3,c);  write(30,f3,cs);
write(30,f3,rs);  write(30,f3,v);  write(30,f3,q);
write(30,f3,b);  write text(30,[[ccc]]);

write text(30,[ramp*clamp, steps[cc]]);
write text(30,[*em*******i**********t********n*****
*****m**********h**********ik1 *********ik2********ina
********ian**********f[c]******ic*****************
irc**********io**********ig*********ik[cc]]);


comment THIS SECTION PROVIDES A PRINTOUT OF ALL THE
        DATA FOR EACH RUN, WRITES THE HEADINGS, AND
        DETERMINES THE FORMAT OF THE DATA OUTPUT;
```

```
tchange:=(emax-e1)/s;
a:=f:=0;
irc:=0;

ratecon(e1);
nmh(0);
no:=n; mo:=m; ho:=h; e:=e1;
icalc(0);

set:=true;

comment PRELIMINARY CALCULATIONS HAVE NOW BEEN
        COMPLETED.  THE MAIN BODY OF THE PROGRAM
        BEGINS BELOW;



up:
a:=a+1;  t:=t+dt;  e:=e+s×dt;
ratecon(e);
nmh(dt);
no:=n;  mo:=m;  ho:=h;
icalc(a);
goto print;

down:
a:=a+1;  t:=t+dt;  e:=e-s×dt;
ratecon(e);
nmh(dt);
no:=n;  mo:=m;  ho:=h;
icalc(a);
goto print;

comment ALL THE CALCULATIONS AT THE END OF EACH
        STEP ARE ACCOMPLISHED BY THIS SECTION;



print:
if entier(f/d)≠entier((f-1)/d) then begin
write(30,f2,e); write(30,f4,i); write(30,f1,t);
write(30,f3,n);  write(30,f3,m); write(30,f3,h);
write(30,f3,iko); write(30,f3,ikt);  write(30,f3,ina);
write(30,f3,ian); write(30,f5,f);
write text(30,[[sss]]);  write(30,f3,ic);
write text(30,[[6s]]);   write(30,f3,irc);
write text(30,[[ss]]);   write(30,f3,io);
write(30,f3,ig);  write(30,f3,iko+ikt);
write text(30,[[c]]) end;

comment THIS SECTION PRINTS THE DATA AT THE END
        OF A STEP ON COMMAND;
```

```
if t<tchange then goto up else
if t=tchange or t>tchange then begin
if pause and set then begin no:=ne; mo:=me; ho:=he;
set:=false end end;
if t<((emax-e1+emax-emin)/s) then goto down else
begin write text(30,[[p]]);  open(20);
goto restart end;

stop:
a:=a;
close(30);

comment THIS SECTION RESETS THE PROGRAM AT THE
        PROPER STARTING PLACE, DEPENDING ON WHETHER
        THE SAWTOOTH CLAMP IS DEPOLARIZING OR
        REPOLARIZING.  IT ALSO STOPS THE PROGRAM
        AT THE END OF THE LAST SET OF DATA, IF THE
        LATTER IS FOLLOWED BY 0;

end→
```

REFERENCES

ADRIAN, R.H. (1965). The rubidium and potassium permeability of frog muscle membrane. J. Physiol. 175, 134-159.

ADRIAN, R.H. & FREYGANG, W.H. (1962). The potassium and chloride conductance of frog muscle membrane. J. Physiol. 163, 61-103.

BARR, L., BERGER, W. & DEWEY, M.M. (1964). The effects of osmolarity on propagation, longitudinal resistance, and the structure of the nexus in frog atrium. Physiologist, 7, 87.

BARR, L., DEWEY, M.M. & BERGER, W. (1965). Propagation of action potentials and the structure of the nexus in cardiac muscle. J. Gen. Physiol. 48, 797-824.

BAYLISS, L.E. (1960). Principles of General Physiology. Volume I. Longmans, Green & Co., Ltd., London.

BENNETT, M.V.L. & GRUNDFEST, H. (1966). Analysis of depolarizing and hyperpolarizing inactivation responses in gymnotid electroplaques. J. Gen. Physiol. 50, 141-170.

BOULPAEP, E. (1963). Permeability of heart muscle to choline. Arch. Intern. Physiol. Biochem. 71, 623-625.

BURGEN, A.S.V. & TERROUX, K.G. (1953). The membrane resting and action potentials of the cat auricle. J. Physiol. 119, 139-152.

CAESAR, R., EDWARDS, G.A. & RUSKA, H. (1958). Electron microscopy of the impulse-conducting system of the sheep heart. Z. Zellforsch. mikroskop. Anat. 48, 698-719.

CARMELIET, E. (1961). Chloride ions and the membrane potential of Purkinje fibres. J. Physiol. 156, 375-388.

CEDERGREN, B. & HARARY, I. (1964). In vitro studies on single beating rat heart cells: electronmicroscopic studies of single cells; ultrastructure of beating cell layer. J. Ultrastruct. Res. 11, 428-442.

COLE, K.S. & CURTIS, H.J. (1939). Electrical impedance of the squid giant axon during activity. J. Gen. Physiol. 22, 649-670.

CORABOEUF, E. & WEIDMANN, S. (1949a). Potentiels de repos et potentiels d'action du muscle cardiaque, mesurés à l'aide d'électrodes internes. Comptes Rendus, 143, 1329-1331.

CORABOEUF, E. & WEIDMANN, S. (1949b). Potentiels d'action du muscle cardiaque obtenus à l'aide de microélectrodes intracellulaires. Présence d'une inversion de potentiel. Comptes Rendus, 143, 1360-1361.

CORABOEUF, E. & WEIDMANN, S. (1954). Temperature effects on the electrical activity of Purkinje fibres. Helv. Physiol. Acta 12, 32-41.

DECK, K.A., KERN, R. & TRAUTWEIN, W. (1964). Voltage clamp technique in mammalian cardiac fibres. Pflügers Arch. ges. Physiol. 280, 50-62.

DECK, K.A. & TRAUTWEIN, W. (1964). Ionic currents in cardiac excitation. Pflügers Arch. ges. Physiol. 280, 63-80.

DELEZE, J. (1965). Calcium ions and the healing-over of heart fibres. In Electrophysiology of the Heart, ed. B. Taccardi & G. Marchetti, pp. 147-148. Pergamon Press, Oxford.

DE MELLO, W.C. & HOFFMAN, B.F. (1960). Potassium ions and electrical activity of specialized cardiac fibres. Am. J. Physiol. 199, 1125-1130.

DEWEY, M.M. & BARR, L. (1962). Intercellular connection between smooth muscle cells: the nexus. Science, 137, 670-672.

DEWEY, M.M. & BARR, L. (1964). A study of the structure and distribution of the nexus. J. Cell. Biol. 23, 553-585.

DRAPER, M.H. & WEIDMANN, S. (1951). Cardiac resting and action potentials recorded with an intracellular electrode. J. Physiol. 115, 74-94.

DUDEL, J., PEPER, K. & TRAUTWEIN, W. (1966). The contribution of Ca^{++} ions to the current voltage relation in cardiac muscle (Purkinje fibres). Pflügers Arch. ges. Physiol. 288, 262-281.

DUDEL, J., PEPER, K., RUDEL, R. & TRAUTWEIN, W. (1966). Excitatory membrane current in heart muscle (Purkinje fibres). Pflügers Arch. ges. Physiol. 292, 255-273.

DUDEL, J., PEPER, K., RUDEL, R. & TRAUTWEIN, W. (1967). The dynamic chloride component of membrane current in Purkinje fibres. Pflügers Arch. ges. Physiol. 295, 197-212.

DUDEL, J. & TRAUTWEIN, W. (1958). Der Mechanismus der automatischen rhythmischen Impulsbildung der Herzmuskelfaser. Pflügers Arch. ges. Physiol. 267, 553-565.

EDWARDS, G.A., RUSKA, H., DE SOUZA SANTOS, P. & VALLEJO-FREIRE, A. (1956). Comparative cytophysiology of striated muscle, with special reference to the role of the endoplasmic reticulum. J. Biophys. Biochem. Cytol. 2, Suppl. 143-156.

FORSSMANN, W.G. & GIRARDIER, L. (1966). Untersuchungen zur Ultrastruktur des Rattenherzmuskels mit besonderer Berücksichtigung des sarkoplasmatischen Retikulums. Z. Zellforsch. mikroskop. Anat. 72, 249-275.

FOZZARD, H.A. (1966). Membrane capacity of the cardiac Purkinje fibre.

J. Physiol. 182, 255-267.

FRANKENHAEUSER, B. (1962). Potassium permeability in myelinated nerve fibres of Xenopus Laevis. J. Physiol. 160, 54-61.

GIRARDIER, L. (1965). The problem of the inward spread of excitation in skeletal and heart muscle cells. In Electrophysiology of the Heart, ed. B. Taccardi & G. Marchetti, pp. 53-70. Pergamon Press, Oxford.

GOLDENBERG, M. & ROTHBERGER, C.J. (1936). Uber das Elektrogramm der spezifischen Herzmuskulatur. Pflügers Arch. ges. Physiol. 237, 295-306.

GOLDMAN, D.E. (1943). Potential, impedance, and rectification in membranes. J. Gen. Physiol. 27, 37-60.

GRIMLEY, P.M. & EDWARDS, G.A. (1960). Ultrastructure of cardiac desmosomes in toad and their relationship to the intercalated disc. J. Biophys. Biochem. Cytol. 8, 305-318.

HALL, A.E., HUTTER, O.F. & NOBLE, D. (1963). Current-voltage relations of Purkinje fibres in sodium-deficient solutions. J. Physiol. 166, 225-240.

HALL, A.E. & NOBLE, D . (1963). The effect of potassium on the repolarizing current in cardiac muscle. J. Physiol. 167, 53-54P.

HARRIS, E.J. & HUTTER, O.F. (1956). The action of acetylcholine on the movements of potassium ions in the sinus venosus of the heart. J. Physiol. 133, 58-59P.

HAWGOOD, J. (1965). Numerical Methods in Algol. McGraw-Hill, Maidenhead, England.

HECHT, H.H. & HUTTER, O.F. (1965). The action of pH on cardiac Purkinje

fibres. In The Electrophysiology of the Heart, ed. B. Taccardi & G. Marchetti, Pergamon Press, Oxford, pp. 105-123.

HILL, A.V. (1949). The abrupt transition from rest to activity in muscle. Proc. Roy. Soc. B., 399-420.

HÖBER, R . (1945). Physical Chemistry of Cells and Tissues. J. & A. Churchill Ltd., London.

HODGKIN, A.L. & HUXLEY, A.F. (1952a). Currents carried by sodium and potassium ions through the membrane of the giant axons of Loligo. J. Physiol. 116, 449-472.

HODGKIN, A.L. & HUXLEY, A.F. (1952b). The components of membrane conductance in the giant axons of Loligo. J. Physiol. 116, 473-496.

HODGKIN, A.L. & HUXLEY, A .F. (1952c). The dual effect of membrane potential on sodium conductance in the giant axon of Loligo. J. Physiol. 116, 497-506.

HODGKIN, A.L. & HUXLEY, A.F. (1952d). A quantitative description of membrane current and its application to conduction and excitation in nerve. J. Physiol. 117, 500-544.

HODGKIN, A.L. HUXLEY, A.F. & KATZ, B. (1952). Measurement of current-voltage relations in the membrane of the giant axon of Loligo. J. Physiol. 116, 424-448.

HODGKIN, A.L. & KATZ, B. (1949). The effect of sodium ions on the electrical activity of the giant axon of the squid. J. Physiol. 108, 37-77.

HOFFMAN, B.F. & CRANEFIELD, P.F. (1960). Electrophysiology of the Heart. McGraw-Hill, New York.

HUTTER, O.F. & NOBLE, D. (1960). Rectifying properties of cardiac

muscle. Nature, 188, 495.

HUTTER, O.F. & NOBLE, D. (1961). Anion conductance of cardiac muscle. J. Physiol. 157, 335-350.

HUXLEY, A.F. (1961). A micromanipulator. J. Physiol. 157, 5-7P.

HUXLEY, A.F. & TAYLOR, R.E. (1958). Local activation of striated muscle fibres. J. Physiol. 144, 426-441.

HUXLEY, H.E. (1964). Evidence for continuity between the central element of the triads and extracellular space in frog sartorius muscle. Nature, 202, 1067-1071.

JOHNSON, E.A. & TILLE, J. (1961). Investigations of the electrical properties of cardiac muscle fibres with the aid of intracellular double-barrelled electrodes. J. Gen. Physiol. 44, 443- 467.

JOHNSON, E.A., TILLE, J. & WILSON, L. (1961). The effect of a change in shape of the cardiac action potential on the ionic conductances. Aust. J. E xp. Biol. 39, 179-186.

KAY, R.H., PHILLIPS, C.G. & TEAL, R.H. (1958). A versatile stimulator. Electronic Engineering, October.

LING, G. & GERARD, R.W. (1949). The normal membrane potential of frog sartorius fibres. J. Cell. Comp. Physiol. 34, 383-396.

MOORE, D.H. & RUSKA, H. (1957). Electron microscope study of mammalian cardiac muscle cells. J. Biophys. Biochem. Cytol. 3, 261-268.

MOORE, E.N., PRESTON, J.B. & MOE, G.K. (1965). Durations of transmembrane action potentials and functional refractory periods of canine false tendon and ventricular myocardium. Circulation Res. 17, 259-273.

MUIR, A.R. (1957). An electron microscope study of the embryology of the intercalated disc in the heart of the rabbit. J. Biophys. Biochem. Cytol. 3, 193-201.

MUIR, A.R. (1965). Further observations on the cellular structure of cardiac muscle. J. Anat. 99, 27-46.

MULLER, P. (1965). Potassium and rubidium exchange across the surface membrane of cardiac Purkinje fibres. J. Physiol. 177, 453-462.

NELSON, D.A. & BENSON, E.S. (1963). On the structural continuities of the transverse tubular system of rabbit and human myocardial cells. J. Cell. Biol. 16, 297-313.

NOBLE, D. (1962a). A modification of the Hodgkin-Huxley equations applicable to Purkinje fibre action and pace-maker potentials. J. Physiol. 160, 317-352.

NOBLE, D. (1962b). The voltage dependence of the cardiac membrane conductance. Biophys. J. 2 381-393.

NOBLE, D. (1965). Electrical properties of cardiac muscle attributable to inward going (anomalous) rectification. J. Cell. Comp. Physiol. 66, Suppl. 2 to No. 3, 127-136.

NOBLE, D. & HALL, A.E. (1963). The conditions for initiating 'all-or-nothing' repolarization in cardiac muscle. Biophys. J. 3, 261-274.

ORKAND, R.K. & NIEDERGERKE, R. (1964). Heart action potential: dependence on external calcium and sodium ions. Science 146, 1176-1177.

PILLAT, B. (1967). Prolongation of the relative refractory period by drugs acting like quinidine; occurrence of propagated spikes in cardiac muscle. Helv. Physiol. Acta 25, 32-39.

PORTER, K.R. (1956). The sarcoplasmic reticulum in muscle cells of amblystoma larvae. J. Biophys. Biochem. Cytol. 2, Suppl. 163-169.

PURKINJE, Prof. (1845). Mikroskopisch - neurologische Beobachtungen. Arch. Anat. Physiol., Leipzig, 12, 281-295.

RAYNS, D.G., SIMPSON, F.O. & BERTAUD, W.S. (1967). Transverse tubule apertures in mammalian myocardial cells: surface array. Science, 156, 656-657.

RENKIN, E.M. (1961). Permeability of frog skeletal muscle to choline. J. Gen. Physiol. 44, 1159-1164.

REUTER, H. (1966). Strom-Spannungsbeziehungen von Purkinje-Fasern bei verschiedenen extracellulären Calcium-Konzentrationen und unter Adrenalineinwirkung. Pflügers Arch. ges. Physiol. 287, 257-367.

SJÖSTRAND, F.S. & ANDERSSON, E. (1954). Electron miscoscopy of the intercalated discs of cardiac muscle tissue. Experientia 10, 369-370.

SJÖSTRAND, F.S., ANDERSSON-CEDERGREN, E. & DEWEY, M.M. (1958). The ultrastructure of the intercalated discs of frog, mouse, and guinea-pig cardiac muscle. J. Ultrastruct. Res. 1, 271-287.

TEMTE, J.V. & DAVIS, L.D. (1967). Effect of calcium concentration on the transmembrane potentials of Purkinje fibres. Circulation,Res. 20, 32-44.

TRAUTWEIN, W. & DUDEL, J. (1954). Aktionspotential und Mechanogramm des Warmblüterherzmuskels als Funktion der Schlagfrequenz. Pflügers Arch. ges. Physiol. 260, 24-39.

TRAUTWEIN, W. & DUDEL, J. (1958a). Zum Mechanismus der Membranwirkung der Acetylcholin an der Herzmuskelfaser. Pflügers Arch. ges.

Physiol. 266, 324-334.

TRAUTWEIN, W. & DUDEL, J. (1958b). Hemmende und 'erregende' Wirkungen des Acetylcholin am Warmblüterherzen. Zur Frage der spontanen Erregungsbild. Pflügers Arch. ges. Physiol. 266, 653-664.

TRAUTWEIN, W., DUDEL, J. & PEPER, K. (1965). Stationary S-shaped current volrage relation and hysteresis in heart muscle fibres. Excitatory phenomena in Na-free bathing solutions. J. Cell. Comp. Physiol. 66, Suppl. 2, 79-90.

TRAUTWEIN, W., GOTTSTEIN, U. & DUDEL, J. (1954). Der Aktionsstrom der Myokardfaser im Sauerstoffmangel. Pflügers Arch. ges. Physiol. 260, 40-60.

TRAUTWEIN, W., GOTTSTEIN, U. & FEDERSCHMIDT, K. (1953). Der Einfluss der Temperatur auf den Aktionsstrom des excidierten Purkinje-fadens, gemessen mit einer intracellulären Elektrode. Pflügers Arch. ges. Physiol. 258, 243-260.

TRAUTWEIN, W. & KASSELBAUM, D.G. (1961). On the mechanism of spontaneous impulse generation in the pacemaker of the heart. J. Gen. Physiol. 45, 317-330.

TROSHIN, A.S. (1966). Problems of Cell Permeability. Pergamon Press, Oxford.

VAN BREEMAN, V.L. (1953). Intercalated discs in heart muscle, studied with the electron microscope. Anat. Rec. 117, 49-56.

VASSALLE, M. (1966). An analysis of cardiac pacemaker potential by means of a 'voltage clamp' technique. Am. J. Physiol. 210, 1335-1341.

VAUGHAN WILLIAMS, E.M. (1959). The effect of changes in extracellular potassium concentration on the intracellular potentials of isolated rabbit atria. J. Physiol. 146, 411-427.

WALKER, S.M. & SCHRODT, G.R. (1965). Continuity of the T-system with the sarcolemma in rat skeletal muscle fibres. J. Cell Biol. 27, 671-676.

WEIDMANN, S. (1951). Effect of current flow on the membrane potential of cardiac muscle. J. Physiol. 115, 227-236.

WEIDMANN, S. (1952). The electrical constants of Purkinje fibres. J. Physiol. 118, 348-360.

WEIDMANN, S. (1955a). Rectifier properties of Purkinje fibres. Am. J. Physiol. 183, 671.

WEIDMANN, S. (1955b). The effect of the cardiac membrane potential on the rapid availability of the sodium-carrying system. J. Physiol. 127, 213-234.

WEIDMANN, S. (1955c). Effects of calcium ions and local anaesthetics on electrical properties of Purkinje fibres. J. Physiol. 129, 568-582.

WEIDMANN, S. (1956a). Elektrophysiologie der Herzmuskelfaser. Huber, Bern.

WEIDMANN, S. (1956b). Shortening of the cardiac action potential due to a brief injection of KCl following the onset of activity. J. Physiol. 132, 157-163.

WEIDMANN, S. (1957). Resting and action potentials of cardiac muscle. Ann. N.Y. Acad. Sci. 65, 663-678.

WEIDMANN, S. (1966). The diffusion of radiopotassium across intercalated discs of mammalian cardiac muscle. J. Physiol. 187, 323-342.